„Power Network Planning and Operation“

Steady-state and quasi-steady-state power system analysis

Prof. Dr.-Ing. habil. Martin Wolter

Otto-von-Guericke Universität Magdeburg

Institute of Electric Power Systems

Chair Electric Power Networks and Renewable Energy Sources

Version 2020

List of content

1 Modal components 1
1.1 General development of transformation matrices 2
1.2 Calculation of powers in modal components 4
1.3 Most common modal components 4
1.3.1 Symmetrical components 4
1.3.2 Diagonal components (Clarke-Transformation) 7
1.3.3 Other transformation methods 8
1.4 Summary of transformation matrices 9

2 Modelling of equipment 11
2.1 Dipoles 11
2.2 Quadrupoles 12
2.2.1 Lines 13
2.2.2 Two-winding transformer 13
2.3 Sextupoles 16
2.4 Octopoles 16

3 Grid equation systems 19
3.1 Multipole theory 19
3.1.1 Description of topology 20
3.1.2 Nodal-based description of the system state 21
3.1.3 Deduced information 22
3.2 Graph theory 22
3.3 Direct arrangement of the bus admittance matrix 25

4 Power flow calculation 27
4.1 Node types and voltage dependency of loads 27
4.2 Gauss-Seidel iteration 29
4.3 Newton-Raphson-approach 32
4.3.1 Newton-Raphson in Cartesian coordinates 33
4.3.2 Newton-Raphson in polar coordinates 36
4.3.3 Initial guess 38
4.3.4 Flow chart of the iteration 39
4.4 Decoupled power flow calculation 40
4.5 Fast decoupled power flow (DC power flow) 40

5 State Estimation 43
5.1 Measurement error and redundancy 43
5.2 State estimation with linear measurement model 45
5.3 State estimation with non-linear measurement model 47
5.4 Construction of the Jacobian 49
5.4.1 Nodal powers 49
5.4.2 Terminal powers 49

5.4.3 Nodal voltage magnitudes ... 50
5.4.4 Nodal current magnitudes ... 50
5.4.5 Terminal current magnitude ... 51
5.4.6 Construction of the equation systems ... 51
5.5 Flow chart of the iteration ... 52

6 Short-circuit calculation ... 55
6.1 Single line diagram of dipoles for short-circuit calculation ... 56
6.2 Exact calculation ... 57
6.3 Superposition approach by Helmholtz and Thévenin ... 58
6.4 Short-circuit calculation according to IEC 60909 ... 60
6.5 Impedance correction ... 61

7 Stability ... 65
7.1 Generator models ... 65
7.2 Description of rotor motion ... 67
7.3 Equivalent network model ... 68
7.4 Grid transfiguration to the generator nodes ... 68
7.5 Small-signal stability ... 69
7.5.1 Demonstration of small-signal stability using the single-machine-problem ... 69
7.5.2 General calculation of small-signal stability ... 71
7.5.3 Measures to increase small-signal stability ... 72
7.6 Transient stability ... 73
7.6.1 Demonstration of transient stability using the single-machine problem ... 74
7.6.2 General determination of transient stability in grids with several generators ... 78
7.6.3 Measures to increase transient stability ... 79

8 Modelling of shunt and series faults ... 81
8.1 Fault conditions ... 81
8.1.1 Fault conditions in natural coordinates ... 82
8.1.2 Fault conditions in symmetrical components ... 84
8.2 General description of shunt faults ... 85
8.3 General description of series faults ... 87
8.4 Balanced faults ... 89

Nomenclature

Notation

Symbol	Description
k, K	scalar
$\underline{k}$, $\underline{K}$	complex value
k'	related value
$\boldsymbol{k}$	vector
$\boldsymbol{K}$	Matrix

Superscript Indices

Symbol	Description
T	transposed
*	complex-conjugated

Subscript Indices

Symbol	Description
a, b, c	Phase index in natural coordinates
A, B, C, D	terminal indexes
act	actual
Beschl	acceleration
BM	equipment
Brems	slowdown
calc	calculated
D	diagonal components
est	estimated
F	faulty
Fe	iron losses
G	Generator
g	mutual impedance
h	Main-
K	node
k	short-circuit
m	modal
p	synchronous generated voltage
q	Source
r	rated
ref	reference
s	self impedance
SK	symmetrical components
SP	neutral point
T	Terminal
TOS	upper voltage side of the transformer
TUS	lower voltage side of the transformer
α, β	system indexes in α, β, 0 coordinates

Symbols

Symbol	Description
δ	voltage angle
φ	phase angle
A	area
a	rotary operator
B	susceptance
C	capacitance
c	correction factor
$\boldsymbol{E}$	unity matrix
g	physical variable
G	Conductance
$\boldsymbol{H, N, M, L}$	submatrix
I	electric current
$\boldsymbol{J}$	Jacobian
k	factor
K	incidence matric
l	length
M	torque
m, n, i, j	control variable
P	active power
Q	reactive power
R	resistance
S	apparent power
$\underline{\boldsymbol{t}}$	eigenvector
$\boldsymbol{T}$	transformation matrix
t	time
U	voltage
x	system state variable
X	reactance
Y	admittance
Z	impedance
ε	threshold
v	iteration counter
σ	standard deviation
τ	transmission ratio
λ	eigenvalue

Preamble

The continuous and reliable availability of electric energy at any place and in a sufficient amount is the backbone of any advanced economy. A highly meshed, stable electric power grid which offers sufficient reserves is necessary to grant the high degree of reliability and security of supply which the customers nowadays are used to. The grid needs to be resilient to cope the various needs of customers at any time.

Economic boom phases and crises, demographic changes, technological breakthroughs and last but not least divergent political interests have led to a continuous change in the utilization of the electric power system in the recent past. Grid extension efforts take much longer than the described changes in grid utilization, so grid reserves are decreasing. This is becoming a more and more severe threat to system security. That is why knowledge of the grid state is of essential importance for grid operators.

In this script, the fundamental algorithms of steady-state and quasi-steady-state power system analysis are presented. It contains the essential approaches of modelling assets and network topology. Furthermore, the most relevant grid state identification algorithms are explained. The algorithms are suitable for the healthy, balanced system as well as for faulty, balanced and unbalanced conditions.

Nowadays, commercial grid calculation software is used to do power system analysis. Nevertheless, a power system engineer should be able to understand the fundamental mathematics behind power system behavior. This will help him to use and parameterize the software and makes it easier to understand the results and derive solutions.

At this point it is necessary to mention, that the script does not replace the lecture course and vice versa. Instead, the script and the lecture supplement each other. In the script, the focus is laid on the mathematical details and algorithms, while, in the lecture, the focus is on understanding the concepts

While reading this script, I hope, the reader will feel the same joy I did, when I was a student and got introduced to power system analysis.

Martin Wolter

August 2020

1 Modal components

The general composition of a three-phase electric power system is given in Fig. 1. Voltages and currents cannot be calculated separately for each phase due to the coupling of the phases.

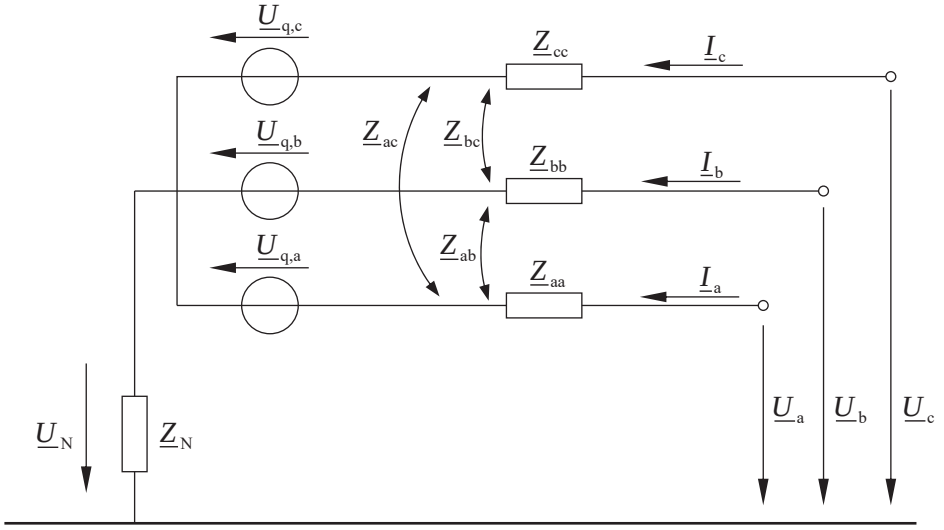

Fig. 1: general composition of a three-phase electric power system in natural coordinates

The coupling of the phases results in a dense impedance matrix $\underline{\boldsymbol{Z}}$ in the linear equation system. Encircling of the three meshes given by the respective phase, the neutral point impedance and ground results in

$$\begin{bmatrix} \underline{U}_a \\ \underline{U}_b \\ \underline{U}_c \end{bmatrix} = \begin{bmatrix} \underline{Z}_{aa} & \underline{Z}_{ab} & \underline{Z}_{ac} \\ \underline{Z}_{ba} & \underline{Z}_{bb} & \underline{Z}_{bc} \\ \underline{Z}_{ca} & \underline{Z}_{cb} & \underline{Z}_{cc} \end{bmatrix} \begin{bmatrix} \underline{I}_a \\ \underline{I}_b \\ \underline{I}_c \end{bmatrix} + \begin{bmatrix} \underline{U}_{q,a} \\ \underline{U}_{q,b} \\ \underline{U}_{q,c} \end{bmatrix} + \begin{bmatrix} \underline{U}_N \\ \underline{U}_N \\ \underline{U}_N \end{bmatrix} \tag{1.1}$$

or in abbreviated diction

$$\underline{\boldsymbol{u}} = \underline{\boldsymbol{Z}}\,\underline{\boldsymbol{i}} + \underline{\boldsymbol{u}}_q + \underline{\boldsymbol{u}}_N \tag{1.2}$$

Usually, a symmetric and balanced three phase system is assumed. That means, that all of the phase impedances and all of the couplings are identical and the source voltages have equal magnitudes and a phase angle difference of 120° each. Usually, phase “a” is considered reference phase and therefore its phase angle is set to 0° to simplify calculations.

Furthermore, assumption of a balanced system results in

$$\begin{aligned} \underline{Z}_{aa} &= \underline{Z}_{bb} = \underline{Z}_{cc} = \underline{Z}_s = R_s + \mathrm{j}X_s \\ \underline{Z}_{ab} &= \underline{Z}_{bc} = \underline{Z}_{ac} = \underline{Z}_{ba} = \underline{Z}_{cb} = \underline{Z}_{ca} = \underline{Z}_m = R_m + \mathrm{j}X_m \end{aligned} \tag{1.3}$$

with the self-impedance $\underline{Z}_s$ and the mutual impedance $\underline{Z}_m$. Using the rotating operator

$$\underline{a} = \mathrm{e}^{\mathrm{j}\frac{2}{3}\pi} \tag{1.4}$$

the source voltages can be expressed as follows

$$\begin{aligned}\underline{U}_{\mathrm{q,a}} &= \underline{U}_{\mathrm{q}} \\ \underline{U}_{\mathrm{q,b}} &= \underline{\mathrm{a}}^2\, \underline{U}_{\mathrm{q}} \\ \underline{U}_{\mathrm{q,c}} &= \underline{\mathrm{a}}\, \underline{U}_{\mathrm{q}}\end{aligned} \tag{1.5}$$

So, in a symmetric three-phase system, the impedance matrix is diagonal-cyclic symmetric. Integration of symmetry into eq. (1.1) results in

$$\begin{bmatrix}\underline{U}_{\mathrm{a}} \\ \underline{U}_{\mathrm{b}} \\ \underline{U}_{\mathrm{c}}\end{bmatrix} = \begin{bmatrix}\underline{Z}_{\mathrm{s}} & \underline{Z}_{\mathrm{g}} & \underline{Z}_{\mathrm{g}} \\ \underline{Z}_{\mathrm{g}} & \underline{Z}_{\mathrm{s}} & \underline{Z}_{\mathrm{g}} \\ \underline{Z}_{\mathrm{g}} & \underline{Z}_{\mathrm{g}} & \underline{Z}_{\mathrm{s}}\end{bmatrix} \begin{bmatrix}\underline{I}_{\mathrm{a}} \\ \underline{I}_{\mathrm{b}} \\ \underline{I}_{\mathrm{c}}\end{bmatrix} + \underline{U}_{\mathrm{q}} \begin{bmatrix}1 \\ \underline{\mathrm{a}}^2 \\ \underline{\mathrm{a}}\end{bmatrix} + \underline{U}_{\mathrm{N}} \begin{bmatrix}1 \\ 1 \\ 1\end{bmatrix} \tag{1.6}$$

Using modal components instead of the natural coordinates a, b, c the equation system can be further simplified and potentially decoupled. Transformation of the natural variables $\underline{\boldsymbol{g}}$ into their modal form $\underline{\boldsymbol{g}}_{\mathrm{m}}$ shall be a linear, reversible and unique mapping which results in the following transformation equations

$$\begin{aligned}\underline{\boldsymbol{g}} &= \underline{\boldsymbol{T}}_{\mathrm{m}}\, \underline{\boldsymbol{g}}_{\mathrm{m}} \\ \underline{\boldsymbol{g}}_{\mathrm{m}} &= \underline{\boldsymbol{T}}_{\mathrm{m}}^{-1}\, \underline{\boldsymbol{g}}\end{aligned} \tag{1.7}$$

Expression of $\underline{\boldsymbol{u}}$ and $\underline{\boldsymbol{i}}$ by their modal equivalent in eq. (1.6) results in

$$\underline{\boldsymbol{T}}_{\mathrm{m}}\, \underline{\boldsymbol{u}}_{\mathrm{m}} = \underline{\boldsymbol{Z}}\, \underline{\boldsymbol{T}}_{\mathrm{m}}\, \underline{\boldsymbol{i}}_{\mathrm{m}} + \underline{\boldsymbol{u}}_{\mathrm{q}} + \underline{\boldsymbol{u}}_{\mathrm{N}} \tag{1.8}$$

Eq. (1.8) can be solved for $\underline{\boldsymbol{u}}_{\mathrm{m}}$ due to the reversibility of the transformation process and results in

$$\begin{aligned}\underline{\boldsymbol{u}}_{\mathrm{m}} &= \underline{\boldsymbol{T}}_{\mathrm{m}}^{-1}\, \underline{\boldsymbol{Z}}\, \underline{\boldsymbol{T}}_{\mathrm{m}}\, \underline{\boldsymbol{i}}_{\mathrm{m}} + \underline{\boldsymbol{T}}_{\mathrm{m}}^{-1}\, \underline{\boldsymbol{u}}_{\mathrm{q}} + \underline{\boldsymbol{T}}_{\mathrm{m}}^{-1}\, \underline{\boldsymbol{u}}_{\mathrm{N}} \\ \underline{\boldsymbol{u}}_{\mathrm{m}} &= \quad \underline{\boldsymbol{Z}}_{\mathrm{m}}\, \underline{\boldsymbol{i}}_{\mathrm{m}} \quad + \quad \underline{\boldsymbol{u}}_{\mathrm{q,m}} \quad + \quad \underline{\boldsymbol{u}}_{\mathrm{N,m}}\end{aligned} \tag{1.9}$$

The described procedure is well-known in math science and called reference frame transformation. It aims at the development of a diagonalized system matrix $\underline{\boldsymbol{Z}}_{\mathrm{m}}$, with the eigenvalues of $\underline{\boldsymbol{Z}}$ on its main diagonal. Most of the modal transformations result in such a decoupled system. Depending on the problem formulation and the field of application, different types of modal transformation are applied. The transformation matrices are developed in the following chapters.

1.1 General development of transformation matrices

The transformation matrix $\underline{\boldsymbol{T}}_{\mathrm{m}}$ contains the eigenvectors that correspond to the respective eigenvalues. They form the modal reference frame and therefore need to be orthogonal.

$$\underline{\boldsymbol{T}}_{\mathrm{m}} = k \begin{bmatrix}\underline{t}_{11} & \underline{t}_{12} & \underline{t}_{13} \\ \underline{t}_{21} & \underline{t}_{22} & \underline{t}_{23} \\ \underline{t}_{31} & \underline{t}_{32} & \underline{t}_{33}\end{bmatrix} = k \begin{bmatrix}\underline{\boldsymbol{t}}_1 & \underline{\boldsymbol{t}}_2 & \underline{\boldsymbol{t}}_3\end{bmatrix} \tag{1.10}$$

This means, $\underline{\boldsymbol{t}}_1$, $\underline{\boldsymbol{t}}_2$ and $\underline{\boldsymbol{t}}_3$ must be linearly independent. Otherwise, the inverse of $\underline{\boldsymbol{T}}_{\mathrm{m}}$ cannot be calculated. k is an arbitrary factor other than zero to scale the result.

The eigenvalues of $\underline{\underline{\boldsymbol{Z}}}$ are obtained by solving the characteristic polygon.

$$\det\left(\underline{\underline{\boldsymbol{Z}}} - \underline{\lambda}\,\boldsymbol{E}\right) = \det\left(\begin{bmatrix} \underline{Z}_\mathrm{s} - \underline{\lambda} & \underline{Z}_\mathrm{g} & \underline{Z}_\mathrm{g} \\ \underline{Z}_\mathrm{g} & \underline{Z}_\mathrm{s} - \underline{\lambda} & \underline{Z}_\mathrm{g} \\ \underline{Z}_\mathrm{g} & \underline{Z}_\mathrm{g} & \underline{Z}_\mathrm{s} - \underline{\lambda} \end{bmatrix}\right) = \left(\underline{Z}_\mathrm{s} - \underline{\lambda}\right)^3 - 3\left(\underline{Z}_\mathrm{s} - \underline{\lambda}\right)\underline{Z}_\mathrm{g}^2 + 2\,\underline{Z}_\mathrm{g}^3 = 0 \quad (1.11)$$

Solving eq. (1.11) results in three eigenvalues, whereof one eigenvalue is double.

$$\begin{aligned} \underline{\lambda}_1 &= \underline{Z}_\mathrm{s} - \underline{Z}_\mathrm{g} \\ \underline{\lambda}_2 &= \underline{Z}_\mathrm{s} - \underline{Z}_\mathrm{g} \\ \underline{\lambda}_3 &= \underline{Z}_\mathrm{s} + 2\,\underline{Z}_\mathrm{g} \end{aligned} \quad (1.12)$$

As described above, for each eigenvalue an eigenvector needs to be found. For $\underline{\lambda}_1$ this results in

$$\left(\underline{\underline{\boldsymbol{Z}}} - \underline{\lambda}_1\,\boldsymbol{E}\right)\underline{\boldsymbol{t}}_1 = \begin{bmatrix} \underline{Z}_\mathrm{g} & \underline{Z}_\mathrm{g} & \underline{Z}_\mathrm{g} \\ \underline{Z}_\mathrm{g} & \underline{Z}_\mathrm{g} & \underline{Z}_\mathrm{g} \\ \underline{Z}_\mathrm{g} & \underline{Z}_\mathrm{g} & \underline{Z}_\mathrm{g} \end{bmatrix} \begin{bmatrix} \underline{t}_{11} \\ \underline{t}_{21} \\ \underline{t}_{31} \end{bmatrix} = \begin{bmatrix} 0 \\ 0 \\ 0 \end{bmatrix} \quad (1.13)$$

It is obvious, that there is no unique solution. In fact, every vector will be suitable, if their coefficients sum up to zero.

$$\underline{t}_{11} + \underline{t}_{21} + \underline{t}_{31} = 0 \quad (1.14)$$

The same solution is obtained for $\underline{\lambda}_2$

$$\underline{t}_{12} + \underline{t}_{22} + \underline{t}_{32} = 0 \quad (1.15)$$

Insertion of $\underline{\lambda}_3$ results in

$$\left(\underline{\underline{\boldsymbol{Z}}} - \underline{\lambda}_3\,\boldsymbol{E}\right)\underline{\boldsymbol{t}}_3 = \underline{Z}_\mathrm{g} \begin{bmatrix} -2 & 1 & 1 \\ 1 & -2 & 1 \\ 1 & 1 & -2 \end{bmatrix} \begin{bmatrix} \underline{t}_{13} \\ \underline{t}_{23} \\ \underline{t}_{33} \end{bmatrix} = \begin{bmatrix} 0 \\ 0 \\ 0 \end{bmatrix} \quad (1.16)$$

In this case, too, a unique solution cannot be found. Besides an infinite number of possible solutions, e.g. eigenvectors whose coefficients are all equal, are suitable.

$$\underline{t}_{13} = \underline{t}_{23} = \underline{t}_{33} \quad (1.17)$$

So, any arbitrary but invertible matrix that complies with eq. (1.14), (1.15) and (1.17) can be used as transformation matrix. In eq. (1.14) and eq. (1.15) two parameters can be chosen, in eq. (1.17) only one. Still, the eigenvectors of $\underline{\lambda}_1$ and $\underline{\lambda}_2$ must stay linearly independent to keep the transformation matrix invertible.

1.2 Calculation of powers in modal components

The overall power of the electric energy system is calculated by the sum of the powers of each component in the system. In natural coordinates this is

$$\underline{S} = \underline{U}_\mathrm{a}\ \underline{I}_\mathrm{a}^* + \underline{U}_\mathrm{b}\ \underline{I}_\mathrm{b}^* + \underline{U}_\mathrm{c}\ \underline{I}_\mathrm{c}^* = \underline{\boldsymbol{u}}^\mathrm{T}\ \underline{\boldsymbol{i}}^* \tag{1.18}$$

and in modal components

$$\underline{S}_\mathrm{m} = \underline{\boldsymbol{u}}_\mathrm{m}^\mathrm{T}\ \underline{\boldsymbol{i}}_\mathrm{m}^* \tag{1.19}$$

Keeping the power constant before and after the transformation between component systems results in

$$\underline{S} = \underline{S}_\mathrm{m} \tag{1.20}$$

Expression of the natural component system as a function of modal variables results in

$$\left(\underline{\boldsymbol{T}}_\mathrm{m}\ \underline{\boldsymbol{u}}_\mathrm{m}\right)^\mathrm{T}\left(\underline{\boldsymbol{T}}_\mathrm{m}\ \underline{\boldsymbol{i}}_\mathrm{m}\right)^* = \underline{\boldsymbol{u}}_\mathrm{m}^\mathrm{T}\ \underline{\boldsymbol{T}}_\mathrm{m}^\mathrm{T}\ \underline{\boldsymbol{T}}_\mathrm{m}^*\ \underline{\boldsymbol{i}}_\mathrm{m}^* \overset{!}{=} \underline{\boldsymbol{u}}_\mathrm{m}^\mathrm{T}\ \underline{\boldsymbol{i}}_\mathrm{m}^* \tag{1.21}$$

This is only possible, if

$$\underline{\boldsymbol{T}}_\mathrm{m}^\mathrm{T}\ \underline{\boldsymbol{T}}_\mathrm{m}^* = \boldsymbol{E} \tag{1.22}$$

and can be realized by choosing a suitable factor k in eq. (1.10). In this case, the transformation matrix is invariant to powers. It is important to mention, that most transformations are not invariant to powers.

1.3 Most common modal components

In practice, only a couple of modal component systems are used, because only they offer the aspired advantages for their specific field of application. Steady-state power system analysis is usually based on symmetrical components, while e.g. power electronics engineering often uses Clarke-Transformation for modelling and control purposes. Drives and generators – especially synchronous machines – are best described using Park-Transformation.

1.3.1 Symmetrical components

Symmetrical components were introduced in 1918 by Charles Legeyt Fortescue. He proved, that any random unsymmetrical n-phase system can be expressed as a sum of n symmetrical separate components. Its transformation matrix

$$\underline{\boldsymbol{T}}_\mathrm{m} = k\begin{bmatrix} 1 & 1 & 1 \\ \underline{\mathrm{a}}^2 & \underline{\mathrm{a}} & 1 \\ \underline{\mathrm{a}} & \underline{\mathrm{a}}^2 & 1 \end{bmatrix} \tag{1.23}$$

shows, that the eigenvector of $\underline{\lambda}_1$ describes a symmetrical system, whose sequence $1 \rightarrow \underline{\mathrm{a}}^2 \rightarrow \underline{\mathrm{a}}$ is in line with the natural phase sequence. It is therefore called “positive sequence system”. The eigenvector of $\underline{\lambda}_2$ describes a system, whose sequence $1 \rightarrow \underline{\mathrm{a}} \rightarrow \underline{\mathrm{a}}^2$ is counter-rotating. It is therefore called „negative sequence system“. The eigenvector of $\underline{\lambda}_3$ shows no rotation. It is

therefore called „zero sequence system“. Due to its special behavior it is no longer indexed 3 but gets the index 0 instead. If k is chosen to be one, this results in

$$\underline{\boldsymbol{T}}_{\mathrm{SK}} = \begin{bmatrix} 1 & 1 & 1 \\ \underline{a}^2 & \underline{a} & 1 \\ \underline{a} & \underline{a}^2 & 1 \end{bmatrix} \qquad \underline{\boldsymbol{T}}_{\mathrm{SK}}^{-1} = \frac{1}{3}\begin{bmatrix} 1 & \underline{a} & \underline{a}^2 \\ 1 & \underline{a}^2 & \underline{a} \\ 1 & 1 & 1 \end{bmatrix} = \frac{1}{3}\left(\underline{\boldsymbol{T}}_{\mathrm{SK}}^{*}\right)^{\mathrm{T}} \tag{1.24}$$

Symmetrical component transformation shall now be applied to eq. (1.9). The source voltages are transformed into

$$\underline{\boldsymbol{u}}_{\mathrm{q,m}} = \frac{1}{3}\begin{bmatrix} 1 & \underline{a} & \underline{a}^2 \\ 1 & \underline{a}^2 & \underline{a} \\ 1 & 1 & 1 \end{bmatrix}\begin{bmatrix} 1 \\ \underline{a}^2 \\ \underline{a} \end{bmatrix}\underline{U}_{\mathrm{q}} = \begin{bmatrix} \underline{U}_{\mathrm{q}} \\ 0 \\ 0 \end{bmatrix} \tag{1.25}$$

and the neutral point voltage

$$\underline{\boldsymbol{u}}_{\mathrm{N,m}} = \frac{1}{3}\begin{bmatrix} 1 & \underline{a} & \underline{a}^2 \\ 1 & \underline{a}^2 & \underline{a} \\ 1 & 1 & 1 \end{bmatrix}\begin{bmatrix} 1 \\ 1 \\ 1 \end{bmatrix}\underline{U}_{\mathrm{N}} = \begin{bmatrix} 0 \\ 0 \\ \underline{U}_{\mathrm{N}} \end{bmatrix} \tag{1.26}$$

Finally, the result is

$$\begin{bmatrix} \underline{U}_1 \\ \underline{U}_2 \\ \underline{U}_0 \end{bmatrix} = \begin{bmatrix} \underline{Z}_1 & & \\ & \underline{Z}_2 & \\ & & \underline{Z}_0 \end{bmatrix}\begin{bmatrix} \underline{I}_1 \\ \underline{I}_2 \\ \underline{I}_0 \end{bmatrix} + \begin{bmatrix} \underline{U}_{\mathrm{q}} \\ 0 \\ 0 \end{bmatrix} + \begin{bmatrix} 0 \\ 0 \\ \underline{U}_{\mathrm{N}} \end{bmatrix} \tag{1.27}$$

Eq. (1.27) shows the special advantage of symmetrical components. In a non-faulty, balanced state, negative and zero sequence systems are passive and do not need to be calculated. This is due to the negative sequence system does not contain sources and $\underline{U}_{\mathrm{N}}$ is only other than zero, if the sum of $\underline{I}_{\mathrm{a}}$, $\underline{I}_{\mathrm{b}}$ and $\underline{I}_{\mathrm{c}}$ is other than zero. So, in a non-faulty state, it is sufficient to only consider the positive sequence system. Only in the case of faults or unbalanced operation points, consideration of negative and zero sequence systems is necessary.

Another advantage of symmetrical components is, that they are invariant to the reference phase. In a balanced operation point negative and zero sequence systems are passive, resulting in

$$\begin{bmatrix} \underline{G}_{\mathrm{a}} \\ \underline{G}_{\mathrm{b}} \\ \underline{G}_{\mathrm{c}} \end{bmatrix} = \begin{bmatrix} 1 & 1 & 1 \\ \underline{a}^2 & \underline{a} & 1 \\ \underline{a} & \underline{a}^2 & 1 \end{bmatrix}\begin{bmatrix} \underline{G}_1 \\ 0 \\ 0 \end{bmatrix} = \begin{bmatrix} \underline{G}_1 \\ \underline{a}^2\,\underline{G}_1 \\ \underline{a}\,\underline{G}_1 \end{bmatrix} \tag{1.28}$$

This means, currents and voltages of the positive sequence system correspond to the currents and voltages of the reference phase “a”. Interpretation of symmetrical components is therefore very easy. Nevertheless, it is important to keep in mind, that

$$\underline{\boldsymbol{T}}_{\mathrm{SK}}^{\mathrm{T}}\,\underline{\boldsymbol{T}}_{\mathrm{SK}}^{*}=\begin{bmatrix}1 & \underline{\mathrm{a}}^{2} & \underline{\mathrm{a}}\\ 1 & \underline{\mathrm{a}} & \underline{\mathrm{a}}^{2}\\ 1 & 1 & 1\end{bmatrix}\begin{bmatrix}1 & 1 & 1\\ \underline{\mathrm{a}} & \underline{\mathrm{a}}^{2} & 1\\ \underline{\mathrm{a}}^{2} & \underline{\mathrm{a}} & 1\end{bmatrix}=\begin{bmatrix}3 & 0 & 0\\ 0 & 3 & 0\\ 0 & 0 & 3\end{bmatrix}=3\,\boldsymbol{E} \tag{1.29}$$

That means, electric power in natural coordinates is three times higher compared to the symmetrical components. Thus, using the given transformation matrix they are not invariant to power. To obtain a power invariant transformation system, it is necessary to set the factor $k=\sqrt{3}$. Unfortunately, this would lead to currents and voltages that are $\sqrt{3}$ times higher compared to the real system. Thus, invariance to the reference phase would be lost. That is why in practice, usually the reference phase invariant transformation is used.

Eq. (1.27) shows that in a non-faulty state, positive, negative and zero sequence system, are decoupled and can be calculated independently.

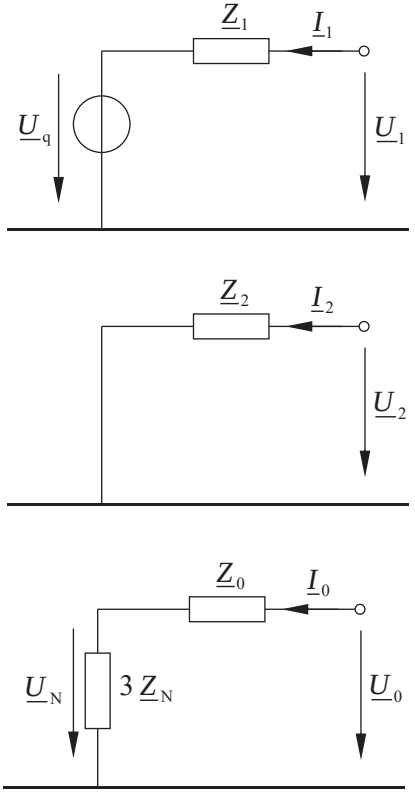

Fig. 2: graphical interpretation of symmetrical components

The neutral point impedance is only considered in the zero-sequence system. It is multiplied with the factor 3 due to

$$\underline{U}_\mathrm{N}=\underline{Z}_\mathrm{N}\,\underline{I}_\mathrm{N}=\underline{Z}_\mathrm{N}\left(\underline{I}_\mathrm{a}+\underline{I}_\mathrm{b}+\underline{I}_\mathrm{c}\right)=\underline{Z}_\mathrm{N}\,3\,\underline{I}_0 \tag{1.30}$$

1.3.2 Diagonal components (Clarke-Transformation)

Diagonal components or $\alpha,\beta,0$-components have been developed by Edith Clarke. With the factor $k=1$ he following transformation matrices are obtained

$$\boldsymbol{T}_{\mathrm{D}}=\begin{bmatrix}1 & 0 & 1\\ -\frac{1}{2} & \frac{\sqrt{3}}{2} & 1\\ -\frac{1}{2} & -\frac{\sqrt{3}}{2} & 1\end{bmatrix}\qquad \boldsymbol{T}_{\mathrm{D}}^{-1}=\frac{1}{3}\begin{bmatrix}2 & -1 & -1\\ 0 & \sqrt{3} & -\sqrt{3}\\ 1 & 1 & 1\end{bmatrix} \tag{1.31}$$

The coefficients can be easily explained by putting the natural coordinate system into a complex-valued plane described by α - und β - vectors.

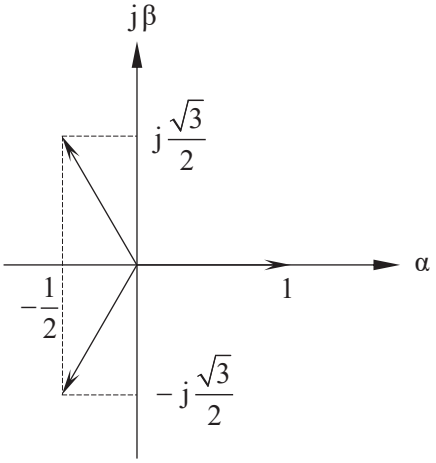

Fig. 3: complex-valued reference frame of diagonal components

The first column of $\boldsymbol{T}_{\mathrm{D}}$ corresponds to the real part of the first column of $\underline{\boldsymbol{T}}_{\mathrm{SK}}$ and the second column of $\boldsymbol{T}_{\mathrm{D}}$ corresponds to the imaginary part of the second column of $\underline{\boldsymbol{T}}_{\mathrm{SK}}$.

Clarke-Transformation shall now be applied to eq. (1.9). With the source voltages

$$\underline{\boldsymbol{u}}_{\mathrm{q,D}}=\frac{1}{3}\begin{bmatrix}2 & -1 & -1\\ 0 & \sqrt{3} & -\sqrt{3}\\ 1 & 1 & 1\end{bmatrix}\begin{bmatrix}1\\ \underline{\mathrm{a}}^2\\ \underline{\mathrm{a}}\end{bmatrix}\underline{U}_{\mathrm{q}}=\begin{bmatrix}\underline{U}_{\mathrm{q}}\\ -\mathrm{j}\underline{U}_{\mathrm{q}}\\ 0\end{bmatrix}=\begin{bmatrix}\underline{U}_{\mathrm{q},\alpha}\\ \underline{U}_{\mathrm{q},\beta}\\ 0\end{bmatrix} \tag{1.32}$$

And the neutral point voltages

$$\underline{\boldsymbol{u}}_{\mathrm{N,D}}=\frac{1}{3}\begin{bmatrix}2 & -1 & -1\\ 0 & \sqrt{3} & -\sqrt{3}\\ 1 & 1 & 1\end{bmatrix}\begin{bmatrix}1\\ 1\\ 1\end{bmatrix}\underline{U}_{\mathrm{N}}=\begin{bmatrix}0\\ 0\\ \underline{U}_{\mathrm{N}}\end{bmatrix} \tag{1.33}$$

This results in the following equation system

$$\begin{bmatrix}\underline{U}_{\alpha}\\ \underline{U}_{\beta}\\ \underline{U}_{0}\end{bmatrix}=\begin{bmatrix}\underline{Z}_{\alpha} & & \\ & \underline{Z}_{\beta} & \\ & & \underline{Z}_{0}\end{bmatrix}\begin{bmatrix}\underline{I}_{\alpha}\\ \underline{I}_{\beta}\\ \underline{I}_{0}\end{bmatrix}+\begin{bmatrix}\underline{U}_{\mathrm{q},\alpha}\\ \underline{U}_{\mathrm{q},\beta}\\ 0\end{bmatrix}+\begin{bmatrix}0\\ 0\\ \underline{U}_{\mathrm{N}}\end{bmatrix} \tag{1.34}$$

The impedance matrix is identical to the symmetrical components. Nevertheless, two significant differences are obvious:

- The transformation matrices are real-valued.
- A single-component system description is not possible anymore. Generally, sources are active in the α - and the β - component.

As already known from the symmetrical components, the transformation leads to three decoupled systems that can be analyzed independently. The neutral point impedance is again only considered in the zeros sequence system.

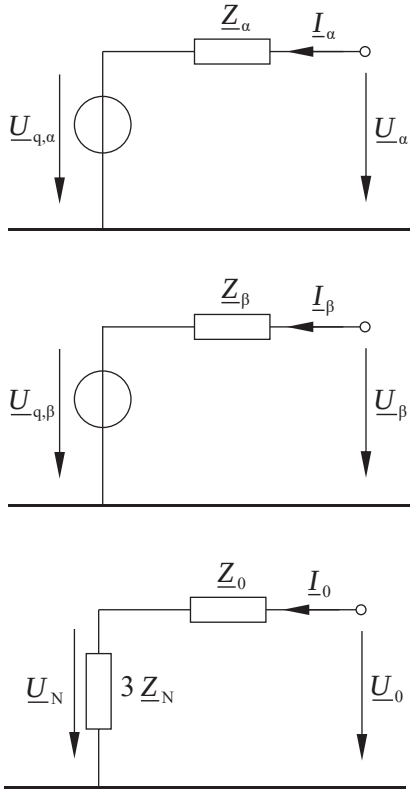

Fig. 4: diagonal components

1.3.3 Other transformation methods

Symmetrical components and diagonal components have in common, that their transformation matrices have constant coefficients. This is not always advantageous, e.g. to model the rotor of a synchronous generator, it is more useful to apply a rotating transformation. This leads to a time-variant transformation matrix but also to constant modal values. This dq0-transformation has been developed by Robert H. Park.

Finally, symmetrical components are only valid to describe steady-state, base frequency models. To model multi-frequency, dynamic performances, space-phasor transformations are needed, which again can be based on steady or rotating reference frames. In fact, it can be shown, that symmetrical components are a special case of the general space-phasor transformation.

1.4 Summary of transformation matrices

Table 1: invariant to reference phase

	$\begin{bmatrix} \underline{g}_a \\ \underline{g}_b \\ \underline{g}_c \end{bmatrix}$	$\begin{bmatrix} \underline{g}_1 \\ \underline{g}_2 \\ \underline{g}_0 \end{bmatrix}$	$\begin{bmatrix} \underline{g}_\alpha \\ \underline{g}_\beta \\ \underline{g}_0 \end{bmatrix}$
$\begin{bmatrix} \underline{g}_a \\ \underline{g}_b \\ \underline{g}_c \end{bmatrix} =$	$\begin{bmatrix} 1 & & \\ & 1 & \\ & & 1 \end{bmatrix}$	$\begin{bmatrix} 1 & 1 & 1 \\ \underline{a}^2 & \underline{a} & 1 \\ \underline{a} & \underline{a}^2 & 1 \end{bmatrix}$	$\frac{1}{2}\begin{bmatrix} 2 & 0 & 2 \\ -1 & \sqrt{3} & 2 \\ -1 & -\sqrt{3} & 2 \end{bmatrix}$
$\begin{bmatrix} \underline{g}_1 \\ \underline{g}_2 \\ \underline{g}_0 \end{bmatrix} =$	$\frac{1}{3}\begin{bmatrix} 1 & \underline{a} & \underline{a}^2 \\ 1 & \underline{a}^2 & \underline{a} \\ 1 & 1 & 1 \end{bmatrix}$	$\begin{bmatrix} 1 & & \\ & 1 & \\ & & 1 \end{bmatrix}$	$\frac{1}{2}\begin{bmatrix} 1 & j & 0 \\ 1 & -j & 0 \\ 0 & 0 & 2 \end{bmatrix}$
$\begin{bmatrix} \underline{g}_\alpha \\ \underline{g}_\beta \\ \underline{g}_0 \end{bmatrix} =$	$\frac{1}{3}\begin{bmatrix} 2 & -1 & -1 \\ 0 & \sqrt{3} & -\sqrt{3} \\ 1 & 1 & 1 \end{bmatrix}$	$\begin{bmatrix} 1 & 1 & 0 \\ -j & j & 0 \\ 0 & 0 & 1 \end{bmatrix}$	$\begin{bmatrix} 1 & & \\ & 1 & \\ & & 1 \end{bmatrix}$

Table 2: invariant to power

	$\begin{bmatrix} \underline{g}_a \\ \underline{g}_b \\ \underline{g}_c \end{bmatrix}$	$\begin{bmatrix} \underline{g}_1 \\ \underline{g}_2 \\ \underline{g}_0 \end{bmatrix}$	$\begin{bmatrix} \underline{g}_\alpha \\ \underline{g}_\beta \\ \underline{g}_0 \end{bmatrix}$
$\begin{bmatrix} \underline{g}_a \\ \underline{g}_b \\ \underline{g}_c \end{bmatrix} =$	$\begin{bmatrix} 1 & & \\ & 1 & \\ & & 1 \end{bmatrix}$	$\frac{1}{\sqrt{3}}\begin{bmatrix} 1 & 1 & 1 \\ \underline{a}^2 & \underline{a} & 1 \\ \underline{a} & \underline{a}^2 & 1 \end{bmatrix}$	$\frac{1}{\sqrt{6}}\begin{bmatrix} 2 & 0 & \sqrt{2} \\ -1 & \sqrt{3} & \sqrt{2} \\ -1 & -\sqrt{3} & \sqrt{2} \end{bmatrix}$
$\begin{bmatrix} \underline{g}_1 \\ \underline{g}_2 \\ \underline{g}_0 \end{bmatrix} =$	$\frac{1}{\sqrt{3}}\begin{bmatrix} 1 & \underline{a} & \underline{a}^2 \\ 1 & \underline{a}^2 & \underline{a} \\ 1 & 1 & 1 \end{bmatrix}$	$\begin{bmatrix} 1 & & \\ & 1 & \\ & & 1 \end{bmatrix}$	$\frac{1}{\sqrt{2}}\begin{bmatrix} 1 & j & 0 \\ 1 & -j & 0 \\ 0 & 0 & \sqrt{2} \end{bmatrix}$
$\begin{bmatrix} \underline{g}_\alpha \\ \underline{g}_\beta \\ \underline{g}_0 \end{bmatrix} =$	$\frac{1}{\sqrt{6}}\begin{bmatrix} 2 & -1 & -1 \\ 0 & \sqrt{3} & -\sqrt{3} \\ \sqrt{2} & \sqrt{2} & \sqrt{2} \end{bmatrix}$	$\frac{1}{\sqrt{2}}\begin{bmatrix} 1 & 1 & 0 \\ -j & j & 0 \\ 0 & 0 & \sqrt{2} \end{bmatrix}$	$\begin{bmatrix} 1 & & \\ & 1 & \\ & & 1 \end{bmatrix}$

2 Modelling of equipment

To model processes and calculate states of electric power systems, a systematic description of grid topology and the physical behavior of all the assets is necessary. Different approaches are available, especially graph theory and multipole theory. For the purpose of steady-state and quasi steady-state grid analysis, the latter offers a couple of advantages, namely:

- Equipment matrices are usually smaller.
- Input and output variables of the equipment equation systems are values that can be directly measured in real grids. Using graph theory, these original terminal values of the equipment need to be calculated first by superposing branch values.
- It is not necessary to (arbitrarily) define directions of branches. Therefore, all solutions are unique.

It is assumed, that all assets are built in a symmetric way. So, it is sufficient to only consider the positive sequence system. Symmetry can be achieved by appropriate construction of the asset or is suitably reached by twisting phases in case of overhead lines.

Multipole theory considers each single piece of equipment a black box with a specific amount of connection points. At these terminals currents and voltages can be directly measured. By doing so, measurement possibilities are modelled very realistic, for the terminal values e.g. at both ends of a cable are exactly the values that can be measured in physical grids, too, whereas voltages and currents inside of the cable e.g. capacitive shunt currents, cannot be directly measured during system operation and need to be calculated. As a general convention, loads are counted positive. Therefore, currents always point into the asset at each terminal and voltages are pointing from phase to ground. For the purpose of steady-state grid analysis, most of the equipment can be described using a linear model due to there is a linear dependency of voltages and currents. Therefore, the physical behavior of the asset is described using a linear equation system. Its size depends on the number of terminals.

In the following, nodal and terminal values need to be separated. Therefore, the index K is used to describe nodal values and index T is used to describe terminal values.

2.1 Dipoles

The general black box representation of a dipole is given in Fig. 5.

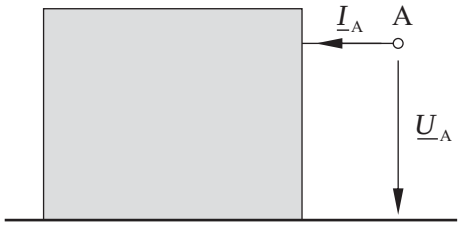

Fig. 5: general model of a dipole

The dipole is characterized by one pair of terminals, whereof one terminal is grounded and therefore not explicitly indexed. The terminal voltage $\underline{U}_A$ can be found between ground and the other terminal which is indexed A.

Due to the linear dependency between terminal voltage and current, the behavior of the diploe can be expressed by a linear equation.

$$\underline{I}_\mathrm{A} = \underline{Y}_\mathrm{A}\,\underline{U}_\mathrm{A} + \underline{I}_\mathrm{q} \tag{2.1}$$

The general equivalent circuit of the dipole can be found in Fig. 6.

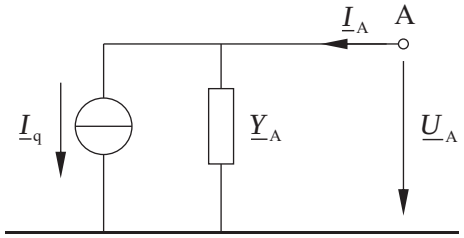

Fig. 6: general equivalent circuit of a dipole

Dipoles are:

- Synchronous and asynchronous machines
- Grid equivalents
- Loads
- Shunt compensators (capacitor banks and reactors)

In case of a synchronous machine

$$\underline{Y}_\mathrm{A} = \frac{1}{R_\mathrm{a} + \mathrm{j}X_\mathrm{d}} \tag{2.2}$$

and

$$\underline{I}_\mathrm{q} = \underline{Y}_\mathrm{A}\,\underline{U}_\mathrm{p} \tag{2.3}$$

2.2 Quadrupoles

The general black box representation of a quadrupole is given in Fig. 7.

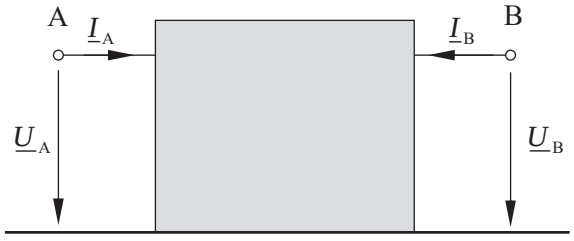

Fig. 7: general representation of a quadrupole

The Quadrupole has two independent terminals (A and B), which results in a 2nd order linear equation system with the equipment admittance matrix $\underline{\boldsymbol{Y}}_\mathrm{T,BM}$.

$$\begin{bmatrix} \underline{I}_\mathrm{A} \\ \underline{I}_\mathrm{B} \end{bmatrix} = \begin{bmatrix} \underline{Y}_\mathrm{AA} & \underline{Y}_\mathrm{AB} \\ \underline{Y}_\mathrm{BA} & \underline{Y}_\mathrm{BB} \end{bmatrix} \begin{bmatrix} \underline{U}_\mathrm{A} \\ \underline{U}_\mathrm{B} \end{bmatrix} \tag{2.4}$$

$$\underline{\boldsymbol{i}}_\mathrm{T,BM} = \quad \underline{\boldsymbol{Y}}_\mathrm{T,BM} \quad \underline{\boldsymbol{u}}_\mathrm{T,BM}$$

Quadrupoles represent lines (overhead lines and cables) as well as two-winding transformers. These assets do not have internal sources, so modelling of a current source is unnecessary. In

the following chapters the coefficients of the admittance matrix of lines and transformers are derived.

2.2.1 Lines

The general equivalent circuit diagram of a line with concentrated parameters is given in Fig. 8. Due to its form it is often called π-equivalent-circuit.

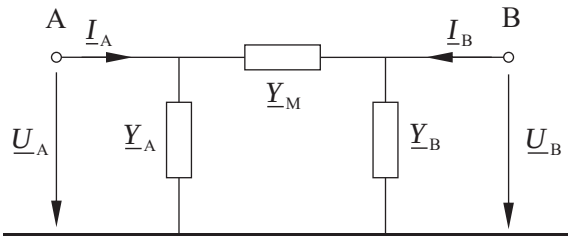

Fig. 8: equivalent circuit diagram of a line

The admittances are calculated as follows

$$\begin{aligned} \underline{Y}_A &= \underline{Y}_B = \frac{1}{2}\left(G + \mathrm{j}\omega C\right) \\ \underline{Y}_M &= \frac{1}{R + \mathrm{j}X} \end{aligned} \tag{2.5}$$

Application of 1st Kirchhoff's law at the left and right branching points results in

$$\begin{bmatrix} \underline{I}_A \\ \underline{I}_B \end{bmatrix} = \begin{bmatrix} \underline{Y}_A + \underline{Y}_M & -\underline{Y}_M \\ -\underline{Y}_M & \underline{Y}_B + \underline{Y}_M \end{bmatrix} \begin{bmatrix} \underline{U}_A \\ \underline{U}_B \end{bmatrix} \tag{2.6}$$

So, the coefficients of the admittance matrix of a line are found. $\underline{Y}_A$, $\underline{Y}_B$ and $\underline{Y}_M$ can be easily derived from the line length l and the resistance loads per unit length.

$$\begin{aligned} R &= r' \, l \\ X &= x' \, l \\ C &= c' \, l \\ G &= g' \, l \end{aligned} \tag{2.7}$$

2.2.2 Two-winding transformer

The general equivalent circuit diagram of a two-winding transformer is given in Fig. 9. Due to its form it is often called T-equivalent circuit. Without loss of generality it is assumed, that the winding at terminal B is regulated and the elements of the equivalent circuit of winding B are related to the rated voltage of winding A. Back-transformation of the related voltages and currents is done using an ideal transformer with the transformation ratio $\underline{\tau}$ which is also used to model regulation, tap changing and phase shifting.

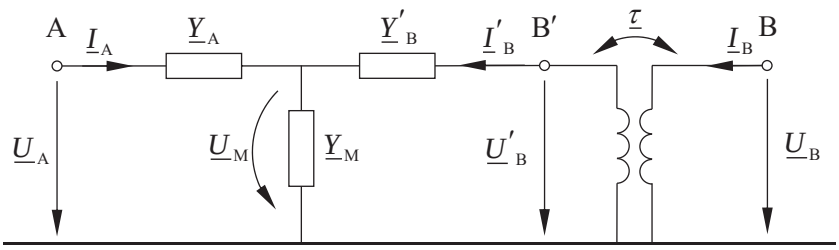

Fig. 9: equivalent circuit diagram of a two-winding transformer

The admittances are calculated as follows

$$\begin{aligned} \underline{Y}_A &= \frac{1}{R_A + jX_A} \\ \underline{Y}'_B &= \frac{1}{R'_B + jX'_B} \\ \underline{Y}_M &= \frac{1}{R_{Fe}} + \frac{1}{jX_h} \end{aligned} \tag{2.8}$$

$\underline{I}_A$ and $\underline{I}'_B$ can be expressed as a function of $\underline{U}_A$, $\underline{U}'_B$ and $\underline{U}_M$.

$$\begin{aligned} \underline{I}_A &= \underline{Y}_A \left(\underline{U}_A - \underline{U}_M\right) \\ \underline{I}'_B &= \underline{Y}'_B \left(\underline{U}'_B - \underline{U}_M\right) \end{aligned} \tag{2.9}$$

Additional application of the 1st Kirchhoff's law at the branching point in the equivalent circuit results in

$$-\underline{I}_A - \underline{I}'_B + \underline{Y}_M \, \underline{U}_M = 0 \tag{2.10}$$

Eq. (2.9) and eq. (2.10) form a linear equation system

$$\begin{bmatrix} \underline{I}_A \\ \underline{I}'_B \\ 0 \end{bmatrix} = \begin{bmatrix} \underline{Y}_A & 0 & -\underline{Y}_A \\ 0 & \underline{Y}'_B & -\underline{Y}'_B \\ -\underline{Y}_A & -\underline{Y}'_B & \underline{Y}_A + \underline{Y}'_B + \underline{Y}_M \end{bmatrix} \begin{bmatrix} \underline{U}_A \\ \underline{U}'_B \\ \underline{U}_M \end{bmatrix} \tag{2.11}$$

Eq. (2.11) still does not have the aspired 2x2 form. With $\underline{U}_M$ the equation system still contains an inner voltage of the transformer which needs to be eliminated. Therefore, the last equation is solved for $\underline{U}_M$, so $\underline{U}_M$ can be expressed as a function of $\underline{U}_A$ and $\underline{U}'_B$.

$$\underline{U}_M = \frac{1}{\underline{Y}_A + \underline{Y}'_B + \underline{Y}_M} \begin{bmatrix} \underline{Y}_A & \underline{Y}'_B \end{bmatrix} \begin{bmatrix} \underline{U}_A \\ \underline{U}'_B \end{bmatrix} \tag{2.12}$$

Insertion of eq. (2.12) in the two upper equations of eq. (2.11) results in

$$\begin{bmatrix} \underline{I}_A \\ \underline{I}'_B \end{bmatrix} = \frac{1}{\underline{Y}_A + \underline{Y}'_B + \underline{Y}_M} \begin{bmatrix} \underline{Y}_A \left(\underline{Y}'_B + \underline{Y}_M\right) & -\underline{Y}_A \, \underline{Y}'_B \\ -\underline{Y}_A \, \underline{Y}'_B & \underline{Y}'_B \left(\underline{Y}_A + \underline{Y}_M\right) \end{bmatrix} \begin{bmatrix} \underline{U}_A \\ \underline{U}'_B \end{bmatrix} \tag{2.13}$$

It is aspired to calculate with the actual voltages and currents which means, the related voltages and currents need to be eliminated. Therefore, the transformation ratio needs to be integrated into the equipment admittance matrix. This is done by

$$\underline{U}'_{\mathrm{B}} = \underline{\tau}\,\underline{U}_{\mathrm{B}} \tag{2.14}$$

with

$$\underline{\tau} = \frac{U_{\mathrm{r,T,A}}}{U_{\mathrm{r,T,B}}}\,\rho\,\mathrm{e}^{\mathrm{j}\left(\frac{\pi}{6}k+\alpha\right)} \tag{2.15}$$

ρ represents the change of voltage magnitude evoked by transformer tapping. It is related to the terminal A nominal voltage. α is the respective change in phase and k is a constant phase shift which is given by the transformer vector group. E.g. $k = 5$ at an Yd5 transformer. An ideal transformer has no losses, so

$$\underline{S}'_{\mathrm{B}} = \underline{S}_{\mathrm{B}} \tag{2.16}$$

Therefore

$$\underline{I}'_{\mathrm{B}} = \frac{1}{\underline{\tau}^{*}}\,\underline{I}_{\mathrm{B}} \tag{2.17}$$

Integration of eq. (2.14) and eq. (2.17) in eq. (2.13) results in

$$\begin{bmatrix}\underline{I}_{\mathrm{A}}\\ \underline{I}_{\mathrm{B}}\end{bmatrix} = \frac{1}{\underline{Y}_{\mathrm{A}}+\underline{Y}'_{\mathrm{B}}+\underline{Y}_{\mathrm{M}}}\begin{bmatrix}\underline{Y}_{\mathrm{A}}\left(\underline{Y}'_{\mathrm{B}}+\underline{Y}_{\mathrm{M}}\right) & -\underline{\tau}\,\underline{Y}_{\mathrm{A}}\,\underline{Y}'_{\mathrm{B}}\\ -\underline{\tau}^{*}\underline{Y}_{\mathrm{A}}\,\underline{Y}'_{\mathrm{B}} & |\underline{\tau}|^{2}\,\underline{Y}'_{\mathrm{B}}\left(\underline{Y}_{\mathrm{A}}+\underline{Y}_{\mathrm{M}}\right)\end{bmatrix}\begin{bmatrix}\underline{U}_{\mathrm{A}}\\ \underline{U}_{\mathrm{B}}\end{bmatrix} \tag{2.18}$$

So, the coefficients of the admittance matrix of a two-winding transformer are found. $\underline{Y}_{\mathrm{A}}$ and $\underline{Y}'_{\mathrm{B}}$ are obtained from a short-circuit test

$$R_{\mathrm{A}} = R'_{\mathrm{B}} = \frac{1}{2}\,\frac{P_{\mathrm{V,k}}}{3\,I^{2}_{\mathrm{r,T,A}}} \tag{2.19}$$

$$X_{\mathrm{A}} = X'_{\mathrm{B}} = \frac{1}{2}\sqrt{\left(u_{\mathrm{k}}\,\frac{U_{\mathrm{r,T,A}}}{\sqrt{3}\,I_{\mathrm{r,T,A}}}\right)^{2} - \left(\frac{P_{\mathrm{V,k}}}{3\,I^{2}_{\mathrm{r,T,A}}}\right)^{2}} \approx \frac{1}{2}\,u_{\mathrm{k}}\,\frac{U_{\mathrm{r,T,A}}}{\sqrt{3}\,I_{\mathrm{r,T,A}}} \tag{2.20}$$

$\underline{Y}_{\mathrm{M}}$ is obtained from an open-loop test

$$R_{\mathrm{Fe}} \approx \frac{U^{2}_{\mathrm{r,T,A}}}{P_{\mathrm{V,0}}} \tag{2.21}$$

$$X_{\mathrm{h}} \approx \frac{U_{\mathrm{r,T,A}}}{\sqrt{3}\,I_{\mathrm{0,A}}} \tag{2.22}$$

2.3 Sextupoles

The general black box representation of a sextupole is given in Fig. 10.

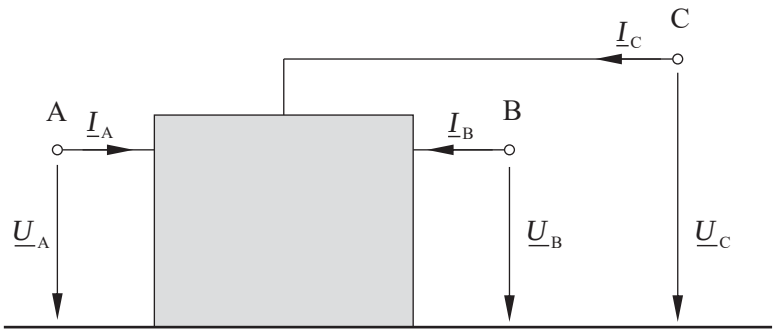

Fig. 10: general equivalent circuit diagram of a sextupole

It is used to model three-winding transformers. Its physical behavior is described by a third order linear equation system.

$$\begin{bmatrix} \underline{I}_A \\ \underline{I}_B \\ \underline{I}_C \end{bmatrix} = \begin{bmatrix} \underline{Y}_{AA} & \underline{Y}_{AB} & \underline{Y}_{AC} \\ \underline{Y}_{BA} & \underline{Y}_{BB} & \underline{Y}_{BC} \\ \underline{Y}_{CA} & \underline{Y}_{CB} & \underline{Y}_{CC} \end{bmatrix} \begin{bmatrix} \underline{U}_A \\ \underline{U}_B \\ \underline{U}_C \end{bmatrix} \tag{2.23}$$

The coefficients of the equipment admittance matrix are calculated the exact same way as shown for the two-winding transformer.

2.4 Octopoles

The general black box representation of an octopole is given in Fig. 11.

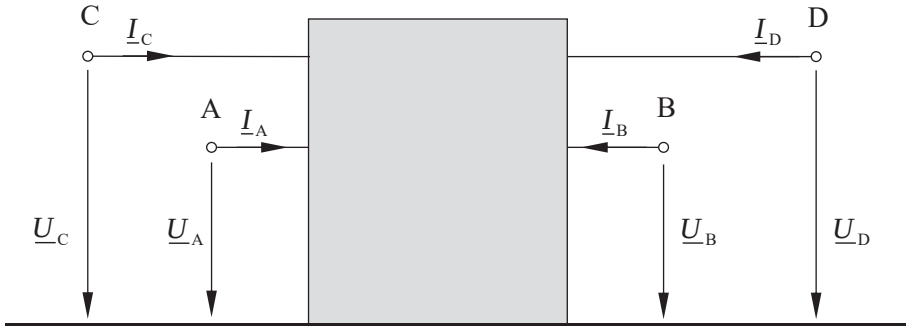

Fig. 11: general equivalent circuit diagram of an octopole

It is used to model parallel systems of lines, e.g. overhead line systems that share the same poles. Although the phases are twisted to reach symmetry, there might be an inductive or capacitive coupling between these systems. The physical behavior of such parallel systems can be described by a forth order linear equation system.

$$\begin{bmatrix} \underline{I}_A \\ \underline{I}_B \\ \underline{I}_C \\ \underline{I}_D \end{bmatrix} = \left[\begin{array}{cc:cc} \underline{Y}_{AA} & \underline{Y}_{AB} & \underline{Y}_{AC} & \underline{Y}_{AD} \\ \underline{Y}_{BA} & \underline{Y}_{BB} & \underline{Y}_{BC} & \underline{Y}_{BD} \\ \hdashline \underline{Y}_{CA} & \underline{Y}_{CB} & \underline{Y}_{CC} & \underline{Y}_{CD} \\ \underline{Y}_{DA} & \underline{Y}_{DB} & \underline{Y}_{DC} & \underline{Y}_{DD} \end{array}\right] \begin{bmatrix} \underline{U}_A \\ \underline{U}_B \\ \underline{U}_C \\ \underline{U}_D \end{bmatrix} \tag{2.24}$$

The 2×2 submatrices on the main diagonal describe the behavior of the respective system as a quadrupole and the submatrices on the secondary diagonal the mutual coupling between these systems.

In the same way overhead-lines carrying three or more systems can be modeled as 12-poles, 16-poles and so on. Usually, the mutual perturbation is neglected and all systems of the overhead-line are modeled as quadrupoles.

3 Grid equation systems

To efficiently perform power system analysis, a suitable equation system is needed, which allows to easily formulate the problem and model the underlying mechanisms. Therefore, a system state vector is aspired which has toe following properties:

- unambiguous and consistent
- lowest possible number of state variables
- simple deduction of other information

Possible system state vectors and mesh currents and nodal voltages. Only the latter fully meet the above requirements.

In the following, different approaches to setup the grid equation systems are introduced.

3.1 Multipole theory

In chapter 2 the physical behavior of different types of assets is described. Up to now, the pieces of equipment are not connected to each other. If all equipment equation systems are put together, this results into a single linear equation system which has a block-diagonal form.

$$\begin{bmatrix} \underline{I}_{\mathrm{A},1} \\ \vdots \\ \underline{I}_{\mathrm{A},\alpha} \\ \underline{I}_{\mathrm{A},\alpha+1} \\ \underline{I}_{\mathrm{B},\alpha+1} \\ \vdots \\ \underline{I}_{\mathrm{A},\alpha+\beta} \\ \underline{I}_{\mathrm{B},\alpha+\beta} \\ \vdots \end{bmatrix} = \begin{bmatrix} \underline{Y}_{\mathrm{A},1} & & & & & & \\ & \ddots & & & & & \\ & & \underline{Y}_{\mathrm{A},\alpha} & & & & \\ & & & \underline{Y}_{\mathrm{AA},\alpha+1} & \underline{Y}_{\mathrm{AB},\alpha+1} & & \\ & & & \underline{Y}_{\mathrm{BA},\alpha+1} & \underline{Y}_{\mathrm{BB},\alpha+1} & & \\ & & & & & \ddots & \\ & & & & & \underline{Y}_{\mathrm{AA},\alpha+\beta} & \underline{Y}_{\mathrm{AB},\alpha+\beta} \\ & & & & & \underline{Y}_{\mathrm{BA},\alpha+\beta} & \underline{Y}_{\mathrm{BB},\alpha+\beta} \\ & & & & & & \ddots \end{bmatrix} \begin{bmatrix} \underline{U}_{\mathrm{A},1} \\ \vdots \\ \underline{U}_{\mathrm{A},\alpha} \\ \underline{U}_{\mathrm{A},\alpha+1} \\ \underline{U}_{\mathrm{B},\alpha+1} \\ \vdots \\ \underline{U}_{\mathrm{A},\alpha+\beta} \\ \underline{U}_{\mathrm{B},\alpha+\beta} \\ \vdots \end{bmatrix} \tag{3.1}$$

In eq. (3.1) the composition is exemplarily given for α dipoles and β quadrupoles. Integration of sextupoles and octopoles is done analogously. The order of the assets or their terminals is not important. Nevertheless, the aspired block-diagonal form can only be achieved, if terminals belonging to the same asset are grouped together.

For the demonstration grid given in Fig. 12 the resulting single-line diagram is shown in Fig. 13 which also gives the enumeration of nodes and terminals.

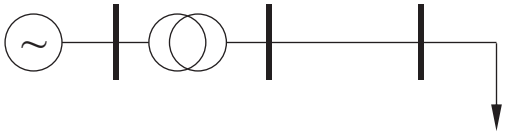

Fig. 12: demonstration grid

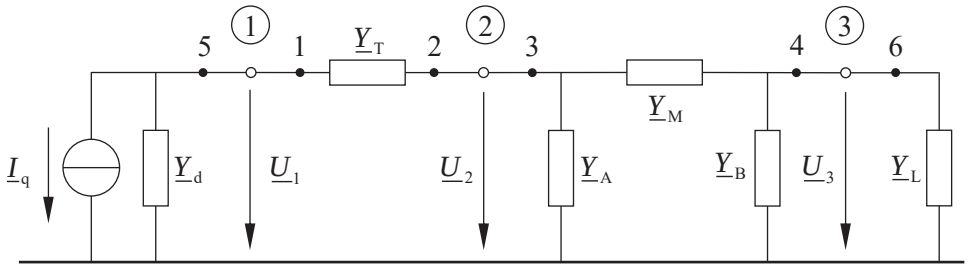

Fig. 13: single-line diagram with node and terminal enumeration

Finally, this results in the full terminal admittance matrix $\underline{\boldsymbol{Y}}_{\mathrm{T.full}}$

$$\underline{\boldsymbol{Y}}_{\mathrm{T,full}} = \left[\begin{array}{cc:cc:c:c} \underline{Y}_T & -\underline{Y}_T & & & & \\ -\underline{Y}_T & \underline{Y}_T & & & & \\ \hdashline & & \underline{Y}_A+\underline{Y}_M & -\underline{Y}_M & & \\ & & -\underline{Y}_M & \underline{Y}_B+\underline{Y}_M & & \\ \hdashline & & & & \underline{Y}_d & \\ \hdashline & & & & & \underline{Y}_L \end{array}\right] \tag{3.2}$$

It can also be composed of a terminal admittance matrix containing only dipoles $\underline{\boldsymbol{Y}}_{\mathrm{T,DP}}$ and a terminal admittance matrix containing all other remaining equipment $\underline{\boldsymbol{Y}}_{\mathrm{T,rem}}$.

$$\underline{\boldsymbol{Y}}_{\mathrm{T,full}} = \begin{bmatrix} \underline{\boldsymbol{Y}}_{\mathrm{T,rem}} & \\ & \underline{\boldsymbol{Y}}_{\mathrm{T,DP}} \end{bmatrix} \tag{3.3}$$

For the purpose of bus-oriented descriptions of the system state, usually only $\underline{\boldsymbol{Y}}_{\mathrm{T,rem}}$ is needed. Therefore, in the following, it is shorter written as $\underline{\boldsymbol{Y}}_{\mathrm{T}}$. At each node, the terminal currents of the adjacent dipoles are summed up to a nodal current $\underline{I}_{\mathrm{K}}$. This simplifies the calculation and it is not necessary to calculate with fictitious internal source currents.

3.1.1 Description of topology

The topology of a grid is described by logically connecting terminals to nodes. This is done using the nodal-terminal-incidence-matrix $\boldsymbol{K}_{\mathrm{KT}}$. If a terminal is logically connected to a node, the respective coefficient of the matrix is set to „1“. All other elements of this column must then be „0“, because a terminal can and must only be connected to exactly one node. So the column sums of the nodal-terminal-incidence-matrix must be exactly „1“ while the row sums represent the degree of intermeshing of a node.

The topology of the demonstration grid given in Fig. 12 is described by $\boldsymbol{K}_{\mathrm{KT,full}}$

$$\boldsymbol{K}_{\mathrm{KT,full}} = \left[\begin{array}{cc:cc:cc} 1 & 0 & 0 & 0 & 1 & 0 \\ 0 & 1 & 1 & 0 & 0 & 0 \\ 0 & 0 & 0 & 1 & 0 & 1 \end{array}\right] \tag{3.4}$$

Like the equipment admittance matrix it can also be composed of a $\boldsymbol{K}_{\mathrm{KT,DP}}$ containing the dipoles and $\boldsymbol{K}_{\mathrm{KT,rem}}$ containing the connectivity of all other remaining assets.

$$\boldsymbol{K}_{\mathrm{KT,full}} = \left[\boldsymbol{K}_{\mathrm{KT,rem}} \quad \boldsymbol{K}_{\mathrm{KT,DP}}\right] \tag{3.5}$$

For the purpose of bus-oriented descriptions of the system state, usually only $\boldsymbol{K}_{\mathrm{KT,rem}}$ is needed. Therefore, in the following, it is shorter written as $\boldsymbol{K}_{\mathrm{KT}}$.

Switching equipment on or off is a change in its physical behavior and therefore must not be modeled by setting or deleting ones in $\boldsymbol{K}_{\mathrm{KT}}$. It must be modeled by changing the respective coefficients of $\underline{\boldsymbol{Y}}_{\mathrm{T}}$. On the other hand, switching a line from one busbar to another is in fact a change of the logical assignment of the terminal to a node. Therefore, this must be modelled by moving the „1“ in the respective column of $\boldsymbol{K}_{\mathrm{KT}}$ from the old to the new node. The physical behavior of the line does not change, so $\underline{\boldsymbol{Y}}_{\mathrm{T}}$ stays constant.

3.1.2 Description of the system state

The multipole approach uses the admittance form to describe the physical behavior of the equipment. It is therefore a nodal based method. Thus, the nodal voltages $\underline{\boldsymbol{u}}_{\mathrm{K}}$ form the system state vector. For example, the terminal voltages $\underline{\boldsymbol{u}}_{\mathrm{T}}$ can easily be expressed.

$$\underline{\boldsymbol{u}}_{\mathrm{T}} = \boldsymbol{K}_{\mathrm{KT}}^{\mathrm{T}}\, \underline{\boldsymbol{u}}_{\mathrm{K}} \tag{3.6}$$

Furthermore, the physical behavior of the assets is known and can be described with a single linear equation system according to eq. (3.1).

$$\underline{\boldsymbol{i}}_{\mathrm{T}} = \underline{\boldsymbol{Y}}_{\mathrm{T}}\, \underline{\boldsymbol{u}}_{\mathrm{T}} \tag{3.7}$$

Finally, 1st Kirchhoff‘s law, says, that the sum of currents at each node has to be zero.

$$\underline{\boldsymbol{i}}_{\mathrm{K}} + \boldsymbol{K}_{\mathrm{KT}}\, \underline{\boldsymbol{i}}_{\mathrm{T}} = \boldsymbol{0} \tag{3.8}$$

In eq. (3.8) the nodal current vector $\underline{\boldsymbol{i}}_{\mathrm{K}}$ is introduced. It summarizes all the dipole currents that are connected to the respective nodes.

$$\underline{\boldsymbol{i}}_{\mathrm{K}} = \boldsymbol{K}_{\mathrm{KT,DP}}\, \underline{\boldsymbol{i}}_{\mathrm{T,DP}} \tag{3.9}$$

Insertion of eq. (3.6) into eq. (3.7) results in

$$\underline{\boldsymbol{i}}_{\mathrm{T}} = \underline{\boldsymbol{Y}}_{\mathrm{T}}\, \boldsymbol{K}_{\mathrm{KT}}^{\mathrm{T}}\, \underline{\boldsymbol{u}}_{\mathrm{K}} \tag{3.10}$$

Insertion of eq. (3.10) into eq. (3.9) and solving for the nodal currents leads to

$$\underline{\boldsymbol{i}}_{\mathrm{K}} = -\boldsymbol{K}_{\mathrm{KT}}\, \underline{\boldsymbol{Y}}_{\mathrm{T}}\, \boldsymbol{K}_{\mathrm{KT}}^{\mathrm{T}}\, \underline{\boldsymbol{u}}_{\mathrm{K}} \tag{3.11}$$

Eq. (3.11) is again written in admittance form, which was already used to describe the physical behavior of the equipment. Nevertheless, all terminal voltages and currents have been replaced by nodal voltages and currents and the description of the physical behavior and topological information are merged into one single equation system. Introduction of the bus admittance matrix $\underline{\boldsymbol{Y}}_{\mathrm{KK}}$

$$\underline{\boldsymbol{Y}}_{\mathrm{KK}} = -\boldsymbol{K}_{\mathrm{KT}}\, \underline{\boldsymbol{Y}}_{\mathrm{T}}\, \boldsymbol{K}_{\mathrm{KT}}^{\mathrm{T}} \tag{3.12}$$

leads to a further simplification

$$\underline{\boldsymbol{i}}_{\mathrm{K}} = \underline{\boldsymbol{Y}}_{\mathrm{KK}}\, \underline{\boldsymbol{u}}_{\mathrm{K}} \tag{3.13}$$

If dipoles were not expressed as nodal currents, then $\underline{\boldsymbol{i}}_{\mathrm{K}}$ would only contain the inner source currents of the dipoles and the dipole admittances would be part of $\underline{\boldsymbol{Y}}_{\mathrm{KK}}$.

$\underline{\boldsymbol{Y}}_{KK}$ has the following properties:

- quadratic
- sparse
- symmetric, if there are no phase shifting transformers in the grid
- singular, if there are no shunt elements in the grid. Even with shunt elements, the determinant is close to zero.

3.1.3 Deduced information

As described above, nodal voltages are particularly suitable to describe the system state, due to all other values can be easily derived. Table 3 gives an overview of a couple the most needed information of interest.

Table 3: derived information

description	formula
terminal voltages	$\underline{\boldsymbol{u}}_T = \boldsymbol{K}_{KT}^T \, \underline{\boldsymbol{u}}_K$
nodal currents	$\underline{\boldsymbol{i}}_K = \underline{\boldsymbol{Y}}_{KK} \, \underline{\boldsymbol{u}}_K$
terminal currents	$\underline{\boldsymbol{i}}_T = \underline{\boldsymbol{Y}}_T \, \underline{\boldsymbol{u}}_T = \underline{\boldsymbol{Y}}_T \, \boldsymbol{K}_{KT}^T \, \underline{\boldsymbol{u}}_K$
nodal powers	$\underline{\boldsymbol{s}}_K = 3 \, \underline{\boldsymbol{U}}_K \, \underline{\boldsymbol{i}}_K^* = 3 \, \underline{\boldsymbol{U}}_K \left(\underline{\boldsymbol{Y}}_{KK} \, \underline{\boldsymbol{u}}_K \right)^*$
terminal powers	$\underline{\boldsymbol{s}}_T = 3 \, \underline{\boldsymbol{U}}_T \, \underline{\boldsymbol{i}}_T^* = 3 \, \underline{\boldsymbol{U}}_T \left(\underline{\boldsymbol{Y}}_T \, \underline{\boldsymbol{u}}_T \right)^*$
grid losses	$\underline{S}_V = -\sum \underline{\boldsymbol{s}}_K = \sum \underline{\boldsymbol{s}}_T$

3.2 Graph theory

Using graph theory, equipment is not modeled as a single piece of asset as described in chapter 2. Instead, the equipment is decomposed into several branches, each containing only a single admittance and possible a parallel current source.

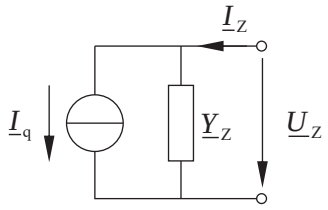

Fig. 14: general presentation of a branch

This results in the branch equation

$$\underline{I}_Z = \underline{Y}_Z \, \underline{U}_Z + \underline{I}_q \tag{3.14}$$

Similar to the multipole approach all branches are enumerated and their equations are joined into a single, decoupled equation system.

$$\begin{bmatrix} \underline{I}_{Z1} \\ \vdots \\ \underline{I}_{Zn} \end{bmatrix} = \begin{bmatrix} \underline{Y}_{Z1} & & \\ & \ddots & \\ & & \underline{Y}_{Zn} \end{bmatrix} \begin{bmatrix} \underline{U}_{Z1} \\ \vdots \\ \underline{U}_{Zn} \end{bmatrix} + \begin{bmatrix} \underline{I}_{q1} \\ \vdots \\ \underline{I}_{qn} \end{bmatrix}$$
$$\underline{\boldsymbol{i}}_Z = \underline{\boldsymbol{Y}}_Z \underline{\boldsymbol{u}}_Z + \underline{\boldsymbol{i}}_q \tag{3.15}$$

For the demonstration grid given in Fig. 12 this results in the following equivalent circuit diagram

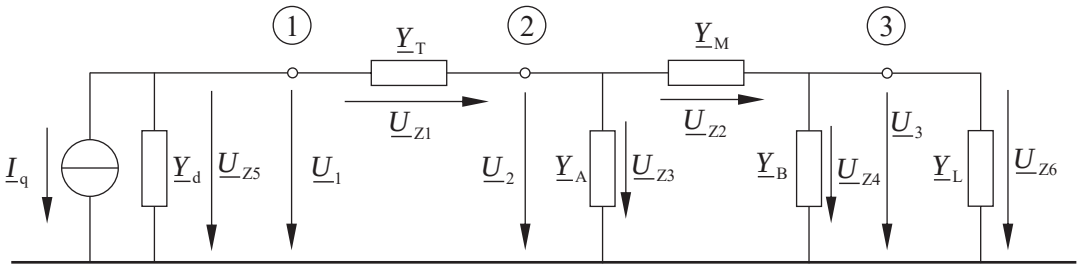

Fig. 15: equivalent circuit diagram in graph theory

The arbitrary chosen direction of the branch currents depicts the direction of the entire branch. In multipole theory, this step is unnecessary, due to the load counting system all terminal currents automatically point into the asset at every terminal. In doing so, a potential source of error is avoided.

According to the branch enumeration the following branch admittance matrix results

$$\underline{\boldsymbol{Y}}_{Z,full} = \left[\begin{array}{c|c} \underline{\boldsymbol{Y}}_Z & \\ \hline & \underline{\boldsymbol{Y}}_{Z,DP} \end{array}\right] = \left[\begin{array}{cccc|cc} \underline{Y}_T & & & & & \\ & \underline{Y}_M & & & & \\ & & \underline{Y}_A & & & \\ & & & \underline{Y}_B & & \\ \hline & & & & \underline{Y}_d & \\ & & & & & \underline{Y}_L \end{array}\right] \tag{3.16}$$

Similar to the multipole theory, it can be divided into the branches of the dipoles and all other branches. Again, at each node, the currents of the adjacent dipoles are summed up to nodal currents.

3.2.1 Topology description

Grid topology is described by logically connecting branches to their adjacent nodes under consideration of the branch direction. This is done using the node-branch-incidence matrix $\boldsymbol{K}_{KZ}$. If a branch is connected to a node but points away from it, a "1" is written at the respective position in $\boldsymbol{K}_{KZ}$. If a branch is connected to a node and points towards it, a "–1" is written at the respective position. In doing so, the ground is neglected.

For the demonstration grid given in Fig. 12 the full topological matrix is

$$\boldsymbol{K}_{KZ,full} = \left[\boldsymbol{K}_{KZ} \mid \boldsymbol{K}_{KZ,DP}\right] = \left[\begin{array}{cccc|cc} 1 & 0 & 0 & 0 & 1 & 0 \\ -1 & 1 & 1 & 0 & 0 & 0 \\ 0 & -1 & 0 & 1 & 0 & 1 \end{array}\right] \tag{3.17}$$

An initial error proof of $\boldsymbol{K}_{\mathrm{KZ}}$ is impossible due to the different signs of the coefficients. Nevertheless – similar to the multipole approach – switching should not be modeled by removing ones from the matrix. As switching is a change in the physical behavior of the branch, this should again be modeled by changing and maybe the source current the admittance of the respective branch.

3.2.2 Description of the system state

The derivation of the grid equation systems is similar to the multipole approach. Due to the admittance form of the branch description, graph theory also is a nodal based approach. The system state vector therefore again consists of the nodal voltages $\underline{\boldsymbol{u}}_{\mathrm{K}}$. The can be used to simply calculate the branch voltages

$$\underline{\boldsymbol{u}}_{\mathrm{Z}} = \boldsymbol{K}_{\mathrm{KZ}}^{\mathrm{T}}\, \underline{\boldsymbol{u}}_{\mathrm{K}} \tag{3.18}$$

Also, modelling of the physical behavior of the branches is done analogously.

$$\underline{\boldsymbol{i}}_{\mathrm{Z}} = \underline{\boldsymbol{Y}}_{\mathrm{Z}}\, \underline{\boldsymbol{u}}_{\mathrm{Z}} \tag{3.19}$$

The branches considered in eq. (3.19) do not contain any sources, due to these are typically only present in dipoles.

Finally, using Kirchhoff's first law, again nodal currents are introduced which sum up to zero together with the adjacent branch currents.

$$\underline{\boldsymbol{i}}_{\mathrm{K}} + \boldsymbol{K}_{\mathrm{KZ}}\, \underline{\boldsymbol{i}}_{\mathrm{Z}} = \boldsymbol{0} \tag{3.20}$$

where the nodal currents can be expressed by the dipole currents, as described above

$$\underline{\boldsymbol{i}}_{\mathrm{K}} = \underline{\boldsymbol{K}}_{\mathrm{KZ,DP}}\, \underline{\boldsymbol{i}}_{\mathrm{Z,DP}} \tag{3.21}$$

Combining eq. (3.19) and eq. (3.20) results in

$$\underline{\boldsymbol{i}}_{\mathrm{Z}} = \underline{\boldsymbol{Y}}_{\mathrm{Z}}\, \boldsymbol{K}_{\mathrm{KZ}}^{\mathrm{T}}\, \underline{\boldsymbol{u}}_{\mathrm{K}} \tag{3.22}$$

Insertion of eq. (3.22) in eq. (3.20) and solving for the nodal current leads to

$$\underline{\boldsymbol{i}}_{\mathrm{K}} = -\boldsymbol{K}_{\mathrm{KZ}}\, \underline{\boldsymbol{Y}}_{\mathrm{Z}}\, \boldsymbol{K}_{\mathrm{KZ}}^{\mathrm{T}}\, \underline{\boldsymbol{u}}_{\mathrm{K}} \tag{3.23}$$

and to the already well-known eq. (3.13) with the same bus admittance matrix

$$\underline{\boldsymbol{Y}}_{\mathrm{KK}} = -\boldsymbol{K}_{\mathrm{KZ}}\, \underline{\boldsymbol{Y}}_{\mathrm{Z}}\, \boldsymbol{K}_{\mathrm{KZ}}^{\mathrm{T}} \tag{3.24}$$

Both approaches lead to identical solutions. Nevertheless, the multipole method is superior due to bypassing any arbitrariness which results from the directed graph. Furthermore, terminal values (e.g. currents and powers at both ends of a cable) exist in the real world and are actually measurable while branch values are mostly fictitious. An additional calculation step is needed to infer from the branch values to measurable values.

3.3 Direct arrangement of the bus admittance matrix

Besides the calculation according to eq. (3.12) $\underline{\boldsymbol{Y}}_{\mathrm{KK}}$ can be directly built manually e.g. for the calculation of small grids.

- Coefficient $\underline{y}_{i,j}$ represents the admittance between the nodes *i* and *j*. If there is no direct connection between *i* and *j*, $\underline{y}_{i,j}$ is zero.
- The elements on the main diagonal $\underline{y}_{i,i}$ are calculated by building the negative sum of line *i* and subtracting the shunt elements at node *i*.

The bus admittance matrix of the demonstration grid shown in Fig. 12 is given below

$$\underline{\boldsymbol{Y}}_{\mathrm{KK}} = \begin{bmatrix} -\underline{Y}_{\mathrm{T}} & \underline{Y}_{\mathrm{T}} & 0 \\ \underline{Y}_{\mathrm{T}} & -\left(\underline{Y}_{\mathrm{T}} + \underline{Y}_{\mathrm{M}} + \underline{Y}_{\mathrm{A}}\right) & \underline{Y}_{\mathrm{M}} \\ 0 & \underline{Y}_{\mathrm{M}} & -\left(\underline{Y}_{\mathrm{M}} + \underline{Y}_{\mathrm{B}}\right) \end{bmatrix} \tag{3.25}$$

The same result is obtained by solving eq. (3.12).

$$\begin{aligned} \underline{\boldsymbol{Y}}_{\mathrm{KK}} &= -\begin{bmatrix} 1 & 0 & 0 & 0 \\ 0 & 1 & 1 & 0 \\ 0 & 0 & 0 & 1 \end{bmatrix} \begin{bmatrix} \underline{Y}_{\mathrm{T}} & -\underline{Y}_{\mathrm{T}} & & \\ -\underline{Y}_{\mathrm{T}} & \underline{Y}_{\mathrm{T}} & & \\ & & \underline{Y}_{\mathrm{A}} + \underline{Y}_{\mathrm{M}} & -\underline{Y}_{\mathrm{M}} \\ & & -\underline{Y}_{\mathrm{M}} & \underline{Y}_{\mathrm{B}} + \underline{Y}_{\mathrm{M}} \end{bmatrix} \begin{bmatrix} 1 & 0 & 0 \\ 0 & 1 & 0 \\ 0 & 1 & 0 \\ 0 & 0 & 1 \end{bmatrix} \\ &= \begin{bmatrix} -\underline{Y}_{\mathrm{T}} & \underline{Y}_{\mathrm{T}} & 0 \\ \underline{Y}_{\mathrm{T}} & -\left(\underline{Y}_{\mathrm{T}} + \underline{Y}_{\mathrm{M}} + \underline{Y}_{\mathrm{A}}\right) & \underline{Y}_{\mathrm{M}} \\ 0 & \underline{Y}_{\mathrm{M}} & -\left(\underline{Y}_{\mathrm{M}} + \underline{Y}_{\mathrm{B}}\right) \end{bmatrix} \end{aligned} \tag{3.26}$$

or eq. (3.24)

$$\begin{aligned} \underline{\boldsymbol{Y}}_{\mathrm{KK}} &= -\begin{bmatrix} 1 & 0 & 0 & 0 \\ -1 & 1 & 1 & 0 \\ 0 & -1 & 0 & 1 \end{bmatrix} \begin{bmatrix} \underline{Y}_{\mathrm{T}} & & & \\ & \underline{Y}_{\mathrm{M}} & & \\ & & \underline{Y}_{\mathrm{A}} & \\ & & & \underline{Y}_{\mathrm{B}} \end{bmatrix} \begin{bmatrix} 1 & -1 & 0 \\ 0 & 1 & -1 \\ 0 & 1 & 0 \\ 0 & 0 & 1 \end{bmatrix} \\ &= \begin{bmatrix} -\underline{Y}_{\mathrm{T}} & \underline{Y}_{\mathrm{T}} & 0 \\ \underline{Y}_{\mathrm{T}} & -\left(\underline{Y}_{\mathrm{T}} + \underline{Y}_{\mathrm{M}} + \underline{Y}_{\mathrm{A}}\right) & \underline{Y}_{\mathrm{M}} \\ 0 & \underline{Y}_{\mathrm{M}} & -\left(\underline{Y}_{\mathrm{M}} + \underline{Y}_{\mathrm{B}}\right) \end{bmatrix} \end{aligned} \tag{3.27}$$

4 Power flow calculation

Power flow calculation is – as well as the state estimation approach – a method of grid state identification. That means, its task is to infer on the grid state, namely to calculate nodal voltages, based on a set of given input variables. The general procedure of grid state identification is given in Fig. 16.

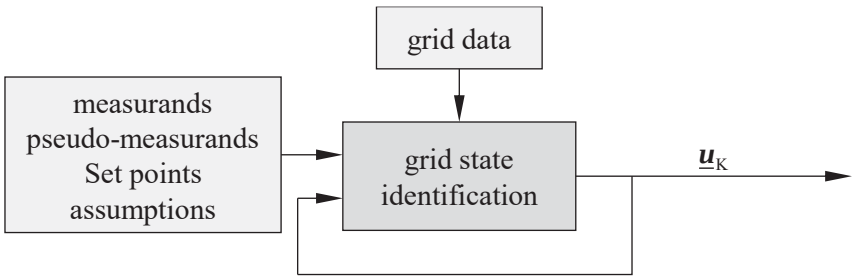

Fig. 16: general procedure of grid state identification

The available methods of grid state identification differ in their algorithms and the available or used set of input parameters. Therefore, they differ in their fields of application as well and are either used for grid planning or grid operation.

The power flow calculation infers on nodal voltages exclusively based on given nodal active and reactive powers as well as some possibly given reference nodal voltages. It is mostly used for offline grid analysis (e.g. grid planning) and is the basis for contingency analyses during system operation.

To obtain information on the grid state, the power flow approach needs to solve a quadratic equation system. The size of the equation system grows with the number of nodes in the grid. Usually, the problem cannot be solved analytically, thus numerical approaches to approximate the solution are applied. For this purpose, fixed-point and tangential approaches are available. Due to their better convergence, the latter are superior, nevertheless, fixed-point approaches offer several advantages, too.

4.1 Node types and voltage dependency of loads

Each node can be assigned four different values: active and reactive nodal power as well as the nodal voltage separated into either real and imaginary part or magnitude and angle. Depending on the available information, different node types are identified.

Table 4: summary of node types

node type	known values	calculated values	amount
load nodes	P, Q	U, δ	> 90 %
Generator nodes	P, U	Q, δ	< 10 %
slack node	U, δ	P, Q	1

Most of the nodes are load nodes, where active and reactive powers are given. Besides that, there are some generator nodes at which active powers and a reference voltage are given. This is in line with the behavior of big power plants that supply active power according to their schedule and offer voltage control. Active and reactive power balancing is granted by a so called

slack node which additionally defines a reference voltage angle. This is necessary, due to power flows on the lines are not defined by the absolute value of the nodal voltage angles but instead by the differences of voltage angles at neighboring nodes.

Theoretically, a fourth node type is thinkable, where Q and δ are given and U and P need to be calculated. There is no physical equivalent to this node type which is why it is usually not used. Nevertheless, it can be a useful tool e.g. for distributed slack calculation, for power flow optimization problems or if reference values for voltage and angle are intended to be given at different locations. Exactly on node must provide a reference angle to make the equation system solvable. If the system does not have any shunt elements, then at least one voltage reference is also necessary.

Active and reactive powers at load nodes may depend on the voltage magnitude. Their characteristic can be expressed by an exponential function.

$$P = P_0 \left(\frac{U}{U_0} \right)^p \tag{4.1}$$

$$Q = Q_0 \left(\frac{U}{U_0} \right)^q \tag{4.2}$$

In Fig. 17 three different special cases are shown:

- $p, q = 0$: active and reactive power are constant and do not depend on the voltage magnitude (e.g. if it is a measured value or the load is power controlled)
- $p, q = 1$: active and reactive currents are constant (e.g. a current controlled load)
- $p, q = 2$: active and reactive powers are proportional to the square of the voltage, i.e. the admittance of the load is constant

In practice, the values of p and q are between 1 and 2.

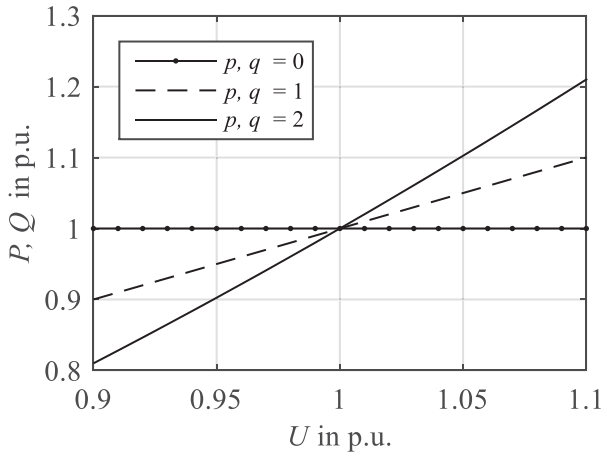

Fig. 17: voltage dependency of active and reactive powers

4.2 Gauss-Seidel iteration

The Gauss-Seidel iteration is a fixed-point approach. It is mainly based on alternatingly solve the power equation

$$\underline{\boldsymbol{i}}_{\mathrm{K}} = \frac{1}{3}\left(\underline{\boldsymbol{U}}_{\mathrm{K}}^{-1}\, \underline{\boldsymbol{s}}_{\mathrm{K}}\right)^{*} \tag{4.3}$$

and the current equation

$$\underline{\boldsymbol{Y}}_{\mathrm{KK}}\, \underline{\boldsymbol{u}}_{\mathrm{K}} = \underline{\boldsymbol{i}}_{\mathrm{K}} \tag{4.4}$$

until the result does not change any more.

The slack voltage $\underline{U}_{\mathrm{s}}$ is given and therefore already known. It can be removed from the solution vector. Hence, the current equation system is separated into the slack equation and the remaining equations.

$$\begin{bmatrix} \underline{Y}_{\mathrm{ss}} & \underline{\boldsymbol{Y}}_{\mathrm{sr}} \\ \underline{\boldsymbol{Y}}_{\mathrm{rs}} & \underline{\boldsymbol{Y}}_{\mathrm{rr}} \end{bmatrix} \begin{bmatrix} \underline{U}_{\mathrm{s}} \\ \underline{\boldsymbol{u}}_{\mathrm{r}} \end{bmatrix} = \begin{bmatrix} \underline{I}_{\mathrm{s}} \\ \underline{\boldsymbol{i}}_{\mathrm{r}} \end{bmatrix} \tag{4.5}$$

The lower part of eq. (4.5) is solved for the remaining voltage vector $\underline{\boldsymbol{u}}_{\mathrm{r}}$

$$\underline{\boldsymbol{u}}_{\mathrm{r}} = \underline{\boldsymbol{Y}}_{\mathrm{rr}}^{-1}\left(\underline{\boldsymbol{i}}_{\mathrm{r}} - \underline{\boldsymbol{Y}}_{\mathrm{rs}}\, \underline{U}_{\mathrm{s}}\right) \tag{4.6}$$

Thereby, $\underline{\boldsymbol{i}}_{\mathrm{r}}$ is the remaining current vector of $\underline{\boldsymbol{i}}_{\mathrm{K}}$ without the current at the slack node.

$$\underline{\boldsymbol{i}}_{\mathrm{K}} = \begin{bmatrix} \underline{I}_{\mathrm{s}} \\ \underline{\boldsymbol{i}}_{\mathrm{r}} \end{bmatrix} \tag{4.7}$$

The voltage vector is obtained iteratively. In each iteration step ν a new remaining current vector is calculated based on the voltage solution of the last iteration step

$$\underline{\boldsymbol{i}}_{\mathrm{r},\nu} = \frac{1}{3}\left(\underline{\boldsymbol{U}}_{\mathrm{r},\nu-1}^{-1}\, \underline{\boldsymbol{s}}_{\mathrm{r},\nu-1}\right)^{*} \tag{4.8}$$

Using these new currents, the voltage vector is updated.

$$\underline{\boldsymbol{u}}_{\mathrm{r},\nu} = \underline{\boldsymbol{Y}}_{\mathrm{rr}}^{-1}\left(\underline{\boldsymbol{i}}_{\mathrm{r},\nu} - \underline{\boldsymbol{Y}}_{\mathrm{rs}}\, \underline{U}_{\mathrm{s}}\right) \tag{4.9}$$

In eq. (4.9) generator nodes are not considered. That means, the voltage $\underline{U}_{g,\nu}$ at the generator node g differs most likely from the reference value $\underline{U}_{g,\mathrm{ref}}$. Therefore, the entire vector $\underline{\boldsymbol{u}}_{\mathrm{r},\nu}$ needs to be corrected. This is done by further decomposing the (remaining) equation system from eq. (4.5) into generator and load nodes

$$\begin{aligned} \left[\underline{\boldsymbol{Y}}_{\mathrm{rs}} \;\vdots\; \underline{\boldsymbol{Y}}_{\mathrm{rr}}\right] \begin{bmatrix} \underline{U}_{\mathrm{s}} \\ \cdots \\ \underline{\boldsymbol{u}}_{\mathrm{r}} \end{bmatrix} &= \underline{\boldsymbol{i}}_{\mathrm{r}} \\ \begin{bmatrix} \underline{\boldsymbol{Y}}_{\mathrm{gs}} & \underline{\boldsymbol{Y}}_{\mathrm{gg}} & \underline{\boldsymbol{Y}}_{\mathrm{gl}} \\ \underline{\boldsymbol{Y}}_{\mathrm{ls}} & \underline{\boldsymbol{Y}}_{\mathrm{lg}} & \underline{\boldsymbol{Y}}_{\mathrm{ll}} \end{bmatrix} \begin{bmatrix} \underline{U}_{\mathrm{s}} \\ \cdots \\ \underline{\boldsymbol{u}}_{\mathrm{g}} \\ \underline{\boldsymbol{u}}_{\mathrm{l}} \end{bmatrix} &= \begin{bmatrix} \underline{\boldsymbol{i}}_{\mathrm{g}} \\ \underline{\boldsymbol{i}}_{\mathrm{l}} \end{bmatrix} \end{aligned} \tag{4.10}$$

Assuming that the newly calculated voltage angle of the generator node is a better approximation than the last one, only the magnitude of the voltage is set back to the reference.

$$\underline{U}_{g,\nu} = \underline{U}_{g,\mathrm{ref}}\, \mathrm{e}^{\mathrm{j}\angle\left\{\underline{U}_{g,\nu}\right\}} \tag{4.11}$$

Changing the voltage magnitudes at the generator nodes has an impact on the voltages of at least all the surrounding load nodes *l*. They can be calculated by the lower equation system of eq. (4.10).

$$\underline{\boldsymbol{u}}_{\mathrm{l},\nu} = \underline{\boldsymbol{Y}}_{\mathrm{ll}}^{-1}\left(\underline{\boldsymbol{i}}_{\mathrm{l},\nu} - \underline{\boldsymbol{Y}}_{\mathrm{lg},\nu}\,\underline{\boldsymbol{u}}_{\mathrm{g},\nu} - \underline{\boldsymbol{Y}}_{\mathrm{ls},\nu}\,\underline{U}_{\mathrm{s}}\right) \tag{4.12}$$

Additionally, the reactive power output of the generator node needs to be modified based on the corrected generator and load voltages.

$$\boldsymbol{q}_{\mathrm{g},\nu} = 3\,\mathrm{Im}\left\{\underline{\boldsymbol{U}}_{\mathrm{g},\nu}\left(\begin{bmatrix}\underline{\boldsymbol{Y}}_{\mathrm{gs}} & \underline{\boldsymbol{Y}}_{\mathrm{gg}} & \underline{\boldsymbol{Y}}_{\mathrm{gl}}\end{bmatrix}\begin{bmatrix}\underline{U}_{\mathrm{s}} \\ \underline{\boldsymbol{u}}_{\mathrm{g},\nu} \\ \underline{\boldsymbol{u}}_{\mathrm{l},\nu}\end{bmatrix}\right)^{*}\right\} \tag{4.13}$$

The resulting vectors of nodal voltages and powers can now be used again in eq. (4.8) to calculate the next iteration step. The powers of the load nodes depend on *p* and *q*. If both *p* and *q* are zero, $\underline{\boldsymbol{s}}_{\mathrm{r}}$ is constant.

$$\begin{aligned} P_{\mathrm{r},\nu,i} &= P_{0,i}\left(\frac{U_{\mathrm{r},\nu-1,i}}{U_{\mathrm{n},i}}\right)^{p_i} \\ Q_{\mathrm{r},\nu,i} &= Q_{0,i}\left(\frac{U_{\mathrm{r},\nu-1,i}}{U_{\mathrm{n},i}}\right)^{q_i} \end{aligned} \tag{4.14}$$

The iteration process is repeated until the maximum voltage difference between two iteration steps is lower than a predefined threshold ε.

$$\max\left(\left|\underline{\boldsymbol{u}}_{\mathrm{r},\nu} - \underline{\boldsymbol{u}}_{\mathrm{r},\nu-1}\right|\right) < \varepsilon \tag{4.15}$$

For the first iteration step, nominal voltages of the nodes can be used as initial guess $\underline{\boldsymbol{u}}_0$. This assumption is called a flat-start. A better initial guess can be achieved if the loads are expressed as equivalent admittances

$$\underline{Y}_{\mathrm{L},i} = \frac{\underline{S}_{\mathrm{L},i}^{*}}{3\,U_{\mathrm{K,n},i}^{2}} \tag{4.16}$$

and integrated on the main diagonal of $\underline{\boldsymbol{Y}}_{\mathrm{KK}}$

$$\underline{\boldsymbol{Y}}_{\mathrm{KK,L}} = \underline{\boldsymbol{Y}}_{\mathrm{KK}} - \underline{\boldsymbol{Y}}_{\mathrm{L}} \tag{4.17}$$

Using the estimated generator currents

$$\underline{\boldsymbol{i}}_{\mathrm{K,g}} = \frac{1}{3}\left(\boldsymbol{U}_{\mathrm{K,n,g}}^{-1}\,\underline{\boldsymbol{s}}_{\mathrm{K,g}}^{*}\right) \tag{4.18}$$

an initial guess $\underline{\boldsymbol{u}}_0$ can be obtained which already includes the effects of phase shifting transformers as well as bulk load and generation. This can help to reduce the number of needed iterations.

$$\underline{\boldsymbol{u}}_0 = \underline{\boldsymbol{Y}}_{\mathrm{KK,L}}^{-1}\, \underline{\boldsymbol{i}}_{\mathrm{K,g}} \tag{4.19}$$

After the iteration has converged, the slack current has to be calculated using the slack line in eq. (4.5). Finally, the voltage and current vectors need to be reassembled

$$\underline{I}_{\mathrm{s}} = \underline{Y}_{\mathrm{ss}}\, \underline{U}_{\mathrm{s}} + \underline{\boldsymbol{Y}}_{\mathrm{sr}}\, \underline{\boldsymbol{u}}_{\mathrm{r}} \tag{4.20}$$

Now, the slack power can be calculated

$$\underline{S}_{\mathrm{s}} = 3\, \underline{U}_{\mathrm{s}}\, \underline{I}_{\mathrm{s}}^{*} \tag{4.21}$$

The flow chart of the Gauss-Seidel iteration is given in Fig. 18.

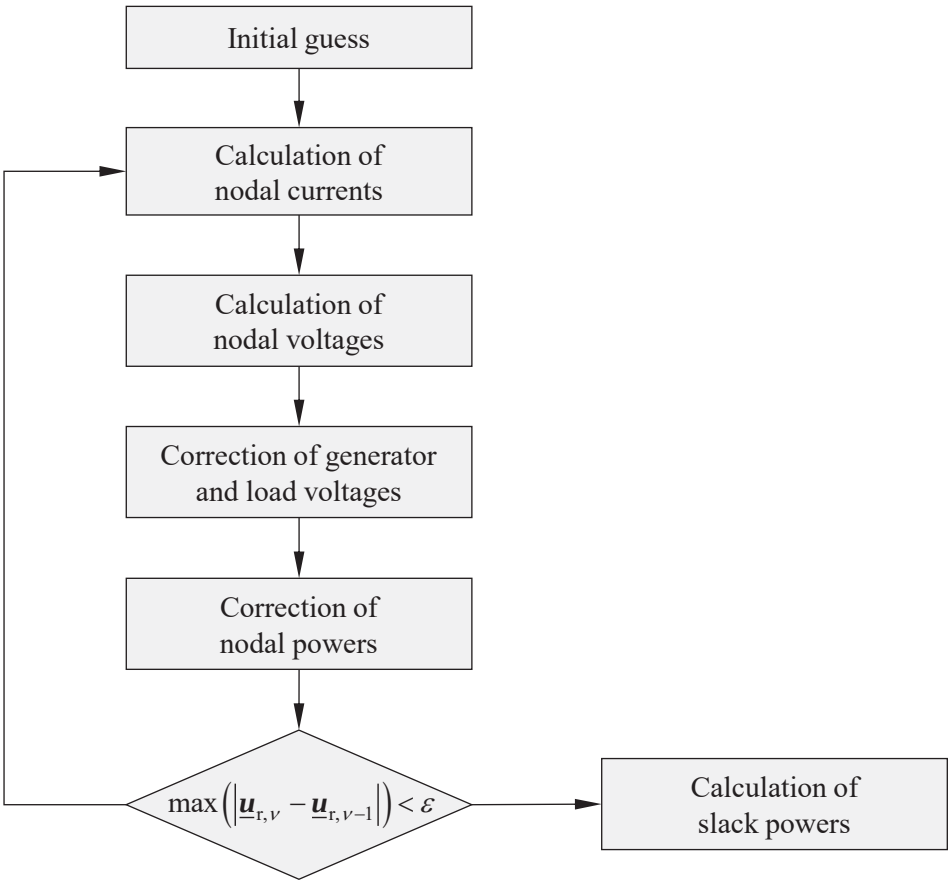

Fig. 18: flow chart of the Gauss-Seidel iteration

The most important properties of the Gauss-Seidel iteration are:

- Large radius of convergence, that means, even if the initial guess is bad, the approach is still able to find a proper solution
- Easy to implement
- The system matrix $\underline{\boldsymbol{Y}}_{\mathrm{rr}}$ is constant. That means it is sufficient to define and invert it once prior to the iteration which saves computation time.
- Low convergence speed, which means a lot of iterations are needed to find a proper solution.

- The number of needed iterations depends strongly on the grid size and increases with the number of nodes.
- Implementation of generator nodes is laborious.

Especially in large grids, the Gauss-Seidel-method often fails to converge within an acceptable amount of time. That is why nowadays it is usually not used anymore. Instead, the superior Newton-Raphson-approach is applied.

4.3 Newton-Raphson-approach

In contrast to the Gauss-Seidel-iteration, the Newton-Raphson-approach is a tangential method to find zeros of a non-linear function $\boldsymbol{f}(\boldsymbol{x})$. Therefore, the function is linearized at an initial guess $\boldsymbol{x}_0$ and the aspired zero position is assumed to be the zero position $\boldsymbol{x}_1$ of the tangent. The so found solution $\boldsymbol{x}_1$ is a better solution than $\boldsymbol{x}_0$ and therefore used as new guess for the zero position of $\boldsymbol{f}(\boldsymbol{x})$ which needs to be linearized at the new solution again until no further improvement can be seen. For a one-dimensional function, the procedure is shown in Fig. 19.

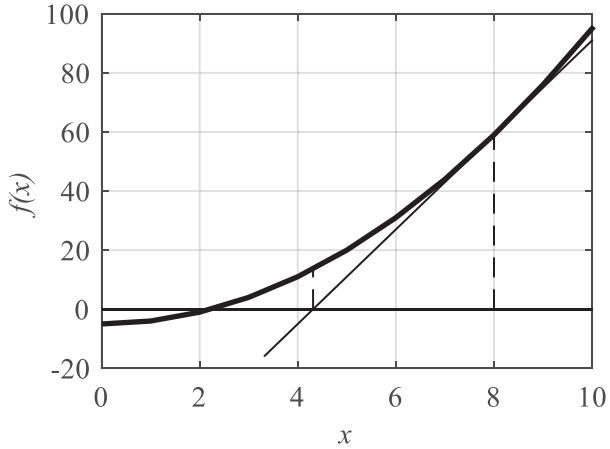

Fig. 19: iteration step of a tangential zero search

For the purpose of power flow calculation, the non-linear function is the power equation which has to be reformulated as a zero search. Therefore, nodal powers that are calculated as a function of nodal voltages

$$\underline{\boldsymbol{s}}_{\mathrm{K,calc}} = 3\,\underline{\boldsymbol{U}}_{\mathrm{K}} \left(\underline{\boldsymbol{Y}}_{\mathrm{KK}}\,\underline{\boldsymbol{u}}_{\mathrm{K}}\right)^{*} \tag{4.22}$$

are supposed to correspond to the actual (given) nodal powers $\underline{\boldsymbol{s}}_{\mathrm{K,act}}$.

$$\underline{\boldsymbol{s}}_{\mathrm{K,calc}} \overset{!}{=} \underline{\boldsymbol{s}}_{\mathrm{K,act}} \tag{4.23}$$

So, the power flow calculation can be defined as the zero search of the difference function of the calculated and actual nodal powers.

$$\Delta\underline{\boldsymbol{s}}_{\mathrm{K}} = \underline{\boldsymbol{s}}_{\mathrm{K,calc}} - \underline{\boldsymbol{s}}_{\mathrm{K,act}} = \boldsymbol{0} \tag{4.24}$$

By doing so, it is necessary to consider that $\underline{\boldsymbol{s}}_{\mathrm{K,act}}$ probably shows a voltage dependent characteristic and needs to be updated in each iteration step (see Fig. 17) along with the improvement of the voltage vector.

Due to the k complex-valued nodal voltages consist of two independent values (magnitude and phase or real and imaginary part), $2\,k$ equations are needed to uniquely solve the problem. Therefore, eq. (4.24) is separated into active and reactive power.

$$\begin{bmatrix} \Delta \boldsymbol{p}_{\mathrm{K}} \\ \Delta \boldsymbol{q}_{\mathrm{K}} \end{bmatrix} = 3 \begin{bmatrix} \mathrm{Re}\left\{ \underline{\boldsymbol{U}}_{\mathrm{K}} \left(\underline{\boldsymbol{Y}}_{\mathrm{KK}}\, \underline{\boldsymbol{u}}_{\mathrm{K}} \right)^{*} \right\} \\ \mathrm{Im}\left\{ \underline{\boldsymbol{U}}_{\mathrm{K}} \left(\underline{\boldsymbol{Y}}_{\mathrm{KK}}\, \underline{\boldsymbol{u}}_{\mathrm{K}} \right)^{*} \right\} \end{bmatrix} - \begin{bmatrix} \boldsymbol{p}_{\mathrm{K,act}} \\ \boldsymbol{q}_{\mathrm{K,act}} \end{bmatrix} \tag{4.25}$$

The linearization of eq. (4.25) needs to be done in each iteration step ν by building a Taylor-series expansion.

$$\boldsymbol{f}\left(\boldsymbol{x}_{\nu}\right) \approx \boldsymbol{f}\left(\boldsymbol{x}_{\nu-1}\right) + \frac{\partial \boldsymbol{f}}{\partial \boldsymbol{x}_{\nu-1}^{\mathrm{T}}} \Delta \boldsymbol{x}_{\nu} \tag{4.26}$$

$\Delta \boldsymbol{x}_{\nu}$ is the difference vector, which needs to be added to $\boldsymbol{x}_{\nu}$ to get a better guess of the zero position.

$$\boldsymbol{x}_{\nu} = \boldsymbol{x}_{\nu-1} + \Delta \boldsymbol{x}_{\nu} \tag{4.27}$$

Application of the Taylor-series expansion to the power flow equation results in

$$\Delta \underline{\boldsymbol{s}}_{\mathrm{K}} = \underline{\boldsymbol{f}}\left(\boldsymbol{x}\right) \tag{4.28}$$

$$\begin{bmatrix} \boldsymbol{0} \\ \boldsymbol{0} \end{bmatrix} \approx \left(\begin{bmatrix} \boldsymbol{p}_{\mathrm{K,calc}}\left(x_{\nu-1}\right) \\ \boldsymbol{q}_{\mathrm{K,calc}}\left(x_{\nu-1}\right) \end{bmatrix} + \begin{bmatrix} \dfrac{\partial \boldsymbol{p}_{\mathrm{K,calc}}}{\partial \boldsymbol{x}_{\nu-1}^{\mathrm{T}}} \\ \dfrac{\partial \boldsymbol{q}_{\mathrm{K,calc}}}{\partial \boldsymbol{x}_{\nu-1}^{\mathrm{T}}} \end{bmatrix} \Delta \boldsymbol{x}_{\nu} \right) - \begin{bmatrix} \boldsymbol{p}_{\mathrm{K,act}} \\ \boldsymbol{q}_{\mathrm{K,act}} \end{bmatrix} \tag{4.29}$$

Reformulation results in

$$\begin{bmatrix} \dfrac{\partial \boldsymbol{p}_{\mathrm{K,calc}}}{\partial \boldsymbol{x}_{\nu-1}^{\mathrm{T}}} \\ \dfrac{\partial \boldsymbol{q}_{\mathrm{K,calc}}}{\partial \boldsymbol{x}_{\nu-1}^{\mathrm{T}}} \end{bmatrix} \Delta \boldsymbol{x}_{\nu} = \begin{bmatrix} \boldsymbol{p}_{\mathrm{K,act}} \\ \boldsymbol{q}_{\mathrm{K,act}} \end{bmatrix} - \begin{bmatrix} \boldsymbol{p}_{\mathrm{K,calc}}\left(x_{\nu-1}\right) \\ \boldsymbol{q}_{\mathrm{K,calc}}\left(x_{\nu-1}\right) \end{bmatrix} \tag{4.30}$$

Or in abbreviated diction with the Jacobian $\boldsymbol{J}$ and the power differences $\Delta \boldsymbol{s}$

$$\boldsymbol{J}_{\nu-1}\, \Delta \boldsymbol{x}_{\nu} = -\Delta \boldsymbol{s}_{\nu-1} \tag{4.31}$$

The Jacobean depends on the chosen reference frame and consists of four submatrices, which are further described in the following.

$$\boldsymbol{J} = \begin{bmatrix} \boldsymbol{H} & \boldsymbol{N} \\ \boldsymbol{M} & \boldsymbol{L} \end{bmatrix} \tag{4.32}$$

4.3.1 Newton-Raphson in Cartesian coordinates

In Cartesian coordinates $\boldsymbol{x}$ consists of the real and imaginary part of the nodal voltages

$$\boldsymbol{x} = \begin{bmatrix} \boldsymbol{u}_{\mathrm{K,r}} \\ \boldsymbol{u}_{\mathrm{K,i}} \end{bmatrix} = \begin{bmatrix} \mathrm{Re}\left\{ \underline{\boldsymbol{u}}_{\mathrm{K}} \right\} \\ \mathrm{Im}\left\{ \underline{\boldsymbol{u}}_{\mathrm{K}} \right\} \end{bmatrix} \tag{4.33}$$

with the bus admittance matrix

$$\underline{\boldsymbol{Y}}_{\mathrm{KK}} = \boldsymbol{G} + \mathrm{j}\,\boldsymbol{B} \tag{4.34}$$

The real and imaginary part of the nodal currents can be calculated. To calculate nodal powers, the complex-conjugate of the nodal currents are needed which is why the imaginary part is already multiplied by -1.

$$\begin{bmatrix} \boldsymbol{i}_{\mathrm{K,r}} \\ -\boldsymbol{i}_{\mathrm{K,i}} \end{bmatrix} = \begin{bmatrix} \boldsymbol{G} & -\boldsymbol{B} \\ -\boldsymbol{B} & -\boldsymbol{G} \end{bmatrix} \begin{bmatrix} \boldsymbol{u}_{\mathrm{K,r}} \\ \boldsymbol{u}_{\mathrm{K,i}} \end{bmatrix} \tag{4.35}$$

So, the nodal powers result in

$$\begin{aligned} \begin{bmatrix} \boldsymbol{p}_{\mathrm{K,calc}} \\ \boldsymbol{q}_{\mathrm{K,calc}} \end{bmatrix} &= 3 \begin{bmatrix} \boldsymbol{U}_{\mathrm{K,r}} & -\boldsymbol{U}_{\mathrm{K,i}} \\ \boldsymbol{U}_{\mathrm{K,i}} & \boldsymbol{U}_{\mathrm{K,r}} \end{bmatrix} \begin{bmatrix} \boldsymbol{G} & -\boldsymbol{B} \\ -\boldsymbol{B} & -\boldsymbol{G} \end{bmatrix} \begin{bmatrix} \boldsymbol{u}_{\mathrm{K,r}} \\ \boldsymbol{u}_{\mathrm{K,i}} \end{bmatrix} \\ &= 3 \begin{bmatrix} \left(\boldsymbol{U}_{\mathrm{K,r}}\,\boldsymbol{G} + \boldsymbol{U}_{\mathrm{K,i}}\,\boldsymbol{B}\right)\boldsymbol{u}_{\mathrm{K,r}} + \left(-\boldsymbol{U}_{\mathrm{K,r}}\,\boldsymbol{B} + \boldsymbol{U}_{\mathrm{K,i}}\,\boldsymbol{G}\right)\boldsymbol{u}_{\mathrm{K,i}} \\ \left(\boldsymbol{U}_{\mathrm{K,i}}\,\boldsymbol{G} - \boldsymbol{U}_{\mathrm{K,r}}\,\boldsymbol{B}\right)\boldsymbol{u}_{\mathrm{K,r}} - \left(\boldsymbol{U}_{\mathrm{K,i}}\,\boldsymbol{B} + \boldsymbol{U}_{\mathrm{K,r}}\,\boldsymbol{G}\right)\boldsymbol{u}_{\mathrm{K,i}} \end{bmatrix} \end{aligned} \tag{4.36}$$

To linearize eq. (4.36), four auxiliary matrices are built

$$\begin{aligned} \boldsymbol{H}_1 &= \boldsymbol{U}_{\mathrm{K,r}}\,\boldsymbol{G} + \boldsymbol{U}_{\mathrm{K,i}}\,\boldsymbol{B} \\ \boldsymbol{H}_2 &= -\boldsymbol{U}_{\mathrm{K,r}}\,\boldsymbol{B} + \boldsymbol{U}_{\mathrm{K,i}}\,\boldsymbol{G} \\ \boldsymbol{H}_3 &= \mathrm{diag}\left(\boldsymbol{G}\,\boldsymbol{u}_{\mathrm{K,r}} - \boldsymbol{B}\,\boldsymbol{u}_{\mathrm{K,i}}\right) \\ \boldsymbol{H}_4 &= \mathrm{diag}\left(\boldsymbol{B}\,\boldsymbol{u}_{\mathrm{K,r}} + \boldsymbol{G}\,\boldsymbol{u}_{\mathrm{K,i}}\right) \end{aligned} \tag{4.37}$$

To include the dependency of the (given) nodal active and reactive powers on the voltage magnitudes, the diagonal matrices of the auxiliary vectors $\boldsymbol{h}_5$, $\boldsymbol{h}_6$, $\boldsymbol{h}_7$ and $\boldsymbol{h}_8$ have to be considered as well. Their coefficients are calculated as follows

$$\begin{aligned} h_{5,i} &= \frac{\partial P_{\mathrm{K,act},i}}{\partial U_{\mathrm{K,r},i}} = p_i\; P_{\mathrm{K,act},i}\,\frac{U_{\mathrm{K,r},i}}{U_{\mathrm{K},i}} \\ h_{6,i} &= \frac{\partial P_{\mathrm{K,act},i}}{\partial U_{\mathrm{K,i},i}} = p_i\; P_{\mathrm{K,act},i}\,\frac{U_{\mathrm{K,i},i}}{U_{\mathrm{K},i}} \\ h_{7,i} &= \frac{\partial Q_{\mathrm{K,act},i}}{\partial U_{\mathrm{K,r},i}} = q_i\; Q_{\mathrm{K,act},i}\,\frac{U_{\mathrm{K,r},i}}{U_{\mathrm{K},i}} \\ h_{8,i} &= \frac{\partial Q_{\mathrm{K,act},i}}{\partial U_{\mathrm{K,i},i}} = q_i\; Q_{\mathrm{K,act},i}\,\frac{U_{\mathrm{K,i},i}}{U_{\mathrm{K},i}} \end{aligned} \tag{4.38}$$

This now results in the Jacobian

$$\boldsymbol{J} = \begin{bmatrix} \dfrac{\partial \boldsymbol{p}_{\mathrm{K}}}{\partial \boldsymbol{u}_{\mathrm{K,r}}^{\mathrm{T}}} & \dfrac{\partial \boldsymbol{p}_{\mathrm{K}}}{\partial \boldsymbol{u}_{\mathrm{K,i}}^{\mathrm{T}}} \\ \dfrac{\partial \boldsymbol{q}_{\mathrm{K}}}{\partial \boldsymbol{u}_{\mathrm{K,r}}^{\mathrm{T}}} & \dfrac{\partial \boldsymbol{q}_{\mathrm{K}}}{\partial \boldsymbol{u}_{\mathrm{K,i}}^{\mathrm{T}}} \end{bmatrix} = 3 \begin{bmatrix} \boldsymbol{H}_1 + \boldsymbol{H}_3 - \boldsymbol{H}_5 & \boldsymbol{H}_2 + \boldsymbol{H}_4 - \boldsymbol{H}_6 \\ \boldsymbol{H}_2 - \boldsymbol{H}_4 - \boldsymbol{H}_7 & \boldsymbol{H}_3 - \boldsymbol{H}_1 - \boldsymbol{H}_8 \end{bmatrix} \tag{4.39}$$

Thus, in Cartesian coordinates, eq. (4.31) has the following form

$$\left[\begin{array}{ccc:ccc} h_{11} & \cdots & h_{1k} & n_{11} & \cdots & n_{1k} \\ \vdots & \ddots & \vdots & \vdots & \ddots & \vdots \\ h_{k1} & \cdots & h_{kk} & n_{k1} & \cdots & n_{kk} \\ \hdashline m_{11} & \cdots & m_{1k} & l_{11} & \cdots & l_{1k} \\ \vdots & \ddots & \vdots & \vdots & \ddots & \vdots \\ m_{k1} & \cdots & m_{kk} & l_{k1} & \cdots & l_{kk} \end{array}\right] \left[\begin{array}{c} \Delta U_{1,\mathrm{r}} \\ \vdots \\ \Delta U_{k,\mathrm{r}} \\ \hdashline \Delta U_{1,\mathrm{i}} \\ \vdots \\ \Delta U_{k,\mathrm{i}} \end{array}\right] = -\left[\begin{array}{c} \Delta P_1 \\ \vdots \\ \Delta P_k \\ \hdashline \Delta Q_1 \\ \vdots \\ \Delta Q_k \end{array}\right] \tag{4.40}$$

At the slack node, the voltage does not change in any iteration step. This means

$$\begin{aligned} \Delta U_{\mathrm{s,r}} &= 0 \\ \Delta U_{\mathrm{s,i}} &= 0 \end{aligned} \tag{4.41}$$

Eq. (4.41) can be inserted into eq. (4.40). Therefore, the active and reactive power difference equations are removed from the original equation system and replaced by the above constraints.

$$\left[\begin{array}{ccccccc:ccccccc} h_{1,1} & \cdots & h_{1,s-1} & 0 & h_{1,s+1} & \cdots & h_{1,k} & n_{1,1} & \cdots & n_{1,s-1} & 0 & n_{1,s+1} & \cdots & n_{1,k} \\ \vdots & \ddots & \vdots & \vdots & \vdots & \ddots & \vdots & \vdots & \ddots & \vdots & \vdots & \vdots & \ddots & \vdots \\ h_{s-1,1} & \cdots & h_{s-1,s-1} & 0 & h_{s-1,s+1} & \cdots & h_{s-1,k} & n_{s-1,1} & \cdots & n_{s-1,s-1} & 0 & n_{s-1,s+1} & \cdots & n_{s-1,k} \\ 0 & \cdots & 0 & 1 & 0 & \cdots & 0 & 0 & \cdots & 0 & 0 & 0 & \cdots & 0 \\ h_{s+1,1} & \cdots & h_{s+1,s-1} & 0 & h_{s+1,s+1} & \cdots & h_{s+1,k} & n_{s+1,1} & \cdots & n_{s+1,s-1} & 0 & n_{s+1,s+1} & \cdots & n_{s+1,k} \\ \vdots & \ddots & \vdots & \vdots & \vdots & \ddots & \vdots & \vdots & \ddots & \vdots & \vdots & \vdots & \ddots & \vdots \\ h_{k,1} & \cdots & h_{k,s-1} & 0 & h_{k,s+1} & \cdots & h_{k,k} & n_{k,1} & \cdots & n_{k,s-1} & 0 & n_{k,s+1} & \cdots & n_{k,k} \\ \hdashline m_{1,1} & \cdots & m_{1,s-1} & 0 & m_{1,s+1} & \cdots & m_{1,k} & l_{1,1} & \cdots & l_{1,s-1} & 0 & l_{1,s+1} & \cdots & l_{1,k} \\ \vdots & \ddots & \vdots & \vdots & \vdots & \ddots & \vdots & \vdots & \ddots & \vdots & \vdots & \vdots & \ddots & \vdots \\ m_{s-1,1} & \cdots & m_{s-1,s-1} & 0 & m_{s-1,s+1} & \cdots & m_{s-1,k} & l_{s-1,1} & \cdots & l_{s-1,s-1} & 0 & l_{s-1,s+1} & \cdots & l_{s-1,k} \\ 0 & \cdots & 0 & 0 & 0 & \cdots & 0 & 0 & \cdots & 0 & 1 & 0 & \cdots & 0 \\ m_{s+1,1} & \cdots & m_{s+1,s-1} & 0 & m_{s+1,s+1} & \cdots & m_{s+1,k} & l_{s+1,1} & \cdots & l_{s+1,s-1} & 0 & l_{s+1,s+1} & \cdots & l_{s+1,k} \\ \vdots & \ddots & \vdots & \vdots & \vdots & \ddots & \vdots & \vdots & \ddots & \vdots & \vdots & \vdots & \ddots & \vdots \\ m_{k,1} & \cdots & m_{k,s-1} & 0 & m_{k,s+1} & \cdots & m_{k,k} & l_{k,1} & \cdots & l_{k,s-1} & 0 & l_{k,s+1} & \cdots & l_{k,k} \end{array}\right] \left[\begin{array}{c} \Delta U_{1,\mathrm{r}} \\ \vdots \\ \Delta U_{\mathrm{s-1,r}} \\ \Delta U_{\mathrm{s,r}} \\ \Delta U_{\mathrm{s+1,r}} \\ \vdots \\ \Delta U_{k,\mathrm{r}} \\ \hdashline \Delta U_{1,\mathrm{i}} \\ \vdots \\ \Delta U_{\mathrm{s-1,i}} \\ \Delta U_{\mathrm{s,i}} \\ \Delta U_{\mathrm{s+1,i}} \\ \vdots \\ \Delta U_{k,\mathrm{i}} \end{array}\right] = -\left[\begin{array}{c} \Delta P_1 \\ \vdots \\ \Delta P_{s-1} \\ 0 \\ \Delta P_{s+1} \\ \vdots \\ \Delta P_k \\ \hdashline \Delta Q_1 \\ \vdots \\ \Delta Q_{s-1} \\ 0 \\ \Delta Q_{s+1} \\ \vdots \\ \Delta Q_k \end{array}\right] \tag{4.42}$$

Setting the remaining elements of the two slack columns to zero has no effect on the solution of the equation system, due to $\Delta U_{\mathrm{s,r}}$ and $\Delta U_{\mathrm{s,i}}$ are zero due to the constraints. Modification of these elements is actually not necessary, but making the Jacobian as sparse as possible may speed up the calculation process and might therefore be advantageous.

In Cartesian form, generator nodes need to be implemented into the equation system in the same way as described for the Gauss-Seidel iteration, which means after the update vector is calculated, it is necessary to reset the voltage magnitude to the reference value and recalculate the reactive power output of the generator. For this reason, usually polar coordinates are used to calculate the power flow. Nevertheless, Cartesian coordinates still provide some useful advantages:

- Simple calculation of the Jacobian.
- The Jacobian is based on gradients of quadratic instead of trigonometric functions.
- Convergence radius is marginally larger.

4.3.2 Newton-Raphson in polar coordinates

In polar coordinates the state vector $\boldsymbol{x}$ consists of the phase angle and the magnitude of the nodal voltages

$$\boldsymbol{x} = \begin{bmatrix} \boldsymbol{\delta}_{\mathrm{K}} \\ \boldsymbol{u}_{\mathrm{K}} \end{bmatrix} \tag{4.43}$$

Using

$$\underline{U}_i = U_i \, \mathrm{e}^{\mathrm{j}\,\delta_i} \tag{4.44}$$

and the coefficients $\underline{Y}_{i,j}$ of the bus admittance matrix

$$\underline{Y}_{i,j} = Y_{i,j} \, \mathrm{e}^{\mathrm{j}\,\alpha_{i,j}} \tag{4.45}$$

Nodal power can be calculated as follows

$$\boldsymbol{p}_{\mathrm{K,calc}} = 3 \, \mathrm{Re}\left\{ \underline{\boldsymbol{U}}_{\mathrm{K}} \left(\underline{\boldsymbol{Y}}_{\mathrm{KK}} \, \underline{\boldsymbol{u}}_{\mathrm{K}} \right)^{*} \right\}$$

$$\begin{bmatrix} P_{1,\mathrm{calc}} \\ \vdots \\ P_{i,\mathrm{calc}} \\ \vdots \\ P_{k,\mathrm{calc}} \end{bmatrix} = 3 \begin{bmatrix} U_1 Y_{11} U_1 \cos\left(-\alpha_{11}\right) + \cdots + U_1 Y_{1i} U_i \cos\left(\delta_1 - \delta_i - \alpha_{1i}\right) + \cdots + U_1 Y_{1k} U_k \cos\left(\delta_1 - \delta_k - \alpha_{1k}\right) \\ \vdots \\ U_i Y_{i1} U_1 \cos\left(\delta_i - \delta_1 - \alpha_{i1}\right) + \cdots + U_i Y_{ii} U_i \cos\left(-\alpha_{ii}\right) + \cdots + U_i Y_{ik} U_k \cos\left(\delta_i - \delta_k - \alpha_{ik}\right) \\ \vdots \\ U_k Y_{k1} U_1 \cos\left(\delta_k - \delta_1 - \alpha_{k1}\right) + \cdots + U_k Y_{ki} U_i \cos\left(\delta_k - \delta_i - \alpha_{ki}\right) + \cdots + U_k Y_{kk} U_k \cos\left(-\alpha_{kk}\right) \end{bmatrix} \tag{4.46}$$

$$\boldsymbol{q}_{\mathrm{K,calc}} = 3 \, \mathrm{Im}\left\{ \underline{\boldsymbol{U}}_{\mathrm{K}} \left(\underline{\boldsymbol{Y}}_{\mathrm{KK}} \, \underline{\boldsymbol{u}}_{\mathrm{K}} \right)^{*} \right\}$$

$$\begin{bmatrix} Q_{1,\mathrm{calc}} \\ \vdots \\ Q_{i,\mathrm{calc}} \\ \vdots \\ Q_{k,\mathrm{calc}} \end{bmatrix} = 3 \begin{bmatrix} U_1 Y_{11} U_1 \sin\left(-\alpha_{11}\right) + \cdots + U_1 Y_{1i} U_i \sin\left(\delta_1 - \delta_i - \alpha_{1i}\right) + \cdots + U_1 Y_{1k} U_k \sin\left(\delta_1 - \delta_k - \alpha_{1k}\right) \\ \vdots \\ U_i Y_{i1} U_1 \sin\left(\delta_i - \delta_1 - \alpha_{i1}\right) + \cdots + U_i Y_{ii} U_i \sin\left(-\alpha_{ii}\right) + \cdots + U_i Y_{ik} U_k \sin\left(\delta_i - \delta_k - \alpha_{ik}\right) \\ \vdots \\ U_k Y_{k1} U_1 \sin\left(\delta_k - \delta_1 - \alpha_{k1}\right) + \cdots + U_k Y_{ki} U_i \sin\left(\delta_k - \delta_i - \alpha_{ki}\right) + \cdots + U_k Y_{kk} U_k \sin\left(-\alpha_{kk}\right) \end{bmatrix} \tag{4.47}$$

Linearization of eq. (4.46) and eq. (4.47) results in

$$\boldsymbol{J} = \begin{bmatrix} \dfrac{\partial \boldsymbol{p}_{\mathrm{K}}}{\partial \boldsymbol{\delta}_{\mathrm{K}}^{\mathrm{T}}} & \dfrac{\partial \boldsymbol{p}_{\mathrm{K}}}{\partial \boldsymbol{u}_{\mathrm{K}}^{\mathrm{T}}} \\ \dfrac{\partial \boldsymbol{q}_{\mathrm{K}}}{\partial \boldsymbol{\delta}_{\mathrm{K}}^{\mathrm{T}}} & \dfrac{\partial \boldsymbol{q}_{\mathrm{K}}}{\partial \boldsymbol{u}_{\mathrm{K}}^{\mathrm{T}}} \end{bmatrix} = \begin{bmatrix} \boldsymbol{H} & \boldsymbol{N} \\ \boldsymbol{M} & \boldsymbol{L} \end{bmatrix} \tag{4.48}$$

Using the diagonal matrices $\boldsymbol{P}_{\mathrm{K,calc}}$ and $\boldsymbol{Q}_{\mathrm{K,calc}}$ obtained from the calculated nodal powers in eq. (4.46) and eq. (4.47), the auxiliary matrix

$$\begin{aligned}\underline{\boldsymbol{S}} &= 3\,\underline{\boldsymbol{U}}_{\mathrm{K}}\left(\underline{\boldsymbol{Y}}_{\mathrm{KK}}\,\underline{\boldsymbol{U}}_{\mathrm{K}}\right)^{*} \\ &= 3\begin{bmatrix} U_1\,Y_{11}\,U_1\,\mathrm{e}^{\mathrm{j}(-\alpha_{11})} & U_1\,Y_{12}\,U_2\,\mathrm{e}^{\mathrm{j}(\delta_1-\alpha_{12}-\delta_2)} & \cdots & U_1\,Y_{1k}\,U_k\,\mathrm{e}^{\mathrm{j}(\delta_1-\alpha_{11}-\delta_k)} \\ \vdots & \vdots & \ddots & \vdots \\ U_k\,Y_{k1}\,U_1\,\mathrm{e}^{\mathrm{j}(\delta_k-\alpha_{k1}-\delta_1)} & U_k\,Y_{k2}\,U_2\,\mathrm{e}^{\mathrm{j}(\delta_k-\alpha_{k2}-\delta_2)} & \cdots & U_k\,Y_{kk}\,U_k\,\mathrm{e}^{\mathrm{j}(-\alpha_{kk})} \end{bmatrix}\end{aligned} \tag{4.49}$$

and the diagonal matrices $\boldsymbol{P}_{\mathrm{p,K,calc}}$ und $\boldsymbol{Q}_{\mathrm{q,K,calc}}$ of the derivation of the voltage magnitude dependency of the nodal active and reactive powers

$$\begin{aligned}\frac{\partial p_{\mathrm{K,calc},i}}{\partial U_{\mathrm{K},i}} &= p_i\,P_{\mathrm{K,calc},i}\,U_{\mathrm{K},i}^{-1} \\ \frac{\partial q_{\mathrm{K,calc},i}}{\partial U_{\mathrm{K},i}} &= q_i\,Q_{\mathrm{K,calc},i}\,U_{\mathrm{K},i}^{-1}\end{aligned} \tag{4.50}$$

the submatrices of the Jacobian can be built

$$\begin{aligned}\boldsymbol{H} &= \mathrm{Im}\left\{\underline{\boldsymbol{S}}\right\} - \boldsymbol{Q}_{\mathrm{K,calc}} \\ \boldsymbol{N} &= \left(\mathrm{Re}\left\{\underline{\boldsymbol{S}}\right\} + \boldsymbol{P}_{\mathrm{K,calc}}\right)\,\boldsymbol{U}_{\mathrm{K}}^{-1} - \boldsymbol{P}_{\mathrm{p,K,calc}} \\ \boldsymbol{M} &= -\mathrm{Re}\left\{\underline{\boldsymbol{S}}\right\} + \boldsymbol{P}_{\mathrm{K,calc}} \\ \boldsymbol{L} &= \left(\mathrm{Im}\left\{\underline{\boldsymbol{S}}\right\} + \boldsymbol{Q}_{\mathrm{K,calc}}\right)\,\boldsymbol{U}_{\mathrm{K}}^{-1} - \boldsymbol{Q}_{\mathrm{q,K,calc}}\end{aligned} \tag{4.51}$$

In polar coordinates eq. (4.31) has the following form

$$\left[\begin{array}{ccc:ccc} h_{11} & \cdots & h_{1k} & n_{11} & \cdots & n_{1k} \\ \vdots & \ddots & \vdots & \vdots & \ddots & \vdots \\ h_{k1} & \cdots & h_{kk} & n_{k1} & \cdots & n_{kk} \\ \hdashline m_{11} & \cdots & m_{1k} & l_{11} & \cdots & l_{1k} \\ \vdots & \ddots & \vdots & \vdots & \ddots & \vdots \\ m_{k1} & \cdots & m_{kk} & l_{k1} & \cdots & l_{kk} \end{array}\right]\left[\begin{array}{c} \Delta\delta_1 \\ \vdots \\ \Delta\delta_k \\ \hdashline \Delta U_1 \\ \vdots \\ \Delta U_k \end{array}\right] = -\left[\begin{array}{c} \Delta P_1 \\ \vdots \\ \Delta P_k \\ \hdashline \Delta Q_1 \\ \vdots \\ \Delta Q_k \end{array}\right] \tag{4.52}$$

At the slack node, voltage magnitude and phase angle do not change

$$\begin{aligned}\Delta\delta_s &= 0 \\ \Delta U_s &= 0\end{aligned} \tag{4.53}$$

Similar to the Cartesian coordinates, these constraints are implemented into the equation system by removing the slack lines and replacing them by the constraints. At the generator nodes, only the voltage magnitude is constant. That means, only in the lower half of the equation system the lines that correspond to a generator node are removed and replaced by the constraint

$$\Delta U_g = 0 \tag{4.54}$$

So, the decisive advantage that makes polar coordinates superior to the other approaches is the extremely simply way of implementing generator nodes into the equation system.

In eq. (4.50) and eq. (4.51) all summands building the submatrices $\boldsymbol{N}$ and $\boldsymbol{L}$ are multiplied by $\boldsymbol{U}_{\mathrm{K}}^{-1}$ from the right. To save some computational effort this multiplication can be avoided, if the voltage magnitudes in the solution vector are related to the voltages of the previous iteration

step. In this case, calculating the improved guess according to eq. (4.27) requires an additional multiplication of the voltage magnitude changes with $\boldsymbol{U}_{\mathrm{K}}$.

4.3.3 Initial guess

Other than the Gauss-Seidel iteration, convergence of the Newton-Raphson-approach strongly depends on the initial guess. If there are no phase-shifting transformers in the grid, usually the flat-start will lead to a good solution again. In other cases, more suitable initial guesses can be found by one of the following methods:

If there are phase-shifting transformers in the grid which do not drive a circular flow, that means there are no parallel branches to the transformer, a suitable initial guess can be found by solving the current equation system for the unloaded grid with all shunt elements deactivated.

$$\begin{bmatrix} \underline{Y}_{1,1} & \cdots & \underline{Y}_{1,s-1} & \underline{Y}_{1,s} & \underline{Y}_{1,s+1} & \cdots & \underline{Y}_{1,k} \\ \vdots & \ddots & \vdots & \vdots & \vdots & \ddots & \vdots \\ \underline{Y}_{s-1,1} & \cdots & \underline{Y}_{s-1,s-1} & \underline{Y}_{s-1,s} & \underline{Y}_{s-1,s+1} & \cdots & \underline{Y}_{s-1,k} \\ \underline{Y}_{s,1} & \cdots & \underline{Y}_{s,s-1} & \underline{Y}_{s,s} & \underline{Y}_{s,s+1} & \cdots & \underline{Y}_{s,k} \\ \underline{Y}_{s+1,1} & \cdots & \underline{Y}_{s+1,s-1} & \underline{Y}_{s+1,s} & \underline{Y}_{s+1,s+1} & \cdots & \underline{Y}_{s+1,k} \\ \vdots & \ddots & \vdots & \vdots & \vdots & \ddots & \vdots \\ \underline{Y}_{k,1} & \cdots & \underline{Y}_{k,s-1} & \underline{Y}_{k,s} & \underline{Y}_{k,s+1} & \cdots & \underline{Y}_{k,k} \end{bmatrix} \begin{bmatrix} \underline{U}_1 \\ \vdots \\ \underline{U}_{s-1} \\ \underline{U}_s \\ \underline{U}_{s+1} \\ \vdots \\ \underline{U}_k \end{bmatrix} = \begin{bmatrix} 0 \\ \vdots \\ 0 \\ \underline{I}_s \\ 0 \\ \vdots \\ 0 \end{bmatrix} \tag{4.55}$$

In eq. (4.55) all voltages except $\underline{U}_s$ are unknown and all currents except $\underline{I}_s$ are known (set to zero). The needed voltages can be obtained by solving eq. (4.6). The resulting voltage vector contains phase-shifting and voltage regulation of the transformers. This guess is therefore closer to the actual voltages than the flat-start.

If there are parallel branches to the phase-shifting transformer, it will drive a circular flow. In this case the described procedure cannot be applied, due to the resulting voltage will be too low. In this case, it is more productive to express the nodal powers as equivalent admittances. Assuming, that the actual voltage magnitude is close to the nominal voltage, the equivalent admittance at node *i* can be calculated

$$\underline{Y}_{\mathrm{L},i} = \frac{\underline{S}_i^*}{U_{\mathrm{n}}^2} \tag{4.56}$$

The equivalent admittances are then implemented into the bus admittance matrix

$$\underline{\boldsymbol{Y}}_{\mathrm{KK,L}} = \underline{\boldsymbol{Y}}_{\mathrm{KK}} - \underline{\boldsymbol{Y}}_{\mathrm{L}} \tag{4.57}$$

In this case, it is better not to remove the shunt elements. The initial voltage guess can now be calculated using eq. (4.55) again.

If the Newton-Raphson-algorithm still does not converge, the initial guess can be further improved by calculating one iteration step of the Gauss-Seidel approach and using its results.

4.3.4 Flow chart of the iteration

The iteration process is similar to the Gauss-Seidel-iteration. After choosing a suitable initial guess, first the right hand side of eq. (4.31) is calculated and afterwards the Jacobian is built depending on the chosen coordinate system. The slack and generator node constraints are now implemented into the equation system. Now, an update vector is calculated which leads to a new and improved guess of the nodal voltages. If the elements of the update vector are smaller than a predefined threshold, the iteration is over, because the solution is sufficiently close to the zero position. Otherwise, an additional iteration step is needed. The flow chart is given in Fig. 20.

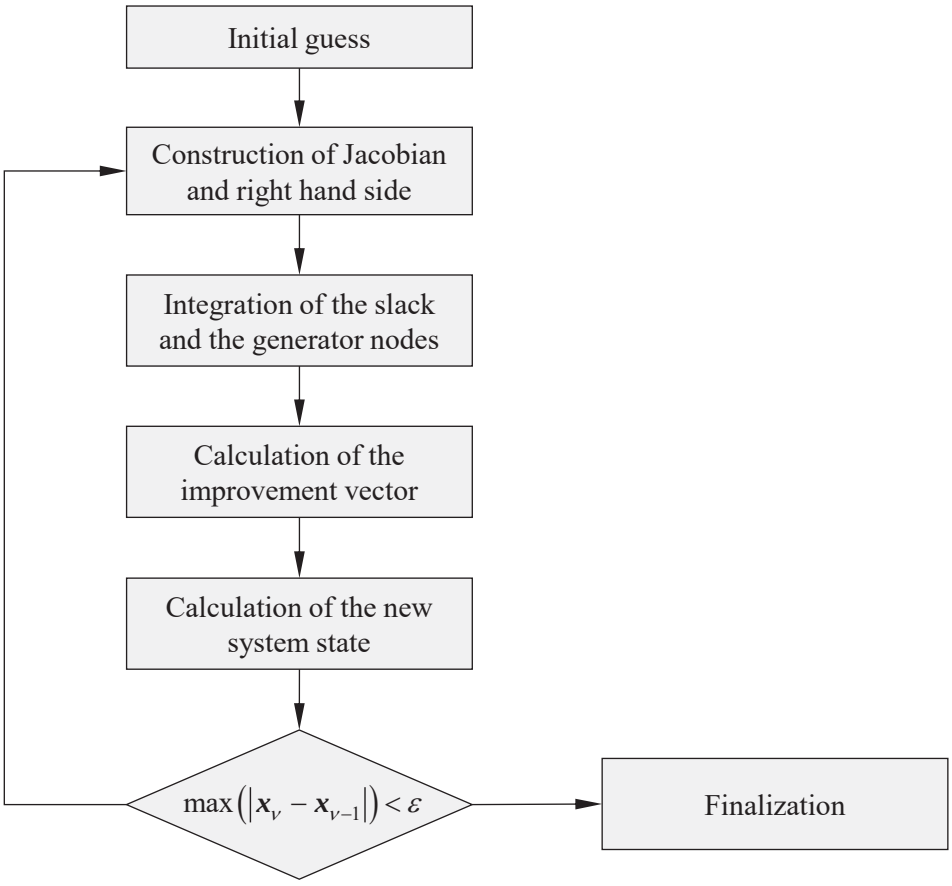

Fig. 20: flow chart of the Newton-Raphson-approach

The most important properties of the Newton-Raphson method are:

- Small convergence radius, that means, if the initial guess is bad, the approach will diverge or find an invalid solution
- High convergence speed, that means, only a few iterations are needed to find a sufficiently good solution.
- The Jacobian needs to be set up entirely new in each iteration step.
- The number of needed iterations is independent from the grid size and should be around three to five iterations depending on the loading of the grid.
- Easy implementation of generator nodes

Programming of the setup of the Jacobian needs to be as efficient as possible, due to this step is computationally intense. To save some time, the Jacobian may be newly calculated e.g. only every second iteration step. Nevertheless, this will lead to the loss of optimal convergence and may require additional iterations.

4.4 Decoupled power flow calculation

Another possibility to save time building the Jacobian is to exploit simplifications that can be applied due to special grid properties. This may result in a slightly different result compared to the entire power flow calculation, but if applied correctly, the deviation stays sufficiently small, such that the gained calculation speed is more advantageous than the loss of accuracy.

The *R*/*X*-ratio in the extra-high voltage level is around 1:10, which means, the grid can be assumed to be entirely inductive and the ohmic part can be neglected. In eq. (4.45), this means, that the phase angle α of the admittance is $\pi/2$. Compared to that, the phase angle difference of the nodal voltages is rather small. In eq. (4.46) and eq. (4.47) this results in

$$\begin{aligned}\cos\left(-\alpha_{i,j}+\delta_i-\delta_j\right) &\approx \cos\left(-\alpha_{i,j}\right) \approx \cos\left(-\frac{\pi}{2}\right)=0\\ \sin\left(-\alpha_{i,j}+\delta_i-\delta_j\right) &\approx \sin\left(-\alpha_{i,j}\right) \approx \sin\left(-\frac{\pi}{2}\right)=-1\end{aligned} \tag{4.58}$$

This simplification leads to the following Jacobian

$$\boldsymbol{J}=\begin{bmatrix}\boldsymbol{H} & \boldsymbol{0}\\ \boldsymbol{0} & \boldsymbol{L}\end{bmatrix} \tag{4.59}$$

with its submatrices

$$\begin{aligned}\boldsymbol{H} &= 3\,\boldsymbol{U}_{\mathrm{K}}\boldsymbol{B}\,\boldsymbol{U}_{\mathrm{K}}\\ \boldsymbol{L} &= 3\left(\boldsymbol{U}_{\mathrm{K}}\boldsymbol{B}+\operatorname{diag}\left(\boldsymbol{B}\,\boldsymbol{u}_{\mathrm{K}}\right)\right)\end{aligned} \tag{4.60}$$

The power flow equation system is now decomposed into two smaller and independent equation systems.

$$\begin{aligned}\boldsymbol{H}\;\Delta\boldsymbol{\delta}_{\mathrm{K}} &= \Delta\boldsymbol{p}_{\mathrm{K}}\\ \boldsymbol{L}\,\Delta\boldsymbol{u}_{\mathrm{K}} &= \Delta\boldsymbol{q}_{\mathrm{K}}\end{aligned} \tag{4.61}$$

They still need to be solved iteratively because the Jacobian depends on the guess of the voltages.

4.5 Fast decoupled power flow (DC power flow)

The fast decoupled power flow, which is also called DC power flow, additionally assumes, that the related voltage magnitudes at each nodes are constant and match e.g. with the nominal voltage. Using this assumption, $\Delta\boldsymbol{u}_{\mathrm{K}}$ does not need to be calculated any more. Furthermore, $\boldsymbol{H}$ becomes constant, due to $\boldsymbol{H}$ does also not depend on phase angles. Thus, iterations are not needed anymore. The resulting nodal voltage phase angle can directly be obtained by solving the linear equation system

$$\boldsymbol{H}\ \boldsymbol{\delta}_{\mathrm{K}} = \boldsymbol{p}_{\mathrm{K}} \tag{4.62}$$

Still, at the slack node, the reference angle needs to be set manually. If it is zero, the slack line and column simply can be removed from the equation system.

Due to the many simplifications and assumptions, the result of the DC power flow differs tremendously from the full power flow result. It is therefore only applied, if a very large number of power flow calculations need to be performed (e.g. in Monte-Carlo-simulations or reliability studies), in studies, that do not focus primarily on the grid result (e.g. market simulations) or to estimate phase angles as an initial guess for the Newton-Raphson-approach. For the purpose of grid planning and especially grid operation, its results are much too defective.

The above mentioned assumptions for the decoupled and the fast decoupled power flow calculation are only valid for the extra-high voltage level. In the high voltage level or below, the R/X-ratio increases. Thus, the calculation error increases that much, such that the results cannot be used.

5 State Estimation

Similar to the power flow calculation, the state estimation is used to find a consistent grid state, i.e. a set of nodal voltages. It is used in system operation to observe the grid and merge the measured information into a consistent system state. Therefore, not only nodal active and reactive powers are used as input parameters, but every possible and available measurement from the grid as well as pseudo measurement. The estimated grid state

$$\boldsymbol{x}_{\text{est}} = \left[\delta_{1,\text{est}} \quad \cdots \quad \delta_{k,\text{est}} \,\vdots\, U_{1,\text{est}} \quad \cdots \quad U_{k,\text{est}} \right]^{\text{T}} \tag{5.1}$$

is supposed to be as close to the actual grid state as possible

$$\boldsymbol{x}_{\text{act}} = \left[\delta_{1,\text{act}} \quad \cdots \quad \delta_{k,\text{act}} \,\vdots\, U_{1,\text{act}} \quad \cdots \quad U_{k,\text{act}} \right]^{\text{T}} \tag{5.2}$$

This can be achieved by using a weighted least-squares approach originally described by Gauss. The estimated grid state is the basis for all other grid calculations, e.g. contingency analysis or short-circuit calculations and is used by the operational staff for decision-making.

In a conventional SCADA-system measured values are typically nodal active und reactive powers, terminal active and reactive powers, nodal voltage magnitudes as well as nodal and terminal current magnitudes. They can be merged to a measurement vector $\boldsymbol{z}_{\text{m}}$.

$$\boldsymbol{z}_{\text{m}} = \left[\boldsymbol{p}_{\text{K,m}}^{\text{T}} \quad \boldsymbol{q}_{\text{K,m}}^{\text{T}} \,\vdots\, \boldsymbol{p}_{\text{T,m}}^{\text{T}} \quad \boldsymbol{q}_{\text{T,m}}^{\text{T}} \,\vdots\, \boldsymbol{u}_{\text{K,m}}^{\text{T}} \,\vdots\, \boldsymbol{i}_{\text{K,m}}^{\text{T}} \quad \boldsymbol{i}_{\text{T,m}}^{\text{T}} \right]^{\text{T}} \tag{5.3}$$

If there are phasor measurement units (PMUs) available in the grid, phasor information can be additionally included in the state estimation process. Nowadays, although PMUs are installed they are typically still not used for operational purposes, due to phase angle differences are quite small in highly meshed grids and a small phasor measurement error may lead to high deviations in the active power flow estimation and therefore do not help to improve the estimation result. The same applies to currents. While active and reactive powers can be measured with correct sign, information of flow direction (load or generation) is lost, if only current magnitudes are measured. Hence, they may have bad influence on the convergence of the state estimation. So, they are usually not used. In fact, the measurement vector in the extra-high voltage level consists of about 75 % terminal powers, 20 % nodal powers and 5 % nodal voltage magnitudes.

5.1 Measurement error and redundancy

While PMUs offer a precise and synchronized measurement, conventional SCADA-technology cannot determine the measured information simultaneously and without error. Generally, all measurands (even those of PMUs) are superposed by inaccuracies. That means, the measured value z_{m} is the sum of the actual value z and the error Δz.

$$z_{\text{m}} = z + \Delta z \tag{5.4}$$

Δz may consist of a systematic and a stochastic component. In the following, it is assumed, that the systematic part is sufficiently eliminated e.g. by calibration such that only the stochastic part needs to be considered. It depends on the chosen measurement process, the measured value and the quality of the measurement device. It is further assumed, that the measurement error is

normally distributed. In Fig. 21 the probability density functions of two measurement devices with different quality are shown.

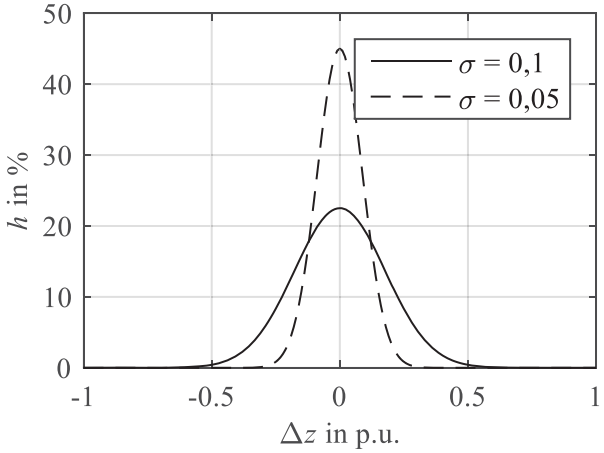

Fig. 21: normally distributed measurement error

The probability function of a normal distribution is

$$h(\Delta z) = \frac{1}{\sqrt{2\,\pi\,\sigma^2}}\,\mathrm{e}^{-\frac{\Delta z^2}{2\,\pi\,\sigma^2}} \tag{5.5}$$

σ is the standard deviation of the normal distribution function. The higher the quality of the measurement device, the lower the standard deviation of the error.

To obtain a consistent grid state out of the bunch of faulty measurement information, and to make this grid state close to the actual one, deviations and even outages of measurement devices need to be compensated. To do so, redundant measurement is necessary, that means, there are more measurement devices in the grid than actually needed to describe the system state. Furthermore, it is assumed, that all measurands and thus all measurement errors are independent. Similar to the power flow approach, the system state is described by the complex-valued nodal voltage vector. So, for a grid with k nodes, 2 k system variables (magnitude and phase angle or real and imaginary part) need to be calculated.

The relation of the number of measurements m and the number of system variables is used to define the amount of redundancy

$$r = \frac{m}{2\,k} - 1 \tag{5.6}$$

To compensate the outage of a measurement device, a redundancy of $r > 1$ is aspired. That means, the number of measurement devices is theoretically four times higher than the number of nodes. In the European transmission system, redundancy is even higher, due to all equipment is fully observed. This includes pseudo measurement which are pieces of information that are well-known although they cannot or do not need to be actually measured. For example, nodal powers of a fictitious node e.g. branching points of overhead lines are always zero and thus known without measuring. Pseudo measurement can be included into the state estimation process with a fictitious, high measurement quality.

5.2 State estimation with linear measurement model

If there is an entirely linear dependency of measurands and system variables, the measurands can be expressed using a linear equation system.

$$\boldsymbol{z} = \boldsymbol{H}\ \boldsymbol{x} \tag{5.7}$$

$\boldsymbol{H}$ is the measurement model matrix and has the dimension $m \times 2k$. Its coefficients are constant and do not depend on $\boldsymbol{x}_{\text{est}}$. Due to the above-mentioned high redundancy, the equation system is overdetermined. It contains more equations than system variables. Such a measurement model can be found in DC grids, if only currents and voltages are used as measurands. In three-phase AC systems a linear measurement model can be achieved, if solely PMU data is used, such that the estimation is based on complex-valued currents and voltages. As soon as powers or magnitudes are used as measurands, the measurement model is non-linear.

According to eq. (5.4) and eq. (5.7) the measured values can be expressed as a function of the system state and the measurement error.

$$\boldsymbol{z}_{\text{m}} = \boldsymbol{H}\ \boldsymbol{x}_{\text{est}} + \Delta\boldsymbol{z} \tag{5.8}$$

The task of state estimation is to find a state vector $\boldsymbol{x}_{\text{est}}$ which minimizes the error in eq. (5.8)

$$\Delta\boldsymbol{z} = \boldsymbol{z}_{\text{m}} - \boldsymbol{H}\ \boldsymbol{x}_{\text{est}} \tag{5.9}$$

By doing so, the respective quality of the measurement device shall be considered. That means a high quality measurand shall be considered more reliable than the information obtained from a device with less quality. This can be achieved b relating the error to the standard deviation of the device so it gets weighted.

$$\Delta\boldsymbol{z}_{\text{g}} = \boldsymbol{S}^{-1}\Delta\boldsymbol{z} = \boldsymbol{S}^{-1}\left(\boldsymbol{z}_{\text{m}} - \boldsymbol{H}\ \boldsymbol{x}_{\text{est}}\right) = \boldsymbol{z}_{\text{m,g}} - \boldsymbol{H}_{\text{g}}\ \boldsymbol{x}_{\text{est}} \tag{5.10}$$

with the weighting matrix $\boldsymbol{S}$

$$\boldsymbol{S}^{-1} = \begin{bmatrix} \frac{1}{\sigma_1} & & \\ & \ddots & \\ & & \frac{1}{\sigma_m} \end{bmatrix} \tag{5.11}$$

The sum of the squared errors

$$F_{\text{g}} = \sum_{i=1}^{m} \Delta\boldsymbol{z}_{\text{g},i}^2 = \Delta\boldsymbol{z}_{\text{g},1}^2 + \cdots + \Delta\boldsymbol{z}_{\text{g},m}^2 \tag{5.12}$$

needs to be minimized and can therefore be expressed using eq. (5.10)

$$\begin{aligned} F_{\text{g}} &= \Delta\boldsymbol{z}_{\text{g}}^{\text{T}}\ \Delta\boldsymbol{z}_{\text{g}} = \left(\boldsymbol{z}_{\text{m,g}} - \boldsymbol{H}_{\text{g}}\ \boldsymbol{x}_{\text{est}}\right)^{\text{T}}\left(\boldsymbol{z}_{\text{m,g}} - \boldsymbol{H}_{\text{g}}\ \boldsymbol{x}_{\text{est}}\right) = \left(\boldsymbol{z}_{\text{m,g}}^{\text{T}} - \boldsymbol{x}_{\text{est}}^{\text{T}}\ \boldsymbol{H}_{\text{g}}^{\text{T}}\right)\left(\boldsymbol{z}_{\text{m,g}} - \boldsymbol{H}_{\text{g}}\ \boldsymbol{x}_{\text{est}}\right) \\ &= \boldsymbol{z}_{\text{m,g}}^{\text{T}}\ \boldsymbol{z}_{\text{m,g}} - \boldsymbol{z}_{\text{m,g}}^{\text{T}}\ \boldsymbol{H}_{\text{g}}\ \boldsymbol{x}_{\text{est}} - \boldsymbol{x}_{\text{est}}^{\text{T}}\ \boldsymbol{H}_{\text{g}}^{\text{T}}\ \boldsymbol{z}_{\text{m,g}} + \boldsymbol{x}_{\text{est}}^{\text{T}}\ \boldsymbol{H}_{\text{g}}^{\text{T}}\ \boldsymbol{H}_{\text{g}}\ \boldsymbol{x}_{\text{est}} \end{aligned} \tag{5.13}$$

To find the minimum of F_{g} its first partial derivations are set to zero.

$$\frac{\partial F_{\mathrm{g}}}{\partial \boldsymbol{x}_{\mathrm{est}}^{\mathrm{T}}} = \frac{\partial\left(\boldsymbol{z}_{\mathrm{m,g}}^{\mathrm{T}}\,\boldsymbol{z}_{\mathrm{m,g}} - \boldsymbol{z}_{\mathrm{m,g}}^{\mathrm{T}}\,\boldsymbol{H}_{\mathrm{g}}\,\boldsymbol{x}_{\mathrm{est}} - \boldsymbol{x}_{\mathrm{est}}^{\mathrm{T}}\,\boldsymbol{H}_{\mathrm{g}}^{\mathrm{T}}\,\boldsymbol{z}_{\mathrm{m,g}} + \boldsymbol{x}_{\mathrm{est}}^{\mathrm{T}}\,\boldsymbol{H}_{\mathrm{g}}^{\mathrm{T}}\,\boldsymbol{H}_{\mathrm{g}}\,\boldsymbol{x}_{\mathrm{est}}\right)}{\partial \boldsymbol{x}_{\mathrm{est}}^{\mathrm{T}}} \overset{!}{=} \boldsymbol{0} \tag{5.14}$$

For the purpose of better understanding, the partial derivations are done separately for each summand. For the first summand, this leads to

$$\frac{\partial\,\boldsymbol{z}_{\mathrm{m,g}}^{\mathrm{T}}\,\boldsymbol{z}_{\mathrm{m,g}}}{\partial\,\boldsymbol{x}_{\mathrm{est}}^{\mathrm{T}}} = \boldsymbol{0} \tag{5.15}$$

due to it only contains measured information and does not depend on $\boldsymbol{x}_{\mathrm{est}}$. The derivation of the second term leads to

$$-\frac{\partial\,\boldsymbol{z}_{\mathrm{m,g}}^{\mathrm{T}}\,\boldsymbol{H}_{\mathrm{g}}\,\boldsymbol{x}_{\mathrm{est}}}{\partial\,\boldsymbol{x}_{\mathrm{est}}^{\mathrm{T}}} = -\boldsymbol{z}_{\mathrm{m,g}}^{\mathrm{T}}\,\boldsymbol{H}_{\mathrm{g}}\frac{\partial\,\boldsymbol{x}_{\mathrm{est}}}{\partial\,\boldsymbol{x}_{\mathrm{est}}^{\mathrm{T}}} \tag{5.16}$$

Analogously, for the third summand

$$-\frac{\partial\,\boldsymbol{x}_{\mathrm{est}}^{\mathrm{T}}\,\boldsymbol{H}_{\mathrm{g}}^{\mathrm{T}}\,\boldsymbol{z}_{\mathrm{m,g}}}{\partial\,\boldsymbol{x}_{\mathrm{est}}^{\mathrm{T}}} = -\frac{\partial\,\boldsymbol{x}_{\mathrm{est}}^{\mathrm{T}}}{\partial\,\boldsymbol{x}_{\mathrm{est}}^{\mathrm{T}}}\boldsymbol{H}_{\mathrm{g}}^{\mathrm{T}}\,\boldsymbol{z}_{\mathrm{m,g}} \tag{5.17}$$

Using the product rule, derivation of the fourth summand leads to

$$\frac{\partial\,\boldsymbol{x}_{\mathrm{est}}^{\mathrm{T}}\,\boldsymbol{H}_{\mathrm{g}}^{\mathrm{T}}\,\boldsymbol{H}_{\mathrm{g}}\,\boldsymbol{x}_{\mathrm{est}}}{\partial\,\boldsymbol{x}_{\mathrm{est}}^{\mathrm{T}}} = \frac{\partial\,\boldsymbol{x}_{\mathrm{est}}^{\mathrm{T}}}{\partial\,\boldsymbol{x}_{\mathrm{est}}^{\mathrm{T}}}\boldsymbol{H}_{\mathrm{g}}^{\mathrm{T}}\,\boldsymbol{H}_{\mathrm{g}}\,\boldsymbol{x}_{\mathrm{est}} + \boldsymbol{x}_{\mathrm{est}}^{\mathrm{T}}\,\boldsymbol{H}_{\mathrm{g}}^{\mathrm{T}}\,\boldsymbol{H}_{\mathrm{g}}\frac{\partial\,\boldsymbol{x}_{\mathrm{est}}}{\partial\,\boldsymbol{x}_{\mathrm{est}}^{\mathrm{T}}} \tag{5.18}$$

F_{g} is a scalar value. That means, its transposed is again F_{g}. The same can be applied to the partial derivations. Thus

$$-\boldsymbol{z}_{\mathrm{m,g}}^{\mathrm{T}}\,\boldsymbol{H}_{\mathrm{g}}\frac{\partial\,\boldsymbol{x}_{\mathrm{est}}}{\partial\,\boldsymbol{x}_{\mathrm{est}}^{\mathrm{T}}} = -\frac{\partial\,\boldsymbol{x}_{\mathrm{est}}^{\mathrm{T}}}{\partial\,\boldsymbol{x}_{\mathrm{est}}^{\mathrm{T}}}\boldsymbol{H}_{\mathrm{g}}^{\mathrm{T}}\,\boldsymbol{z}_{\mathrm{m,g}} \tag{5.19}$$

and

$$\frac{\partial\,\boldsymbol{x}_{\mathrm{est}}^{\mathrm{T}}}{\partial\,\boldsymbol{x}_{\mathrm{est}}^{\mathrm{T}}}\boldsymbol{H}_{\mathrm{g}}^{\mathrm{T}}\,\boldsymbol{H}_{\mathrm{g}}\,\boldsymbol{x}_{\mathrm{est}} = \boldsymbol{x}_{\mathrm{est}}^{\mathrm{T}}\,\boldsymbol{H}_{\mathrm{g}}^{\mathrm{T}}\,\boldsymbol{H}_{\mathrm{g}}\frac{\partial\,\boldsymbol{x}_{\mathrm{est}}}{\partial\,\boldsymbol{x}_{\mathrm{est}}^{\mathrm{T}}} \tag{5.20}$$

So, eq. (5.14) can be reformulated

$$\frac{\partial F_{\mathrm{g}}}{\partial\,\boldsymbol{x}_{\mathrm{est}}^{\mathrm{T}}} = 2\frac{\partial\,\boldsymbol{x}_{\mathrm{est}}^{\mathrm{T}}}{\partial\,\boldsymbol{x}_{\mathrm{est}}^{\mathrm{T}}}\left(-\boldsymbol{H}_{\mathrm{g}}^{\mathrm{T}}\,\boldsymbol{z}_{m,g} + \boldsymbol{H}_{\mathrm{g}}^{\mathrm{T}}\,\boldsymbol{H}_{\mathrm{g}}\,\boldsymbol{x}_{\mathrm{est}}\right) \overset{!}{=} \boldsymbol{0} \tag{5.21}$$

Due to

$$\frac{\partial\,\boldsymbol{x}_{\mathrm{est}}^{\mathrm{T}}}{\partial\,\boldsymbol{x}_{\mathrm{est}}^{\mathrm{T}}} = \boldsymbol{E} \tag{5.22}$$

eq. (5.22) is only true, if

$$\boldsymbol{H}_{\mathrm{g}}^{\mathrm{T}}\,\boldsymbol{H}_{\mathrm{g}}\,\boldsymbol{x}_{\mathrm{est}} = \boldsymbol{H}_{\mathrm{g}}^{\mathrm{T}}\,\boldsymbol{z}_{m,g} \tag{5.23}$$

or in more detail

$$\begin{aligned} \boldsymbol{H}^{\mathrm{T}}\ \boldsymbol{R}^{-1}\ \boldsymbol{H}\ \boldsymbol{x}_{\mathrm{est}} &= \boldsymbol{H}^{\mathrm{T}}\ \boldsymbol{S}^{-1}\ \boldsymbol{z}_{\mathrm{m}} \\ \boldsymbol{A}\ \boldsymbol{x}_{\mathrm{est}} &= \boldsymbol{y} \end{aligned} \tag{5.24}$$

Eq. (5.24) is the Gaussian weighted normal equation with the covariance matrix $\boldsymbol{R}^{-1}$

$$\boldsymbol{R}^{-1} = \boldsymbol{S}^{-1}\ \boldsymbol{S}^{-1} \tag{5.25}$$

The system matrix $\boldsymbol{A}$ has the dimension $2k \times 2k$. It is positive definite and symmetric. In opposition to the non-linear measurement model, $\boldsymbol{A}$ is of rank $2k$ as soon as at least one voltage measurement is included. Eq. (5.24) can directly be solved for $\boldsymbol{x}_{\mathrm{est}}$. The resulting solution is the estimated, consistent system state, which best fits the measured values under consideration of their different qualities.

5.3 State estimation with non-linear measurement model

The linear measurement model cannot be applied to an electric power supply system using conventional SCADA technology. On the one hand, this is due to the fact that phase shifts occur, and on the other hand due to the necessity of powers and voltage magnitudes in the measurement vector. Eq. (5.7) therefore needs to be rewritten more generally

$$\boldsymbol{z} = \boldsymbol{h}\left(\boldsymbol{x}\right) \tag{5.26}$$

Accordingly, eq. (5.8) results in

$$\boldsymbol{z}_{\mathrm{m}} = \boldsymbol{h}\left(\boldsymbol{x}_{\mathrm{est}}\right) + \Delta\boldsymbol{z} \tag{5.27}$$

and eq. (5.9) respectively

$$\Delta\boldsymbol{z} = \boldsymbol{z}_{\mathrm{m}} - \boldsymbol{h}\left(\boldsymbol{x}_{\mathrm{est}}\right) \tag{5.28}$$

Similar to the linear measurement model, the errors are again related to the standard deviation to make high quality measurands more important during the estimation process.

$$\Delta\boldsymbol{z}_{\mathrm{g}} = \boldsymbol{S}^{-1}\ \Delta\boldsymbol{z} = \boldsymbol{S}^{-1}\ \boldsymbol{z}_{\mathrm{m}} - \boldsymbol{S}^{-1}\ \boldsymbol{h}\left(\boldsymbol{x}_{\mathrm{est}}\right) = \boldsymbol{z}_{\mathrm{m,g}} - \boldsymbol{h}_{\mathrm{g}}\left(\boldsymbol{x}_{\mathrm{est}}\right) \tag{5.29}$$

The weighted squared sum of F_{g} results in

$$\begin{aligned} F_{\mathrm{g}} &= \Delta\boldsymbol{z}_{\mathrm{g}}^{\mathrm{T}}\ \Delta\boldsymbol{z}_{\mathrm{g}} = \left(\boldsymbol{z}_{\mathrm{g,m}}^{\mathrm{T}} - \boldsymbol{h}_{\mathrm{g}}^{\mathrm{T}}\left(\boldsymbol{x}_{\mathrm{est}}\right)\right)\left(\boldsymbol{z}_{\mathrm{g,m}} - \boldsymbol{h}_{\mathrm{g}}\left(\boldsymbol{x}_{\mathrm{est}}\right)\right) \\ &= \boldsymbol{z}_{\mathrm{g,m}}^{\mathrm{T}}\ \boldsymbol{z}_{\mathrm{g,m}} - \boldsymbol{z}_{\mathrm{g,m}}^{\mathrm{T}}\ \boldsymbol{h}_{\mathrm{g}}\left(\boldsymbol{x}_{\mathrm{est}}\right) - \boldsymbol{h}_{\mathrm{g}}^{\mathrm{T}}\left(\boldsymbol{x}_{\mathrm{est}}\right)\boldsymbol{z}_{\mathrm{g,m}} + \boldsymbol{h}_{\mathrm{g}}^{\mathrm{T}}\left(\boldsymbol{x}_{\mathrm{est}}\right)\boldsymbol{h}_{\mathrm{g}}\left(\boldsymbol{x}_{\mathrm{est}}\right) \\ &= \boldsymbol{z}_{\mathrm{g,m}}^{\mathrm{T}}\ \boldsymbol{z}_{\mathrm{g,m}} - 2\,\boldsymbol{h}_{\mathrm{g}}^{\mathrm{T}}\left(\boldsymbol{x}_{\mathrm{est}}\right)\boldsymbol{z}_{\mathrm{g,m}} + \boldsymbol{h}_{\mathrm{g}}^{\mathrm{T}}\left(\boldsymbol{x}_{\mathrm{est}}\right)\boldsymbol{h}_{\mathrm{g}}\left(\boldsymbol{x}_{\mathrm{est}}\right) \end{aligned} \tag{5.30}$$

To minimize the error function, all partial derivations need to be built and set to zero again.

$$\frac{\partial F_{\mathrm{g}}}{\partial\ \boldsymbol{x}_{\mathrm{est}}^{\mathrm{T}}} = \frac{\partial\left(\boldsymbol{z}_{\mathrm{g,m}}^{\mathrm{T}}\ \boldsymbol{z}_{\mathrm{g,m}} - 2\,\boldsymbol{h}_{\mathrm{g}}^{\mathrm{T}}\left(\boldsymbol{x}_{\mathrm{est}}\right)\boldsymbol{z}_{\mathrm{g,m}} + \boldsymbol{h}_{\mathrm{g}}^{\mathrm{T}}\left(\boldsymbol{x}_{\mathrm{est}}\right)\boldsymbol{h}_{\mathrm{g}}\left(\boldsymbol{x}_{\mathrm{est}}\right)\right)}{\partial\ \boldsymbol{x}_{\mathrm{est}}^{\mathrm{T}}} \overset{!}{=} \boldsymbol{0} \tag{5.31}$$

Similar to the linear measurement model, the construction of the partial derivations is done separately for each summand. Derivation of the first term results in

$$\frac{\partial\ \boldsymbol{z}_{\mathrm{g,m}}^{\mathrm{T}}\ \boldsymbol{z}_{\mathrm{g,m}}}{\partial\ \boldsymbol{x}_{\mathrm{est}}^{\mathrm{T}}} = \boldsymbol{0} \tag{5.32}$$

Due to it is again independent from $\boldsymbol{x}_{\text{est}}$. Derivation of the second term results in

$$\frac{\partial\left(-2\,\boldsymbol{h}_{\text{g}}^{\text{T}}\left(\boldsymbol{x}_{\text{est}}\right)\boldsymbol{z}_{\text{g,m}}\right)}{\partial\,\boldsymbol{x}_{\text{est}}^{\text{T}}}=-2\frac{\partial\,\boldsymbol{h}_{\text{g}}^{\text{T}}\left(\boldsymbol{x}_{\text{est}}\right)}{\partial\,\boldsymbol{x}_{\text{est}}^{\text{T}}}\boldsymbol{z}_{\text{g,m}}=-2\,\boldsymbol{H}_{\text{g}}^{\text{T}}\,\boldsymbol{z}_{\text{g,m}} \tag{5.33}$$

$\boldsymbol{H}_{\text{g}}^{\text{T}}$ is the transposed Jacobian of $\boldsymbol{h}\left(\boldsymbol{x}_{\text{est}}\right)$. It does not depend on the system state, thus the coefficients are constant.

Using the product rule, derivation of the third term results in

$$\begin{aligned}\frac{\partial\,\boldsymbol{h}_{\text{g}}^{\text{T}}\left(\boldsymbol{x}_{\text{est}}\right)\boldsymbol{h}_{\text{g}}\left(\boldsymbol{x}_{\text{est}}\right)}{\partial\,\boldsymbol{x}_{\text{est}}^{\text{T}}}&=\frac{\partial\,\boldsymbol{h}_{\text{g}}^{\text{T}}\left(\boldsymbol{x}_{\text{est}}\right)}{\partial\,\boldsymbol{x}_{\text{est}}^{\text{T}}}\boldsymbol{h}_{\text{g}}\left(\boldsymbol{x}_{\text{est}}\right)+\boldsymbol{h}_{\text{g}}^{\text{T}}\left(\boldsymbol{x}_{\text{est}}\right)\frac{\partial\,\boldsymbol{h}_{\text{g}}\left(\boldsymbol{x}_{\text{est}}\right)}{\partial\,\boldsymbol{x}_{\text{est}}^{\text{T}}}\\&=2\,\boldsymbol{H}_{\text{g}}^{\text{T}}\,\boldsymbol{h}_{\text{g}}\left(\boldsymbol{x}_{\text{est}}\right)\end{aligned} \tag{5.34}$$

In conclusion the derivation results in

$$\frac{\partial\,F_{\text{g}}}{\partial\,\boldsymbol{x}_{\text{est}}^{\text{T}}}=-2\,\boldsymbol{H}_{\text{g}}^{\text{T}}\,\boldsymbol{z}_{\text{g,m}}+2\,\boldsymbol{H}_{\text{g}}^{\text{T}}\,\boldsymbol{h}_{\text{g}}\left(\boldsymbol{x}_{\text{est}}\right)=-2\boldsymbol{H}_{\text{g}}^{\text{T}}\left(\boldsymbol{z}_{\text{g,m}}-\boldsymbol{h}_{\text{g}}\left(\boldsymbol{x}_{\text{est}}\right)\right)=\boldsymbol{0} \tag{5.35}$$

and accordingly

$$\boldsymbol{H}_{\text{g}}^{\text{T}}\,\boldsymbol{h}_{\text{g}}\left(\boldsymbol{x}_{\text{est}}\right)=\boldsymbol{H}_{\text{g}}^{\text{T}}\,\boldsymbol{z}_{\text{g,m}} \tag{5.36}$$

Eq. (5.36) still is non-linear due to its dependency on $\boldsymbol{h}\left(\boldsymbol{x}_{\text{est}}\right)$. Thus, the search for the optimal estimated system state has to be done iteratively using e.g. a tangential approach. To do so, $\boldsymbol{h}\left(\boldsymbol{x}_{\text{est}}\right)$ is expressed by a Taylor series expansion in each iteration step μ.

$$\boldsymbol{h}_{\text{g}}\left(\boldsymbol{x}_{\text{est},\mu+1}\right)\approx\boldsymbol{h}_{\text{g}}\left(\boldsymbol{x}_{\text{est},\mu}\right)+\frac{\partial\,\boldsymbol{h}_{\text{g}}\left(\boldsymbol{x}_{\text{est},\mu}\right)}{\partial\,\boldsymbol{x}_{\text{est},\mu}^{\text{T}}}\Delta\boldsymbol{x}_{\text{est},\mu+1}=\boldsymbol{h}_{\text{g}}\left(\boldsymbol{x}_{\text{est},\mu}\right)+\boldsymbol{H}_{\text{g},\mu}\,\Delta\boldsymbol{x}_{\text{est},\mu+1} \tag{5.37}$$

Insertion of eq. (5.37) in eq. (5.36) results in

$$\boldsymbol{H}_{\text{g},\mu}^{\text{T}}\left(\boldsymbol{h}_{\text{g}}\left(\boldsymbol{x}_{\text{est},\mu}\right)+\boldsymbol{H}_{\text{g},\mu}\,\Delta\boldsymbol{x}_{\text{est},\mu+1}\right)=\boldsymbol{H}_{\text{g},\mu}^{\text{T}}\,\boldsymbol{z}_{\text{g,m}} \tag{5.38}$$

which leads to the following equation system

$$\begin{aligned}\boldsymbol{H}_{\text{g},\mu}^{\text{T}}\,\boldsymbol{H}_{\text{g},\mu}\,\Delta\boldsymbol{x}_{\text{est},\mu+1}&=\boldsymbol{H}_{\text{g},\mu}^{\text{T}}\left(\boldsymbol{z}_{\text{g,m}}-\boldsymbol{h}_{\text{g}}\left(\boldsymbol{x}_{\text{est},\mu}\right)\right)\\\boldsymbol{A}_{\mu}\,\Delta\boldsymbol{x}_{\text{est},\mu+1}&=\Delta\boldsymbol{y}_{\mu}\end{aligned} \tag{5.39}$$

The system matrix $\boldsymbol{A}_{\mu}$ again has the dimension $2k\times 2k$. It is still positive definite and symmetric. Usually, its rank is only $2k-1$, especially if there are no shunt elements in the grid. This is mainly due to the fact that power flows are driven by (complex-valued) nodal voltage differences rather than their absolute value. To overcome this problem, a reference phase angle can be manually defined. This can be done in a similar way to the Newton-Raphson power flow calculation.

5.4 Construction of the Jacobian

As described initially, the measurement vector contains power, voltage magnitude and potentially even current magnitude information. The system state vector $\boldsymbol{x}_{\text{est}}$ may be based on either Cartesian or polar coordinates. In the following, polar coordinates are used as shown in eq. (5.1).

5.4.1 Nodal powers

Nodal powers can be calculated using the power equation eq. (4.22). The partial derivations with respect to voltage angle and magnitude are already known from the Newton-Raphson-approach based on polar coordinates. Hence the Jacobian $\boldsymbol{J}$ developed in chapter 4.3.2 can also be used for state estimation.

$$\boldsymbol{J}_{\text{SK}} = \begin{bmatrix} \dfrac{\partial\, \boldsymbol{p}_{\text{K}}}{\partial\, \boldsymbol{\delta}_{\text{K}}^{\text{T}}} & \dfrac{\partial\, \boldsymbol{p}_{\text{K}}}{\partial\, \boldsymbol{u}_{\text{K}}^{\text{T}}} \\ \dfrac{\partial\, \boldsymbol{q}_{\text{K}}}{\partial\, \boldsymbol{\delta}_{\text{K}}^{\text{T}}} & \dfrac{\partial\, \boldsymbol{q}_{\text{K}}}{\partial\, \boldsymbol{u}_{\text{K}}^{\text{T}}} \end{bmatrix} \tag{5.40}$$

For the purpose of state estimation only the lines of $\boldsymbol{J}_{\text{SK}}$ are actually needed, that represent a node at which active or reactive powers are measured. This selection can be applied using the nodal powers measurand incidence matrix $\boldsymbol{M}_{\text{SK}}$.

$$\boldsymbol{H}_{\text{SK}} = \boldsymbol{M}_{\text{SK}}\, \boldsymbol{J}_{\text{SK}} \tag{5.41}$$

5.4.2 Terminal powers

In its construction the terminal power equation

$$\underline{\boldsymbol{s}}_{\text{T}} = 3\, \underline{\boldsymbol{U}}_{\text{T}} \left(\underline{\boldsymbol{Y}}_{\text{T}}\, \underline{\boldsymbol{u}}_{\text{T}} \right)^{*} \tag{5.42}$$

is similar to the nodal power equation. That means their partial derivations can be done the exact same way as for the nodal power. Therefore, $\underline{\boldsymbol{Y}}_{\text{KK}}$ simply needs to be replaced by $\underline{\boldsymbol{Y}}_{\text{T}}$ and instead of $\underline{\boldsymbol{u}}_{\text{K}}$ $\underline{\boldsymbol{u}}_{\text{T}}$ is used. This results in a Jacobian $\boldsymbol{J}_{\text{ST}}$ with dimension $2t \times 2t$. The derivation with respect to terminal values needs to be reassigned to nodal values. Due to terminal voltages are a linear function of nodal voltages

$$\underline{\boldsymbol{u}}_{\text{T}} = \boldsymbol{K}_{\text{KT}}^{\text{T}}\, \underline{\boldsymbol{u}}_{\text{K}} \tag{5.43}$$

this can be applied to the system variables as well

$$\begin{bmatrix} \boldsymbol{\delta}_{\text{T}} \\ \boldsymbol{u}_{\text{T}} \end{bmatrix} = \begin{bmatrix} \boldsymbol{K}_{\text{KT}}^{\text{T}} & \boldsymbol{0} \\ \boldsymbol{0} & \boldsymbol{K}_{\text{KT}}^{\text{T}} \end{bmatrix} \begin{bmatrix} \boldsymbol{\delta}_{\text{K}} \\ \boldsymbol{u}_{\text{K}} \end{bmatrix} \tag{5.44}$$

Using the terminal powers measurand incidence matrix $\boldsymbol{M}_{\text{ST}}$ this results in

$$\boldsymbol{H}_{\text{ST}} = \boldsymbol{M}_{\text{ST}}\, \boldsymbol{J}_{\text{ST}} \begin{bmatrix} \boldsymbol{K}_{\text{KT}}^{\text{T}} & \boldsymbol{0} \\ \boldsymbol{0} & \boldsymbol{K}_{\text{KT}}^{\text{T}} \end{bmatrix} \tag{5.45}$$

5.4.3 Nodal voltage magnitudes

Nodal voltage magnitudes are system variables themselves. Thus, construction of the Jacobian $\boldsymbol{H}_{\mathrm{U}}$ is trivial. Due to phase angles and magnitudes are independent values, on the left-hand side a $k \times k$ empty matrix is used and on the right-hand side the unity matrix. Multiplication with $\boldsymbol{M}_{\mathrm{U}}$ removes the nodes without voltage magnitude measurement.

$$\boldsymbol{H}_{\mathrm{U}} = \boldsymbol{M}_{\mathrm{U}} \begin{bmatrix} \boldsymbol{0} & \boldsymbol{E} \end{bmatrix} \tag{5.46}$$

$\boldsymbol{H}_{\mathrm{U}}$ is the only constant submatrix and therefore only needs to be constructed once prior to the iteration.

5.4.4 Nodal current magnitudes

To calculate the Jacobian, the nodal currents

$$\underline{\boldsymbol{i}}_{\mathrm{K}} = \underline{\boldsymbol{Y}}_{\mathrm{KK}}\, \underline{\boldsymbol{u}}_{\mathrm{K}} \tag{5.47}$$

are split into real and imaginary part

$$\begin{aligned} I_{\mathrm{K,r},\nu} &= \sum_{\gamma=1}^{k} Y_{\mathrm{KK},\nu,\gamma}\, U_{\mathrm{K},\gamma}\, \cos\left(\alpha_{\nu,\gamma} + \delta_{\gamma}\right) \\ I_{\mathrm{K,i},\nu} &= \sum_{\gamma=1}^{k} Y_{\mathrm{KK},\nu,\gamma}\, U_{\mathrm{K},\gamma}\, \sin\left(\alpha_{\nu,\gamma} + \delta_{\gamma}\right) \end{aligned} \tag{5.48}$$

such that the current magnitude results can be calculated

$$I_{\nu} = \sqrt{I_{\mathrm{K,r},\nu}^2 + I_{\mathrm{K,i},\nu}^2} \tag{5.49}$$

Using the chain rule the partial derivations are now performed. Derivation with respect to the phase angle results in

$$J_{\mathrm{I\delta},\nu,\gamma} = \frac{\partial\, I_{\mathrm{K},\nu}}{\partial\, \delta_{\mathrm{K},\gamma}} = \frac{Y_{\mathrm{KK},\nu,\gamma}\, U_{\mathrm{K},\gamma}}{\sqrt{I_{\mathrm{K,r},\nu}^2 + I_{\mathrm{K,i},\nu}^2}} \left(-I_{\mathrm{K,r},\nu}\, \sin\left(\alpha_{\nu,\gamma} + \delta_{\gamma}\right) + I_{\mathrm{K,i},\nu}\, \cos\left(\alpha_{\nu,\gamma} + \delta_{\gamma}\right) \right) \tag{5.50}$$

Derivation with respect to the magnitude results in

$$J_{\mathrm{IU},\nu,\gamma} = \frac{\partial\, I_{\mathrm{K},\nu}}{\partial\, U_{\mathrm{K},\gamma}} = \frac{Y_{\mathrm{KK},\nu,\gamma}}{\sqrt{I_{\mathrm{K,r},\nu}^2 + I_{\mathrm{K,i},\nu}^2}} \left(I_{\mathrm{K,r},\nu}\, \cos\left(\alpha_{\nu,\gamma} + \delta_{\gamma}\right) + I_{\mathrm{K,i},\nu}\, \sin\left(\alpha_{\nu,\gamma} + \delta_{\gamma}\right) \right) \tag{5.51}$$

Using the nodal current magnitude measurand incidence matrix $\boldsymbol{M}_{\mathrm{IK}}$ the Jacobian $\boldsymbol{H}_{\mathrm{IK}}$ is

$$\boldsymbol{H}_{\mathrm{IK}} = \boldsymbol{M}_{\mathrm{IK}} \begin{bmatrix} \boldsymbol{J}_{\mathrm{I\delta}} & \boldsymbol{J}_{\mathrm{IU}} \end{bmatrix} \tag{5.52}$$

5.4.5 Terminal current magnitude

In its construction the terminal current equation

$$\underline{\boldsymbol{i}}_{\mathrm{T}} = \underline{\boldsymbol{Y}}_{\mathrm{T}}\, \underline{\boldsymbol{u}}_{\mathrm{T}} \tag{5.53}$$

is similar to the nodal power equation. That means their partial derivations can be done the exact same way as for the nodal power. Therefore, $\underline{\boldsymbol{Y}}_{\mathrm{KK}}$ simply needs to be replaced by $\underline{\boldsymbol{Y}}_{\mathrm{T}}$ and instead of $\underline{\boldsymbol{u}}_{\mathrm{K}}$ $\underline{\boldsymbol{u}}_{\mathrm{T}}$ is used. Similar to the terminal powers, the partial derivations with respect to terminal voltages need to be reassigned to nodal voltages using the nodal-terminal incidence matrix.

$$\boldsymbol{H}_{\mathrm{IT}} = \boldsymbol{M}_{\mathrm{IT}}\, \boldsymbol{J}_{\mathrm{IT}} \begin{bmatrix} \boldsymbol{K}_{\mathrm{KT}}^{\mathrm{T}} & \boldsymbol{0} \\ \boldsymbol{0} & \boldsymbol{K}_{\mathrm{KT}}^{\mathrm{T}} \end{bmatrix} \tag{5.54}$$

5.4.6 Construction of the equation systems

The submatrices of $\boldsymbol{H}$ are arranged according to the measurement vector in eq. (5.3).

$$\boldsymbol{H} = \begin{bmatrix} \frac{\partial \boldsymbol{p}_{\mathrm{K}}}{\partial \boldsymbol{\delta}_{\mathrm{K}}^{\mathrm{T}}} & \frac{\partial \boldsymbol{p}_{\mathrm{K}}}{\partial \boldsymbol{u}_{\mathrm{K}}^{\mathrm{T}}} \\ \frac{\partial \boldsymbol{q}_{\mathrm{K}}}{\partial \boldsymbol{\delta}_{\mathrm{K}}^{\mathrm{T}}} & \frac{\partial \boldsymbol{q}_{\mathrm{K}}}{\partial \boldsymbol{u}_{\mathrm{K}}^{\mathrm{T}}} \\ \hdashline \frac{\partial \boldsymbol{p}_{\mathrm{T}}}{\partial \boldsymbol{\delta}_{\mathrm{K}}^{\mathrm{T}}} & \frac{\partial \boldsymbol{p}_{\mathrm{T}}}{\partial \boldsymbol{u}_{\mathrm{K}}^{\mathrm{T}}} \\ \frac{\partial \boldsymbol{q}_{\mathrm{T}}}{\partial \boldsymbol{\delta}_{\mathrm{K}}^{\mathrm{T}}} & \frac{\partial \boldsymbol{q}_{\mathrm{T}}}{\partial \boldsymbol{u}_{\mathrm{K}}^{\mathrm{T}}} \\ \hdashline \frac{\partial \boldsymbol{u}_{\mathrm{K}}}{\partial \boldsymbol{\delta}_{\mathrm{K}}^{\mathrm{T}}} & \frac{\partial \boldsymbol{u}_{\mathrm{K}}}{\partial \boldsymbol{u}_{\mathrm{K}}^{\mathrm{T}}} \\ \hdashline \frac{\partial \boldsymbol{i}_{\mathrm{K}}}{\partial \boldsymbol{\delta}_{\mathrm{K}}^{\mathrm{T}}} & \frac{\partial \boldsymbol{i}_{\mathrm{K}}}{\partial \boldsymbol{u}_{\mathrm{K}}^{\mathrm{T}}} \\ \hdashline \frac{\partial \boldsymbol{i}_{\mathrm{T}}}{\partial \boldsymbol{\delta}_{\mathrm{K}}^{\mathrm{T}}} & \frac{\partial \boldsymbol{i}_{T}}{\partial \boldsymbol{u}_{\mathrm{K}}^{\mathrm{T}}} \end{bmatrix} = \begin{bmatrix} \boldsymbol{H}_{\mathrm{SK}} \\ \boldsymbol{H}_{\mathrm{ST}} \\ \boldsymbol{H}_{\mathrm{U}} \\ \boldsymbol{H}_{\mathrm{IK}} \\ \boldsymbol{H}_{\mathrm{IT}} \end{bmatrix} \tag{5.55}$$

Additionally, they are weighted

$$\boldsymbol{H}_{\mathrm{g}} = \boldsymbol{S}^{-1}\, \boldsymbol{H} \tag{5.56}$$

This results in the overdetermined equation system

$$\boldsymbol{H}_{\mathrm{g}} \begin{bmatrix} \Delta\boldsymbol{\delta}_{\mathrm{K}} \\ \Delta\boldsymbol{u}_{\mathrm{K}} \end{bmatrix} = \Delta\boldsymbol{z}_{\mathrm{g}} \tag{5.57}$$

To solve it, it is multiplied with $\boldsymbol{H}_{\mathrm{g}}^{\mathrm{T}}$ as described in eq. (5.39). According to eq. (5.39)

$$\begin{aligned} \boldsymbol{A} &= \boldsymbol{H}_{\mathrm{g}}^{\mathrm{T}}\, \boldsymbol{H}_{\mathrm{g}} \\ \Delta\boldsymbol{y} &= \boldsymbol{H}_{\mathrm{g}}^{\mathrm{T}}\, \Delta\boldsymbol{z}_{\mathrm{g}} \end{aligned} \tag{5.58}$$

To manually set a reference phase angle at one node, similar to the power flow approach, in the equation system

$$\boldsymbol{A}\begin{bmatrix}\Delta\boldsymbol{\delta}_{\mathrm{K}}\\ \Delta\boldsymbol{u}_{\mathrm{K}}\end{bmatrix}=\Delta\boldsymbol{y} \tag{5.59}$$

the additional constraint

$$\Delta\delta_{\mathrm{K,ref}}=0 \tag{5.60}$$

is added.

5.5 Flow chart of the iteration

The flow chart of the iteration is given in Fig. 22. It is similar to the flow chart of the power flow iteration. Based on the current estimated system state the measured values are reproduced with the system model and the difference to the measured information is calculated. Subsequently, the Jacobians are constructed and the equation system to calculate the minimum squared error is solved after the integration of the voltage reference angle. This results in an update of the current estimated grid state. The procedure is repeated until the update is smaller than a predefined threshold.

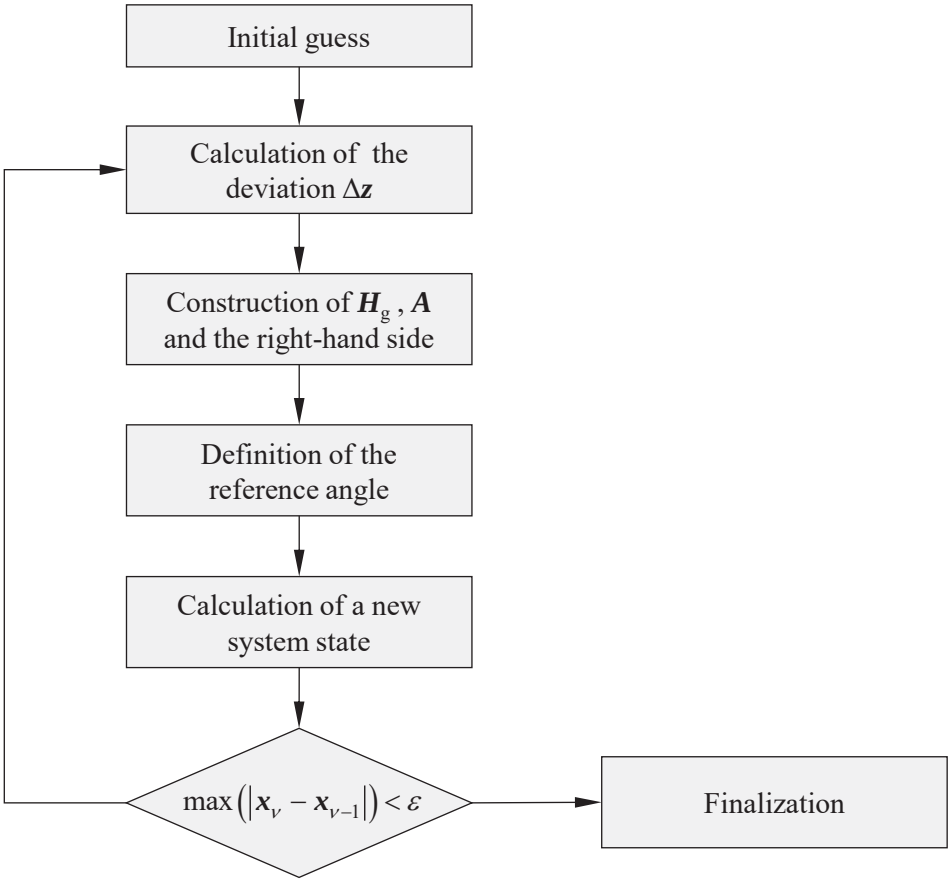

Fig. 22: flow chart of the state estimation iteration

It is advantageous to use measured voltages for the initial guess. For the remaining voltage the nominal value can be assumed. If needed, it is compulsory to set reference angles correctly for the initial guess.

6 Short-circuit calculation

Short-circuits are a high electric, thermal and mechanical threat to the electric power supply system. The intensity of the short-circuit current and its impact on the assets and the surroundings need to be considered not only during system operation but also during the grid planning phase. That means, the assets and protection systems need to be dimensioned and parameterized under uncertain conditions for highest and lowest possible short-circuits. In doing so, it is assumed, that the three-phase fault results in the highest short-circuit currents. In this case, only the positive sequence system needs to be modelled, due to the fault is symmetric.

The time-series of a three-phase fault at zero-crossing of the voltage close to a synchronous generator is given in Fig. 23 together with some characteristic parameters.

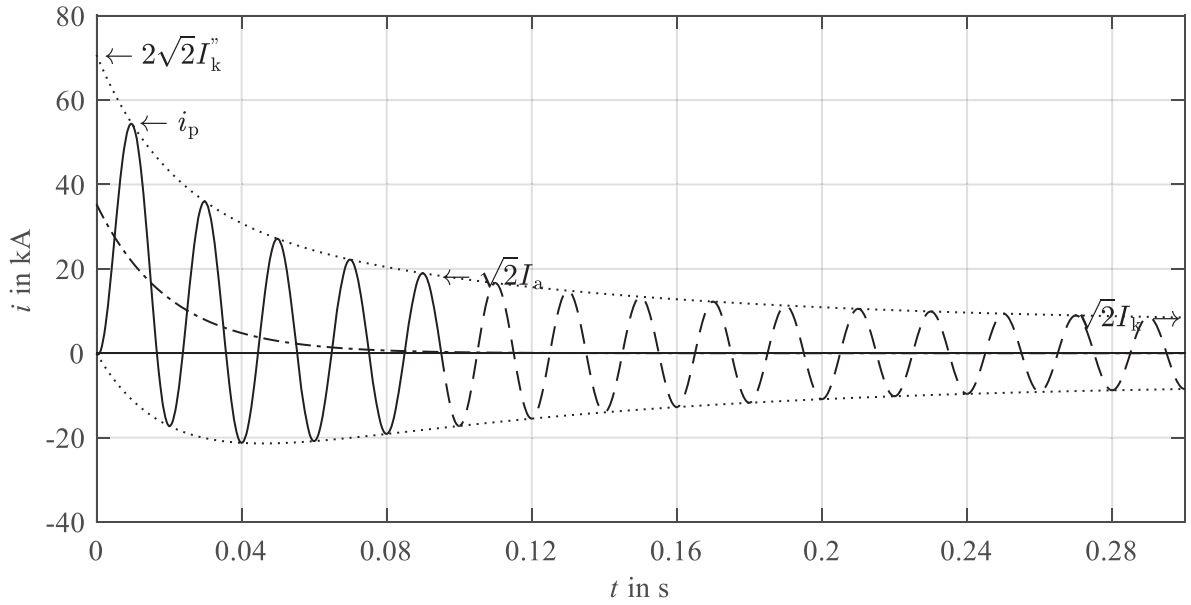

Fig. 23: exemplary time-series of a short-circuit current

The objective of short-circuit calculation – during planning as well as the operational phase – is the calculation of the initial symmetrical short-circuit current I_k''. To avoid constructing and solving a differential equation system, the standard IEC 60909 defines some factors which allows to sufficiently precise infer on other important parameters. These are mainly:

- the maximum aperiodic short-circuit current i_p
- the breaking current I_a
- the steady-state short-circuit current I_k
- the thermal equivalent current I_{th}

The approximation of these characteristic parameters using IEC 60909 factors shall only be applied to public energy supply grids showing a homogenous R/X-ratio and only a couple of rotating machines. In industrial grids and grids for station supply, which are characterized by a high amount of drives, the error of estimation increases to such an extent that only solving the differential equation will lead to a reliable solution.

While the objective of the short-circuit calculation is always the same, the input data is different during grid planning and grid operation. Grid operators can rely on actual, online grid information, e.g. the estimated grid state, which includes load and generation information as well as tap positions and switching states. Thus, it is possible to apply a detailed short-circuit calculation that is based on the estimated grid state. Besides the initial symmetrical short-circuit current it is also possible to calculate the exact nodal voltages during the fault or the time-series of currents and voltages by solving the differential equation.

Short-circuit calculation during the grid planning phase is characterized by a high amount of uncertainty. Neither switching states nor the exact load and generation situation are known. Nevertheless, based on only little information, it is important to still get a good estimation of biggest and smallest possible short-circuit currents. Due to the computational intensity, it is not productive to obtain this estimation by simulating different scenarios. Instead, the extrema are estimated by applying simplifications and assumptions that are considered to safely model the worst-case and best-case scenarios. So, all possible short-circuits that may later occur during grid operation are definitely inside this interval.

6.1 Single line diagram of dipoles for short-circuit calculation

Short-circuits are fed by all rotating machines – generators and drives – as well as equivalent networks. As seen in Fig. 23 the initial symmetrical short-circuit current is a fictitious RMS value, that would envelope the short-circuit current in the initial moment. To calculate the share of the generators their subtransient model is needed. As usual, the admittance form given in Fig. 24 is most advantageous.

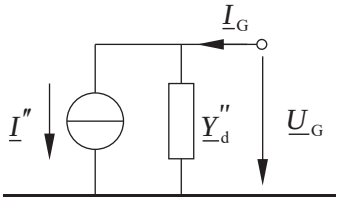

Fig. 24: subtransient single line diagram of synchronous generators

with the subtransient direct axis admittance

$$\underline{Y}''_d = \frac{1}{R_a + j\,X''_d} \tag{6.1}$$

It is used, due to $\underline{I}''$ solely depends on rotor fluxes, which stay constant in the moment of transition from the non-faulty to the faulty state. Induction machines do not have a subtransient state. They are described using the transient model

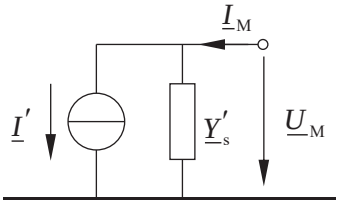

Fig. 25: transient single line diagram of induction machines

with the transient admittance

$$\underline{Y}'_{\mathrm{s}} = \frac{1}{R_{\mathrm{s}} + \mathrm{j}\, X'_{\mathrm{s}}} \tag{6.2}$$

Equivalent networks are modeled analogously to synchronous machines as shown in Fig. 26

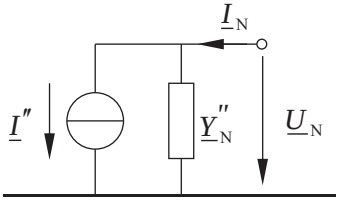

Fig. 26: single line diagram of an equivalent network

with the short-circuit admittance

$$\underline{Y}''_{\mathrm{N}} = \frac{1}{R_{\mathrm{N}} + \mathrm{j}\, X_{\mathrm{N}}} \tag{6.3}$$

It is obtained from the R/X-ratio of the grid and its short-circuit power S''_{k}

$$S''_{\mathrm{k}} = 1{,}1\, Y''_{\mathrm{N}}\, U^2_{\mathrm{nN}} \tag{6.4}$$

Loads without spinning reserve do not contribute to the short-circuit current. It is sufficient to model them as passive dipoles, as nodal currents or as equivalent admittances which are included in $\underline{\boldsymbol{Y}}_{\mathrm{KK}}$.

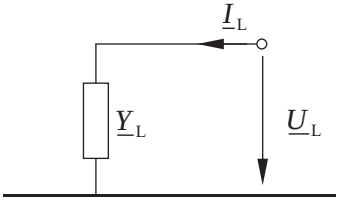

Fig. 27: single line diagram of a load without spinning reserve

6.2 Exact calculation

The exact calculation of the initial symmetrical short-circuit current is only possible during system operation, due to switching states have a high impact on the occurring currents and the grid state prior to the fault needs to be known e.g. in form of estimated nodal voltages. In the nodal current equation

$$\underline{\boldsymbol{Y}}_{\mathrm{KK}}\, \underline{\boldsymbol{u}}_{\mathrm{K}} = \underline{\boldsymbol{i}}_{\mathrm{K}} \tag{6.5}$$

the nodal currents are the sum of currents of dipoles which are connected to the respective nodes. They are now replaced by the single line diagrams given in chapter 6.1. Shunt admittances are added to the bus admittance matrix while source currents remain on the right-hand side. So, eq. (6.5) results in

$$\begin{aligned} \left(\underline{\boldsymbol{Y}}_{\mathrm{KK}} - \underline{\boldsymbol{Y}}''\right) \underline{\boldsymbol{u}}_{\mathrm{K}} &= \boldsymbol{K}_{\mathrm{KT,ZP}}\, \underline{\boldsymbol{i}}''_{\mathrm{q}} \\ \underline{\boldsymbol{Y}}''_{\mathrm{KK}} \quad \underline{\boldsymbol{u}}_{\mathrm{K}} &= \underline{\boldsymbol{i}}''_{\mathrm{q,K}} \end{aligned} \tag{6.6}$$

$\underline{\boldsymbol{Y}}''$ is a diagonal matrix with the shunt admittances of the dipoles on the main diagonal and $\underline{\boldsymbol{i}}_{\mathrm{q}}''$ is the vector of source currents. Loads without spinning reserves are entirely modelled as admittance, thus $\underline{\boldsymbol{i}}_{\mathrm{q}}''$ is zero at nodes without machines. $\underline{\boldsymbol{Y}}_{\mathrm{KK}}''$ is invertible due to the additional elements on the main diagonal.

If a three-phase fault occurs at node *i* the voltage at this node is set to zero and a potential source current at this node is superposed to all of the short-circuit contributions of the other dipoles. This results in the initial symmetrical short-circuit current $\underline{I}_{\mathrm{k}}''$ at node *i*.

$$\begin{bmatrix} \underline{Y}''_{1,1} & \cdots & \underline{Y}''_{1,i-1} & \underline{Y}''_{1,i} & \underline{Y}''_{1,i+1} & \cdots & \underline{Y}''_{1,k} \\ \vdots & \ddots & \vdots & \vdots & \vdots & \ddots & \vdots \\ \underline{Y}''_{i-1,1} & \cdots & \underline{Y}''_{i-1,i-1} & \underline{Y}''_{i-1,i} & \underline{Y}''_{i-1,i+1} & \cdots & \underline{Y}''_{i-1,k} \\ \underline{Y}''_{i,1} & \cdots & \underline{Y}''_{i,i-1} & \underline{Y}''_{i,i} & \underline{Y}''_{i,i+1} & \cdots & \underline{Y}''_{i,k} \\ \underline{Y}''_{i+1,1} & \cdots & \underline{Y}''_{i+1,i-1} & \underline{Y}''_{i+1,i} & \underline{Y}''_{i+1,i+1} & \cdots & \underline{Y}''_{i+1,k} \\ \vdots & \ddots & \vdots & \vdots & \vdots & \ddots & \vdots \\ \underline{Y}''_{k,1} & \cdots & \underline{Y}''_{k,i-1} & \underline{Y}''_{k,i} & \underline{Y}''_{k,i+1} & \cdots & \underline{Y}''_{k,k} \end{bmatrix} \begin{bmatrix} \underline{U}_{\mathrm{k},1} \\ \vdots \\ \underline{U}_{\mathrm{k},i-1} \\ 0 \\ \underline{U}_{\mathrm{k},i+1} \\ \vdots \\ \underline{U}_{\mathrm{k},k} \end{bmatrix} = \begin{bmatrix} \underline{I}''_{\mathrm{q},1} \\ \vdots \\ \underline{I}''_{\mathrm{q},i-1} \\ \underline{I}''_{\mathrm{k}} \\ \underline{I}''_{\mathrm{q},i+1} \\ \vdots \\ \underline{I}''_{\mathrm{q},k} \end{bmatrix} \tag{6.7}$$

Eq. (6.7) can be solved, by removing the *i*-th column and row. The reduced equation system is solved for the faulted nodal voltage vector $\underline{\boldsymbol{u}}_{\mathrm{K,k}}$. It is afterwards used to solve the previously removed *i*-th row for $\underline{I}_{\mathrm{k}}''$.

System operators need to know the impact of a potential short-circuit at each node. Therefore, eq. (6.7) would need to be constructed and solved for each node separately. Using today's computational power and the possibility to parallelize the process, computational time is tolerable even in bigger grids with lots of nodes. Nevertheless, it can be minimized, if the (reduced) system matrix of the equation system would not depend on the fault location and therefore becomes constant. In this case, the equation system would only have to be constructed and inverted once. This can be achieved by using a superposition approach which allows to still calculate short-circuit voltages and currents correctly.

6.3 Superposition approach by Helmholtz and Thévenin

The superposition approach aims at calculating the faulted system state as a superposition of the non-faulty state and a differential state. Eq. (6.6) is therefore expressed as follows

$$\begin{aligned} \underline{\boldsymbol{Y}}''_{\mathrm{KK}} \left(\underline{\boldsymbol{u}}_{\mathrm{K}} + \Delta \underline{\boldsymbol{u}}_{\mathrm{K,k}} \right) &= \underline{\boldsymbol{i}}_{\mathrm{q}}'' + \Delta \underline{\boldsymbol{i}}_{\mathrm{K,k}} \\ \underline{\boldsymbol{Y}}''_{\mathrm{KK}} \quad \underline{\boldsymbol{u}}_{\mathrm{K,k}} \quad &= \quad \underline{\boldsymbol{i}}_{\mathrm{K,k}} \end{aligned} \tag{6.8}$$

Eq. (6.8) consists of the initial state prior to the fault

$$\underline{\boldsymbol{Y}}''_{\mathrm{KK}} \, \underline{\boldsymbol{u}}_{\mathrm{K}} = \underline{\boldsymbol{i}}_{\mathrm{q}}'' \tag{6.9}$$

and the differential state

$$\underline{\boldsymbol{Y}}''_{\mathrm{KK}} \, \Delta \underline{\boldsymbol{u}}_{\mathrm{K,k}} = \Delta \underline{\boldsymbol{i}}_{\mathrm{K,k}} \tag{6.10}$$

As described above, the system matrix is constant and does not depend on the fault location. Furthermore, due to it contains additional elements on the main diagonal, $\underline{\boldsymbol{Y}}''_{\mathrm{KK}}$ is invertible. Therefore, eq. (6.10) can be directly expressed in its impedance form

$$\underline{\boldsymbol{Z}}''_{\mathrm{KK}}\ \Delta\underline{\boldsymbol{i}}_{\mathrm{K,k}} = \Delta\underline{\boldsymbol{u}}_{\mathrm{K,k}} \tag{6.11}$$

To model the short-circuit constraints at node i in accordance to eq. (6.7), at the fault location, the differential state corresponds to the negative voltage prior to the fault

$$\Delta\underline{U}_{\mathrm{K,k},i} = -\underline{U}_{\mathrm{K},i} \tag{6.12}$$

The short-circuit current only occurs at the fault location i. Furthermore, source currents of generators and drives are constant. Therefore, $\Delta\underline{\boldsymbol{i}}_{\mathrm{K,k}}$ is zero, except at position i. Thus, eq. (6.11) can be written in more detail

$$\left[\begin{array}{ccc:c:ccc}
\underline{Z}''_{1,1} & \cdots & \underline{Z}''_{1,i-1} & \underline{Z}''_{1,i} & \underline{Z}''_{1,i+1} & \cdots & \underline{Z}''_{1,k} \\
\vdots & \ddots & \vdots & \vdots & \vdots & \ddots & \vdots \\
\underline{Z}''_{i-1,1} & \cdots & \underline{Z}''_{i-1,i-1} & \underline{Z}''_{i-1,i} & \underline{Z}''_{i-1,i+1} & \cdots & \underline{Z}''_{i-1,k} \\
\hdashline
\underline{Z}''_{i,1} & \cdots & \underline{Z}''_{i,i-1} & \underline{Z}''_{i,i} & \underline{Z}''_{i,i+1} & \cdots & \underline{Z}''_{i,k} \\
\hdashline
\underline{Z}''_{i+1,1} & \cdots & \underline{Z}''_{i+1,i-1} & \underline{Z}''_{i+1,i} & \underline{Z}''_{i+1,i+1} & \cdots & \underline{Z}''_{i+1,k} \\
\vdots & \ddots & \vdots & \vdots & \vdots & \ddots & \vdots \\
\underline{Z}''_{k,1} & \cdots & \underline{Z}''_{k,i-1} & \underline{Z}''_{k,i} & \underline{Z}''_{k,i+1} & \cdots & \underline{Z}''_{k,k}
\end{array}\right]
\left[\begin{array}{c}
0 \\ \vdots \\ 0 \\ \hdashline \Delta\underline{I}''_{i,\mathrm{k}} \\ \hdashline 0 \\ \vdots \\ 0
\end{array}\right] =
\left[\begin{array}{c}
\Delta\underline{U}_{1,\mathrm{k}} \\ \vdots \\ \Delta\underline{U}_{i-1,\mathrm{k}} \\ \hdashline -\underline{U}_i \\ \hdashline \Delta\underline{U}_{i+1,\mathrm{k}} \\ \vdots \\ \Delta\underline{U}_{k,\mathrm{k}}
\end{array}\right] \tag{6.13}$$

In the i-th row of eq. (6.13), $\Delta\underline{I}''_{i,\mathrm{k}}$ can be directly calculated

$$\Delta\underline{I}''_{i,\mathrm{k}} = -\frac{1}{\underline{Z}''_{i,i}}\underline{U}_i \tag{6.14}$$

After that, the differential voltages at all the other nodes can be obtained by multiplying $\Delta\underline{I}''_{i,\mathrm{k}}$ with the i-th column of the impedance matrix. This differential state is finally superposed with the initial state according to eq. (6.8). The differential state is also called Thévenin equivalent.

A graphical representation of the superposition approach is given in Fig. 28. The grid and all of its non-spinning loads, shunt elements, drives and generators are summarized as a black box and only the short-circuit position at note i is drawn separately. The faulty state (left hand side) consists of the initial state (middle) and the differential state (right hand side), which contains the voltage constraints at the fault location.

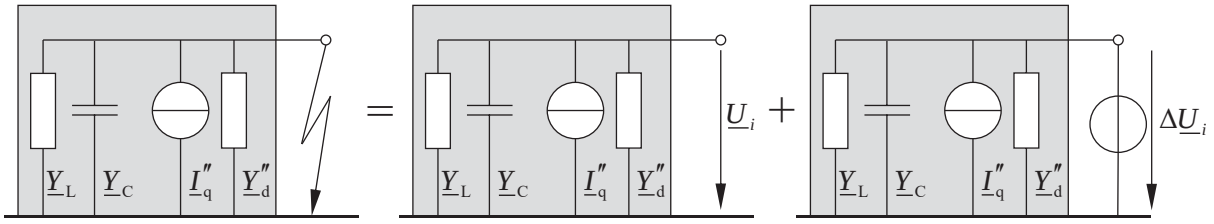

Fig. 28: principle of superposition

Using the superposition principle, a change in the fault location can be implemented by simply changing the right hand side of the equation system given in eq. (6.13). The system matrix does

not need to be reconstructed or reinverted. If $\underline{\boldsymbol{D}}$ is the diagonal matrix of $\underline{\boldsymbol{Z}}''_{\mathrm{KK}}$, then the differential states of all short-circuits at every node can be calculated in one single step.

$$\begin{aligned} \Delta \underline{\boldsymbol{i}}''_{\mathrm{K,k}} &= -\underline{\boldsymbol{D}}^{-1}\, \underline{\boldsymbol{u}}_{\mathrm{K}} \\ \Delta \underline{\boldsymbol{U}}_{\mathrm{K,k}} &= -\underline{\boldsymbol{Z}}''_{\mathrm{KK}}\, \underline{\boldsymbol{D}}^{-1}\, \underline{\boldsymbol{U}}_{\mathrm{K}} \end{aligned} \tag{6.15}$$

6.4 Short-circuit calculation according to IEC 60909

To exactly calculate the short-circuit currents, a dedicated system state described by a consistent nodal voltage vector needs to be available. This is not the case during grid planning, due to information on load and generation can only be approximated and switching states as well as tapping positions need to be assumed. The method of placing an equivalent voltage source at the fault location according to the standard IEC 60909 is a suitable approach, which minimizes the need for exact input information but is still able to estimate biggest and smallest possible short-circuit currents at a fault location.

The method is loosely based on the superposition approach. Nevertheless, information on the initial state is not available due to the lack of operational information. Thus, only the differential state is considered. Additionally, some simplifications are used:

- Loads without spinning reserve used to be modeled entirely as admittance in the equation system. During the fault, voltages over the loads are very low. Thus, they are neglected. By doing so, load uncertainty has been bypassed.
- For the same reason of low voltages during the fault, shunt elements of the equipment (mainly capacitive shunts of lines) are neglected.
- To overcome the uncertainty of generation, all sources in the grid are passivated, which means, current sources are opened and voltage sources are short-circuited.
- Shunt elements of drives, generators and equivalent networks are kept in the grid.

By doing so a source-free, unloaded grid is constructed, which only contains the shunt elements of drives, generators and equivalent networks but besides this has no connection to ground.

Now, at the fault location an auxiliary voltage source U_{aux} is connected, which drives the short-circuit current. Due to the exact voltage magnitude is unknown, the nominal voltage and a correction factor c is used.

$$U_{\mathrm{aux}} = -c\,\frac{U_{\mathrm{nN}}}{\sqrt{3}} \tag{6.16}$$

The described grid is shown in Fig. 29 as a black box again.

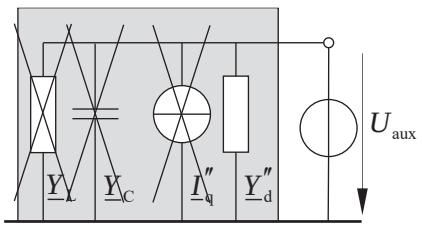

Fig. 29: short-circuit calculation according to IEC 60909

It is obvious, that using this approach the short-circuit contributions of machines and equivalent networks are almost proportional to their internal admittance. The method of the auxiliary voltage source at the fault location aims at approximating the short-circuit currents close to the fault location. With increasing distance to the fault, the error of estimation increases as well. The same is valid for the voltages.

By trend, neglecting shunt elements and load admittances leads to short-circuit currents that are estimated lower than the actual ones. This can be compensated by the correction factor *c*. IEC 60909 suggests the following factors for transmission systems

$$c = \begin{cases} 1{,}1 & \text{to calculate maximum short-circuit currents} \\ 1{,}0 & \text{to calculate minimum short-circuit currents} \end{cases} \tag{6.17}$$

In distribution systems, even $c < 1$ is possible.

Estimation of biggest short-circuit currents is used to dimension and parameterize assets, insulation and bearings in such a way, that they can bear the maximum thermal, mechanic and electric stress. On the other hand, estimation of smallest short-circuit currents is used, to correctly parameterize the protection system to make sure that all faults – even those with low impact on currents and voltages – are securely detected and switched off.

The calculation of the short-circuit currents is done analogously to the calculation of the differential state of the superposition approach. The system matrix is constant and invertible. To calculate the short-circuit current at the *i*-th node, first, the initial symmetrical short-circuit current is obtained from the *i*-th row. Usually, this information is sufficient during grid planning, so the process can be stopped at this point. To additionally calculate the currents on the lines and the contribution of each generator, the voltage differences can be obtained by multiplication of the *i*-th column of the equation system with the initial symmetrical short-circuit current.

The equation system is similar to the equation system of the superposition approach.

$$\begin{bmatrix} \underline{Z}''_{1,1} & \cdots & \underline{Z}''_{1,i-1} & \underline{Z}''_{1,i} & \underline{Z}''_{1,i+1} & \cdots & \underline{Z}''_{1,k} \\ \vdots & \ddots & \vdots & \vdots & \vdots & \ddots & \vdots \\ \underline{Z}''_{i-1,1} & \cdots & \underline{Z}''_{i-1,i-1} & \underline{Z}''_{i-1,i} & \underline{Z}''_{i-1,i+1} & \cdots & \underline{Z}''_{i-1,k} \\ \underline{Z}''_{i,1} & \cdots & \underline{Z}''_{i,i-1} & \underline{Z}''_{i,i} & \underline{Z}''_{i,i+1} & \cdots & \underline{Z}''_{i,k} \\ \underline{Z}''_{i+1,1} & \cdots & \underline{Z}''_{i+1,i-1} & \underline{Z}''_{i+1,i} & \underline{Z}''_{i+1,i+1} & \cdots & \underline{Z}''_{i+1,k} \\ \vdots & \ddots & \vdots & \vdots & \vdots & \ddots & \vdots \\ \underline{Z}''_{k,1} & \cdots & \underline{Z}''_{k,i-1} & \underline{Z}''_{k,i} & \underline{Z}''_{k,i+1} & \cdots & \underline{Z}''_{k,k} \end{bmatrix} \begin{bmatrix} 0 \\ \vdots \\ 0 \\ \underline{I}''_{i,\mathrm{k}} \\ 0 \\ \vdots \\ 0 \end{bmatrix} = \begin{bmatrix} \underline{U}_{1,\mathrm{k}} \\ \vdots \\ \underline{U}_{i-1,\mathrm{k}} \\ \underline{U}_{\mathrm{ers}} \\ \underline{U}_{i+1,\mathrm{k}} \\ \vdots \\ \underline{U}_{k,\mathrm{k}} \end{bmatrix} \tag{6.18}$$

6.5 Impedance correction

As described above, using an auxiliary voltage source at the fault location leads to short-circuit currents that are not very precise. According to experience, contributions on power plants (synchronous machines) are estimated up to 40 % too low and contributions of drives (induction machines) too high. Due to the inner sources of the machines are passivized, the only possibility

to correct the respective short-circuit contribution is to modify the impedance of the machines to artificially increase or decrease their short-circuit current.

The process is explained using a generator which runs at the rated operation point prior to the faults. This means,

$$\begin{aligned} \underline{U}_{\mathrm{G}} &= \frac{U_{\mathrm{rG}}}{\sqrt{3}} \\ \underline{I}_{\mathrm{G}} &= -I_{\mathrm{rG}} \left(\cos\left(\varphi_{\mathrm{rG}}\right) - \mathrm{j} \sin\left(\varphi_{\mathrm{rG}}\right) \right) \end{aligned} \tag{6.19}$$

If there is a three-phase fault at the terminal of the generator and the armature resistance R_{a} is neglected, this leads to the following short-circuit contribution

$$\underline{I}_{\mathrm{k,G}} = \frac{U_{\mathrm{rG}} - \mathrm{j}\sqrt{3}\, X''_{\mathrm{d}}\, \underline{I}_{\mathrm{G}}}{\sqrt{3}\, \mathrm{j}\, X''_{\mathrm{d}}} \tag{6.20}$$

If the same case is modeled using the auxiliary voltage source at the generator terminal, this will result in

$$\underline{I}_{\mathrm{k,F}} = \frac{-U_{\mathrm{aux}}}{\mathrm{j}\, X''_{\mathrm{d}}} = \frac{c\, U_{\mathrm{nN}}}{\mathrm{j}\sqrt{3}\, X''_{\mathrm{d}}} \tag{6.21}$$

To match $\underline{I}_{\mathrm{k,G}}$ and $\underline{I}_{\mathrm{k,F}}$, in eq. (6.21) a correction factor $\underline{k}_{\mathrm{G}}$ is introduced to modify the subtransient direct axis impedance.

$$\frac{U_{\mathrm{rG}} - \mathrm{j}\sqrt{3}\, X''_{\mathrm{d}}\, \underline{I}_{\mathrm{G}}}{\sqrt{3}\, \mathrm{j}\, X''_{\mathrm{d}}} = \frac{c\, U_{\mathrm{nN}}}{\mathrm{j}\sqrt{3}\, \underline{k}_{\mathrm{G}} X''_{\mathrm{d}}} \tag{6.22}$$

Eq. (6.22) is solved for $\underline{k}_{\mathrm{G}}$

$$\underline{k}_{\mathrm{G}} = \frac{c\, U_{\mathrm{nN}}}{U_{\mathrm{rG}} - \sqrt{3}\, \mathrm{j}\, X''_{\mathrm{d}}\, \underline{I}_{\mathrm{rG}}} \tag{6.23}$$

Using the rated generator current in eq. (6.19) and the definition of the subtransient direct axis impedance

$$X''_{\mathrm{d}} = x''_{\mathrm{d}} \frac{U_{\mathrm{rG}}^2}{S_{\mathrm{rG}}} = x''_{\mathrm{d}} \frac{U_{\mathrm{rG}}}{\sqrt{3}\, I_{\mathrm{rG}}} \tag{6.24}$$

eq. (6.23) can also be expressed

$$\begin{aligned} \underline{k}_{\mathrm{G}} &= \frac{c\, U_{\mathrm{nN}}}{U_{\mathrm{rG}} - \mathrm{j}\, x''_{\mathrm{d}} \dfrac{U_{\mathrm{rG}}}{I_{\mathrm{rG}}}\, \underline{I}_{\mathrm{rG}}} = \frac{c\, U_{\mathrm{nN}}}{U_{\mathrm{rG}} + \mathrm{j}\, x''_{\mathrm{d}}\, U_{\mathrm{rG}} \left(\cos\left(\varphi_{\mathrm{rG}}\right) + \mathrm{j} \sin\left(\varphi_{\mathrm{rG}}\right) \right)} \\ &= \frac{U_{\mathrm{nN}}}{U_{\mathrm{rG}}} \frac{c}{1 - x''_{\mathrm{d}} \sin\left(\varphi_{\mathrm{rG}}\right) + \mathrm{j}\, x''_{\mathrm{d}} \cos\left(\varphi_{\mathrm{rG}}\right)} \end{aligned} \tag{6.25}$$

The imaginary part of $\underline{k}_{\mathrm{G}}$ is small compared to the real part. So, it is suitable to neglect it, which also leads to a real-valued correction factor.

$$k_{\mathrm{G}} = \frac{U_{\mathrm{nN}}}{U_{\mathrm{rG}}} \frac{c}{1 - x''_{\mathrm{d}} \sin\left(\varphi_{\mathrm{rG}}\right)} \tag{6.26}$$

Usually, $\underline{k}_{\mathrm{G}}$ is smaller than one. So, the correction factor will decrease the impedance of the generator and thus increase its contribution to the short-circuit current.

The development of the correction factor for drives is done analogously. Usually, the rated voltage of the drive is equal to the nominal grid voltage. This results in

$$k_{\mathrm{M}} = \frac{c}{1 - x'_{\mathrm{S}} \sin\left(\varphi_{\mathrm{rM}}\right)} \tag{6.27}$$

k_{M} is usually greater than one. So, the correction factor will increase the impedance of the drive and thus decrease its contribution to the short-circuit current.

7 Stability

Stability of the electric power supply system describes the capability of generators to stay synchronized even in dynamic situations like load changes, faults and fault clearance. The system is fed by a large number of differently sized generators, mostly synchronous machines. Their big gyrating mass mainly contributes to the inertia of the entire system and leads to the comfortable fact, that electro-mechanical transients proceed rather slowly which simplifies control of the grid. Thus, generators define the stability of the system.

Usually, stability is understood as rotor angle stability of the generators (in contrast to voltage stability and frequency stability). Rotor angle stability can be further divided into

- Steady-state stability (small-signal stability), to prove the existence of stable operation points, that means analysis of the capability of the generators to stay synchronized at a given operation point
- transient stability, which analyzes the capability of generators to find a new stable and synchronized operation point after a bigger disturbance.

Besides rotor angle stability, also frequency stability (long term stability) and voltage stability are of interest. They are not dealt with in this chapter.

7.1 Generator models

To analyze small-signal and transient stability, different generator models need to be applied. They can either be implemented as voltage or current source. Both ways are comparable. While the current source is advantageous for grid calculations based on admittance matrices implementation of voltage sources is more descriptive and allows the transfiguration of the grid.

Small-signal stability is a steady-state problem. That is why the steady-state generator model is used. The synchronous generated voltage drives the generator current and is connected to the grid via the synchronous impedance which consists of the armature resistance and the synchronous direct axis reactance.

$$\underline{Z}_\mathrm{G} = \frac{1}{\underline{Y}_\mathrm{G}} = R_\mathrm{a} + \mathrm{j}X_\mathrm{d} \tag{7.1}$$

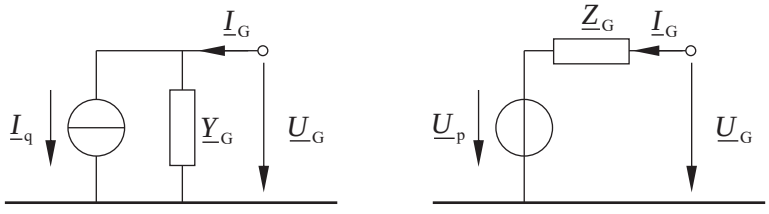

Fig. 30: steady-state generator model

The synchronous generated voltage linearly depends on the rotor speed ω and the excitation current I_f. If there is a sudden disturbance in the grid, this will lead to an abrupt reaction of the rotor currents, to keep the flux linkage constant. This reaction has such a strong influence on the synchronous generated voltage, so that it cannot be used for transient analysis.

Other than the synchronous generated voltage, the transient generated voltage does not depend on the excitation current but only on the rotor flux linkage. If the effects of the damper winding

are neglected, there will be an abrupt reaction as well. Nevertheless, it is sufficiently small. Additionally, the transient generated voltage fades only little after the fault. So, in a good approximation it can be seen almost constant during the entire time. It is therefore the best choice to model phenomena that occur in the transient domain.

The single line diagram of the transient state is similar to the steady-state model. Besides the transient generated voltage or current, the transient direct axis impedance is used, which is about one fifth of the synchronous direct axis impedance.

$$\underline{Z}'_{\mathrm{G}} = \frac{1}{\underline{Y}'_{\mathrm{G}}} = R_{\mathrm{a}} + \mathrm{j}X'_{\mathrm{d}} \tag{7.2}$$

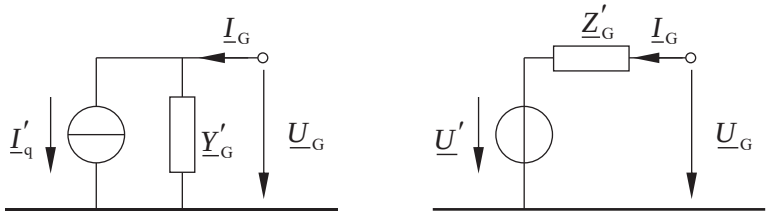

Fig. 31: transient generator model

The phasor diagram summarizes steady-state and transient operation points of the synchronous generator.

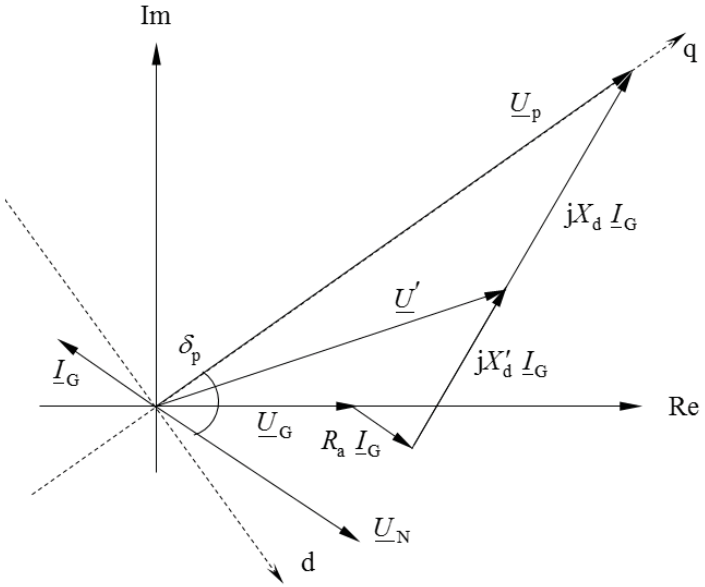

Fig. 32: phasor diagram of a synchronous generator

The synchronous generated voltage rotates synchronously with the rotor and lies in the quadrature axis q of the generator. Its phase angle in relation to the phase angle of the reference voltage $\underline{U}_{\mathrm{N}}$ describes the rotor position.

7.2 Description of rotor motion

The equation of motion of the rotor of a synchronous machine is described by the principle of conservation of angular momentum

$$J\,\dot{\Omega} = \sum M \tag{7.3}$$

Ω is the mechanical rotor speed. It can be converted to the electric rotor speed by multiplication with the number of pole pairs of the generator.

$$\omega_\mathrm{L} = p\,\Omega_\mathrm{L} \tag{7.4}$$

The generator is accelerated by the mechanical torque M_m provided by the turbine and slowed down by the electrical torque M_e which results from the infeed of active power into the grid. If rotor speed and grid frequency differ, this results in a change of the rotor angle.

$$\dot{\delta} = \omega_\mathrm{L} - \omega_0 \tag{7.5}$$

Eq. (7.3) and eq. (7.5) form a first order differential equation system.

$$\begin{bmatrix} 1 & 0 \\ 0 & J \end{bmatrix}\begin{bmatrix} \dot{\delta} \\ \dot{\omega}_\mathrm{L} \end{bmatrix} + \begin{bmatrix} 0 & -1 \\ 0 & 0 \end{bmatrix}\begin{bmatrix} \delta \\ \omega_\mathrm{L} \end{bmatrix} = \begin{bmatrix} -\omega_0 \\ p\left(M_\mathrm{m} + M_\mathrm{e}\right) \end{bmatrix} \tag{7.6}$$

To analyze stability issues, it is more productive to only look at deviations from synchronous operation. Thus, only changes of the rotor position in relation to the reference phase angle are calculated. Eq. (7.6) is therefore rewritten

$$\begin{bmatrix} 1 & 0 \\ 0 & J \end{bmatrix}\begin{bmatrix} \Delta\dot{\delta} \\ \Delta\dot{\omega}_\mathrm{L} \end{bmatrix} + \begin{bmatrix} 0 & -1 \\ 0 & 0 \end{bmatrix}\begin{bmatrix} \Delta\delta \\ \Delta\omega_\mathrm{L} \end{bmatrix} = \begin{bmatrix} 0 \\ p\left(M_\mathrm{m} + M_\mathrm{e}\right) \end{bmatrix} \tag{7.7}$$

In explicit form

$$\begin{bmatrix} \Delta\dot{\delta} \\ \Delta\dot{\omega}_\mathrm{L} \end{bmatrix} = \begin{bmatrix} 0 & 1 \\ 0 & 0 \end{bmatrix}\begin{bmatrix} \Delta\delta \\ \Delta\omega_\mathrm{L} \end{bmatrix} + \begin{bmatrix} 0 \\ \dfrac{p}{J}\left(M_\mathrm{m} + M_\mathrm{e}\right) \end{bmatrix} \tag{7.8}$$

The operation points of the turbine and the generator are usually expressed using powers instead of torques. Via the relationship

$$\begin{aligned} M_\mathrm{m} &= \frac{P_\mathrm{T}}{\Omega_\mathrm{L}} = P_\mathrm{T}\frac{p}{\omega_\mathrm{L}} \\ M_\mathrm{e} &= \frac{P_\mathrm{e}}{\Omega_0} = P_\mathrm{e}\frac{p}{\omega_0} \end{aligned} \tag{7.9}$$

torques can be replaced in eq. (7.8).

$$\begin{bmatrix} \Delta\dot{\delta} \\ \Delta\dot{\omega}_\mathrm{L} \end{bmatrix} = \begin{bmatrix} 0 & 1 \\ 0 & 0 \end{bmatrix}\begin{bmatrix} \Delta\delta \\ \Delta\omega_\mathrm{L} \end{bmatrix} + \begin{bmatrix} 0 \\ \dfrac{p^2}{J\,\omega_\mathrm{L}}\left(P_\mathrm{T} + \dfrac{\omega_\mathrm{L}}{\omega_0}P_\mathrm{e}\right) \end{bmatrix} \tag{7.10}$$

The question of rotor angle stability is answered within a couple of seconds after the disturbance and potentially its clearance. During this time, due to the big gyrating mass, rotor speed does

not change very much. Thus, it can be assumed, that the rotor speed is still almost equal to the grid frequency.

$$\omega_{\mathrm{L}} \approx \omega_0 \tag{7.11}$$

Using the mechanical time constant of the generator

$$T_{\mathrm{m}} = \frac{J\ \omega_0^2}{S_{\mathrm{r,G}}\ p^2} \tag{7.12}$$

and the assumption of eq. (7.11), a machine factor k_{m} can be introduced

$$k_{\mathrm{m}} = \frac{p^2}{J\ \omega_{\mathrm{L}}} \approx \frac{\omega_0}{T_{\mathrm{m}}\ S_{\mathrm{r,G}}} \tag{7.13}$$

which further simplifies eq. (7.10)

$$\begin{bmatrix} \Delta\dot{\delta} \\ \Delta\dot{\omega}_{\mathrm{L}} \end{bmatrix} = \begin{bmatrix} 0 & 1 \\ 0 & 0 \end{bmatrix} \begin{bmatrix} \Delta\delta \\ \Delta\omega_{\mathrm{L}} \end{bmatrix} + \begin{bmatrix} 0 \\ k_{\mathrm{m}} \left(P_{\mathrm{T}} + P_{\mathrm{e}} \right) \end{bmatrix} \tag{7.14}$$

7.3 Equivalent network model

Similar to generators, equivalent networks are modeled as dipoles. Nevertheless, the phase angle of the inner source is always synchronous to the grid frequency. The initial value can be obtained from a power flow calculation of the steady-state operation point prior to the disturbance. It stays constant the entire time.

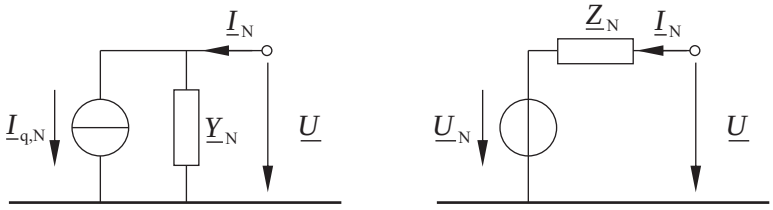

Fig. 33: voltage and current source single line diagrams of equivalent network models

7.4 Grid transfiguration to the generator nodes

For the purpose of stability analysis, usually generators and equivalent networks are modeled as voltage sources. The main disadvantage of this approach is, that the *k* actual grid nodes are supplemented by *g* fictitious, inner generator nodes. Nevertheless, for this analysis only generator voltages and currents are needed, thus the grid can be reduced to the inner generator nodes. This procedure is called transfiguration. All loads without inner sources are expressed again as equivalent admittances $\underline{Y}_{\mathrm{L}}$ and included on the main diagonal of the bus admittance matrix. So, all currents at nodes without drives or generators are zero. The equation system consists of *k* grid nodes and *g* inner generator nodes which are connected to the rest of the grid via $\underline{Y}_{\mathrm{G}}$.

$$\begin{aligned} \underline{Y}_{\mathrm{G}} &= \frac{1}{R_{\mathrm{a}} + \mathrm{j}X_{\mathrm{d}}} \quad \text{for the purpose of small-signal stability} \\ \underline{Y}_{\mathrm{G}} &= \frac{1}{R_{\mathrm{a}} + \mathrm{j}X'_{\mathrm{d}}} \quad \text{for the purpose of transient stability} \end{aligned} \tag{7.15}$$

The generator incidence matrix $\boldsymbol{K}_{\mathrm{KG}}$ describes the connection of a generator to a grid node. It is built analogously to $\boldsymbol{K}_{\mathrm{KT}}$. This results in the following equation system

$$\begin{bmatrix} \underline{\boldsymbol{Y}}_{\mathrm{KK}} - \underline{\boldsymbol{Y}}_{\mathrm{L}} - \boldsymbol{K}_{\mathrm{KG}}\, \underline{\boldsymbol{Y}}_{\mathrm{G}}\, \boldsymbol{K}_{\mathrm{KG}}^{\mathrm{T}} & \boldsymbol{K}_{\mathrm{KG}}\, \underline{\boldsymbol{Y}}_{\mathrm{G}} \\ \underline{\boldsymbol{Y}}_{\mathrm{G}}\, \boldsymbol{K}_{\mathrm{KG}}^{\mathrm{T}} & -\underline{\boldsymbol{Y}}_{\mathrm{G}} \end{bmatrix} \begin{bmatrix} \underline{\boldsymbol{u}}_{\mathrm{K}} \\ \underline{\boldsymbol{u}}_{\mathrm{G}} \end{bmatrix} = \begin{bmatrix} \boldsymbol{0} \\ \underline{\boldsymbol{i}}_{\mathrm{G}} \end{bmatrix} \tag{7.16}$$

Using the abbreviation

$$\underline{\boldsymbol{Y}}_{\mathrm{KK,G,L}} = \underline{\boldsymbol{Y}}_{\mathrm{KK}} - \underline{\boldsymbol{Y}}_{\mathrm{L}} - \boldsymbol{K}_{\mathrm{KG}}\, \underline{\boldsymbol{Y}}_{\mathrm{G}}\, \boldsymbol{K}_{\mathrm{KG}}^{\mathrm{T}} \tag{7.17}$$

The upper half of the equation system can be solved fur $\underline{\boldsymbol{u}}_{\mathrm{K}}$. The result is inserted into the lower equation system

$$-\left(\underline{\boldsymbol{Y}}_{\mathrm{G}}\, \boldsymbol{K}_{\mathrm{KG}}^{\mathrm{T}}\, \underline{\boldsymbol{Y}}_{\mathrm{KK,G,L}}^{-1}\, \boldsymbol{K}_{\mathrm{KG}}\, \underline{\boldsymbol{Y}}_{\mathrm{G}} + \underline{\boldsymbol{Y}}_{\mathrm{G}}\right) \underline{\boldsymbol{u}}_{\mathrm{G}} = \underline{\boldsymbol{Y}}_{\mathrm{GG}}\, \underline{\boldsymbol{u}}_{\mathrm{G}} = \underline{\boldsymbol{i}}_{\mathrm{G}} \tag{7.18}$$

Eq. (7.18) now has the dimension $g \times g$. The resulting system matrix is dense. If $\underline{\boldsymbol{Y}}_{\mathrm{KK}}$ is symmetric it will be symmetric, too. Their diagonal elements are called feeder admittance and the other elements transmission admittance.

7.5 Small-signal stability

Small-signal stability describes the capability of generators to stay in a synchronous operation point under steady-state conditions. Calculation of small-signal stability is therefore the search for the existence of stable, steady-state operation points. Besides the active power infeed of the generator, additional parameters e.g. voltage control may be included.

7.5.1 Demonstration of small-signal stability using the single-machine-problem

To visualize the process of small-signal stability analysis, the single-machine problem is used. The generator is connected to a grid given in Fig. 34. All assets are considered entirely inductive so losses are neglected. The generator feeds into the grid via a two-winding transformer and a system of two parallel lines.

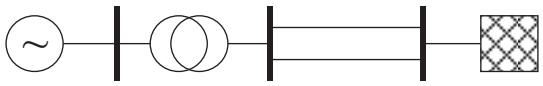

Fig. 34: single-machine problem

This results in the following single line diagram.

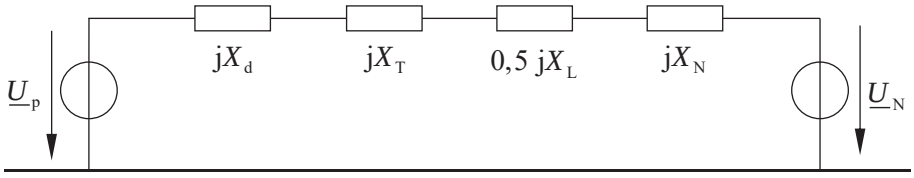

Fig. 35: single line diagram of the grid

The power exchange of the grid and the generator is defined by the inner voltages and the impedances between them.

$$\underline{S} = 3\frac{\underline{U}_\mathrm{p}\,\underline{U}_\mathrm{N}^*}{\left(\mathrm{j}\left(X_\mathrm{d} + X_\mathrm{T} + \frac{1}{2}X_\mathrm{L} + X_\mathrm{N}\right)\right)^*} \tag{7.19}$$

The inner voltage of the grid is usually defined as reference voltage and the reference phase angle is set to zero. Thus, it is real-valued. If the synchronous generated voltage is expressed by magnitude and phase, the active power output of the generator in eq. (7.19) can be expressed as follows

$$P_\mathrm{G} = -3\frac{U_\mathrm{p}\,U_\mathrm{N}}{X_\mathrm{d} + X_\mathrm{T} + \frac{1}{2}X_\mathrm{L} + X_\mathrm{N}}\sin\left(\delta_\mathrm{p}\right) \tag{7.20}$$

Due to the grid is considered entirely inductive without ohmic losses, the active power infeed of the generator corresponds with the active power consumption of the grid.

$$P_\mathrm{N} = -P_\mathrm{G} \tag{7.21}$$

The power curve of the system is given in Fig. 36.

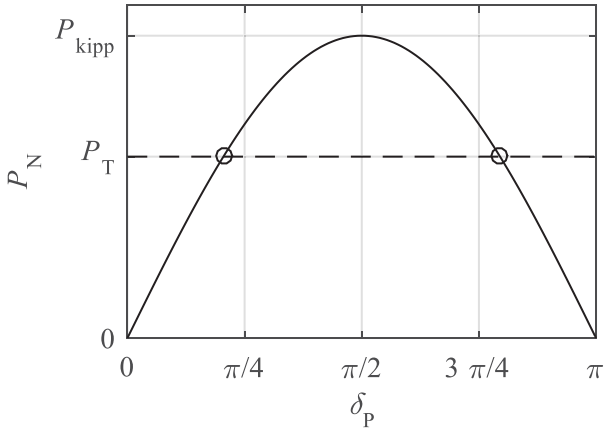

Fig. 36: operation points of the generator

The intersections of the power curve with the active power output of the turbine are possible, steady-state operation points of the generator, due to the sum of power is balanced. Proof of small-signal stability of the two operation points shall be done with a thought experiment.

First, the left operation point is reviewed:

- If the generator accelerates, the rotor angle increases a little bit. At that moment, it feeds more power into the grid as actually provided by the turbine. This difference has to be taken from the kinetic energy, which means the generator slows down until the power balance is reached again. Thus, the generator returns to its original operation point.
- If the generator is slowed down, the rotor angle decreases a little bit. At that moment, it feeds less power into the grid as actually provided by the turbine. This difference is used

to reaccelerate the generator until the power balance is reached again. Thus, the generator returns to its original operation point.

Consequently, the left operation point is stable. The experiment is repeated for the right operation point:

- If the generator accelerates, the rotor angle increases a little bit. At that moment, it feeds less power into the grid as actually provided by the turbine. The difference is used to accelerate the rotor even more, which means, the rotor angle is further increasing. Thus, the generator is drifting apart from the operation point and will not return to it.
- If the generator is slowed down, the rotor angle decreases a little bit. At that moment, it feeds more power into the grid as actually provided by the turbine. This difference has to be taken from the kinetic energy, which means, the rotor is further slowed down and the rotor angle is further decreasing. Thus, the generator is drifting apart from the operation point and will not return to it.

Consequently, the right operation point is instable. Having a look at Fig. 36 a stability limit can be found at π/2. Furthermore, it is obvious, that a smaller rotor angle means a more stable system.

7.5.2 General calculation of small-signal stability

Small-signal stability can be described using eigenvalue analysis. Due to the displacement in the thought experiment is a small signal, a linearization of the motion equation system of the generators around the operation point is valid. For g generators eq. (7.14) is converted to matrix form

$$\begin{bmatrix} \Delta\dot{\boldsymbol{\delta}}_\mathrm{p} \\ \Delta\dot{\boldsymbol{\omega}}_\mathrm{L} \end{bmatrix} = \begin{bmatrix} \boldsymbol{0} & \boldsymbol{E} \\ \boldsymbol{0} & \boldsymbol{0} \end{bmatrix} \begin{bmatrix} \Delta\boldsymbol{\delta}_\mathrm{p} \\ \Delta\boldsymbol{\omega}_\mathrm{L} \end{bmatrix} + \begin{bmatrix} \boldsymbol{0} \\ \boldsymbol{K}_\mathrm{m}\left(\boldsymbol{p}_\mathrm{T} + \boldsymbol{p}_\mathrm{e}\right) \end{bmatrix} \tag{7.22}$$

Due to the active power output $\boldsymbol{p}_\mathrm{e}$ of the generators is a trigonometric function of the rotor angle, the system is non-linear. Linearization is achieved by the application of a Taylor-series expansion.

$$\begin{bmatrix} \Delta\dot{\boldsymbol{\delta}}_\mathrm{p} \\ \Delta\dot{\boldsymbol{\omega}}_\mathrm{L} \end{bmatrix} = \begin{bmatrix} \boldsymbol{0} & \boldsymbol{E} \\ \boldsymbol{0} & \boldsymbol{0} \end{bmatrix} \begin{bmatrix} \Delta\boldsymbol{\delta}_\mathrm{p} \\ \Delta\boldsymbol{\omega}_\mathrm{L} \end{bmatrix} + \begin{bmatrix} \boldsymbol{0} \\ \boldsymbol{K}_\mathrm{m}\left(\boldsymbol{p}_\mathrm{T} + \boldsymbol{p}_{\mathrm{e},0} + \dfrac{\partial \boldsymbol{p}_\mathrm{e}\left(\boldsymbol{\delta}_{\mathrm{p},0}\right)}{\partial \Delta\boldsymbol{\delta}_\mathrm{p}^\mathrm{T}} \Delta\boldsymbol{\delta}_\mathrm{p}\right) \end{bmatrix} \tag{7.23}$$

The linearized part of the active power output is included into the system matrix. Due to the system has been linearized around an existing operation point, $\boldsymbol{p}_\mathrm{T}$ and $\boldsymbol{p}_{\mathrm{e},0}$ sum up to zero. This results in the remaining equation system.

$$\begin{bmatrix} \Delta\dot{\boldsymbol{\delta}}_\mathrm{p} \\ \Delta\dot{\boldsymbol{\omega}}_\mathrm{L} \end{bmatrix} = \begin{bmatrix} \boldsymbol{0} & \boldsymbol{E} \\ \boldsymbol{K}_\mathrm{m} \dfrac{\partial \boldsymbol{p}_\mathrm{e}\left(\boldsymbol{\delta}_{\mathrm{p},0}\right)}{\partial \Delta\boldsymbol{\delta}_\mathrm{p}^\mathrm{T}} & \boldsymbol{0} \end{bmatrix} \begin{bmatrix} \Delta\boldsymbol{\delta}_\mathrm{p} \\ \Delta\boldsymbol{\omega}_\mathrm{L} \end{bmatrix} \tag{7.24}$$

The eigenvalues of the system matrix of eq. (7.24) are a description of the self-oscillation of the uncontrolled generator. As long as no eigenvalue has a positive real part, the system is

stable. Differentiation of the active power output with respect to the rotor angle is done analogously to the construction of the respective submatrix of the Jacobian of the power flow equations in polar coordinates.

Exemplarily, in case of the single machine problem, the result is

$$\frac{\partial p_\mathrm{e}}{\partial \delta_\mathrm{p}} = \frac{\partial p_\mathrm{G}}{\partial \delta_\mathrm{p}} = -3\frac{U_\mathrm{p}\,U_\mathrm{N}}{\sum X}\cos\left(\delta_\mathrm{p}\right) \tag{7.25}$$

This results in the characteristic polygon

$$\left\| \begin{bmatrix} -\underline{\lambda} & 1 \\ -3\,k_\mathrm{m}\dfrac{U_\mathrm{p}\,U_\mathrm{N}}{\sum X}\cos\left(\delta_{\mathrm{p},0}\right) & -\underline{\lambda} \end{bmatrix} \right| = \underline{\lambda}^2 + 3\,k_\mathrm{m}\frac{U_\mathrm{p}\,U_\mathrm{N}}{\sum X}\cos\left(\delta_{\mathrm{p},0}\right) \overset{!}{=} 0 \tag{7.26}$$

with the eigenvalues

$$\underline{\lambda}_{1,2} = \sqrt{-3\,k_\mathrm{m}\frac{U_\mathrm{p}\,U_\mathrm{N}}{\sum X}\cos\left(\delta_{\mathrm{p},0}\right)} \tag{7.27}$$

As long as $\cos\left(\delta_{\mathrm{p},0}\right) > 0$, which means $\delta_{\mathrm{p},0} < \pi/2$ eq. (7.27) results in a complex-valued pair of eigenvalues without real part. Thus, the generator is stable. If $\delta_{\mathrm{p},0} > \pi/2$, which means $\cos\left(\delta_{\mathrm{p},0}\right) < 0$, a real-valued pair of eigenvalues is obtained, whereof one eigenvalue is positive. In this case, the generator is instable.

7.5.3 Measures to increase small-signal stability

To increase small-signal stability, it is necessary to find an operation point far away from the stability limit. Furthermore, to increase the capability of the generators to keep synchronism, it is aspired to get a high gradient of the generator's active power output. According to eq. (7.20) several possible solutions are thinkable. To decrease $\sin\left(\delta_\mathrm{p}\right)$ but keep P_G constant, the numerator needs to get as big as possible and the denominator as small as possible.

Decreasing the denominator means, to reduce the impedance between the generator and the grid. This can be achieved by increasing the number of meshes in the grid, parallel lines or by series compensation to reduce the dominating inductive part of the impedance.

The grid voltage can only be changed within a small band around the nominal value. Thus, the only way to increase the numerator is to control the synchronous generated voltage. This is done by excitation of the synchronous machine. The synchronous generated voltage is a linear function of the excitation current. For the purpose of simplification, the degree of excitation ε is introduced.

$$\varepsilon = \frac{U_\mathrm{p}}{U_\mathrm{N}} \tag{7.28}$$

With ε eq. (7.20) can be rewritten

$$P_\mathrm{G} = -3\varepsilon\frac{U_\mathrm{N}^2}{\sum X}\sin\left(\delta_\mathrm{p}\right) \tag{7.29}$$

A higher excitation increases the breakdown torque of the generator and the stable operation point moves towards smaller rotor angles. The power output diagram of the single-machine problem is given in Fig. 37 for several degrees of excitation.

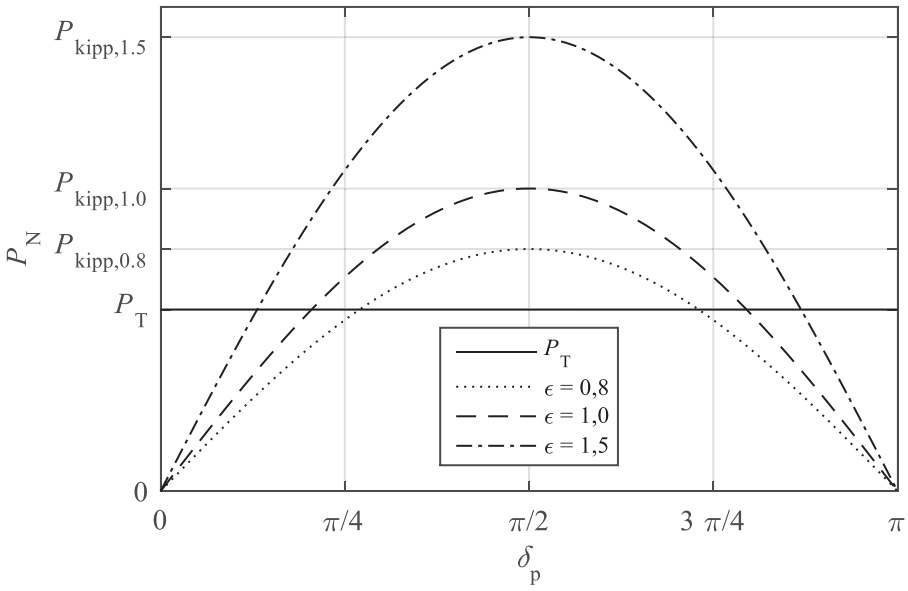

Fig. 37: impact of excitation on the position of the operation point

It is obvious, that small-signal stability decreases with decreasing excitation. These operation points are necessary, if capacitive shunts e.g. of lines in the grid provide a sufficient amount of reactive power. In this case the generator is only little excited or even under-excited to push the voltage down again. So, in contrast to all other contingencies in the grid, the biggest threat to rotor angle stability is not the highly loaded grid but the unloaded grid due to the lines provide enough reactive power themselves. This can only be reduced by switching off lines to higher burden the remaining grid. But this is limited by additional constraints mainly due to the n-1-criterion.

7.6 Transient stability

Transient stability is the capability of generators to return into a new stable operation point after a disturbance in the electric energy supply system. Usually, the three-phase short-circuit is considered the biggest possible disturbance. It leads on the one hand to the biggest imbalance of power but on the other hand, it is symmetric and can be modelled using only the positive sequence system.

In contrast to the small-signal stability, the disturbance is so big, a linearization at the operation point prior to the fault cannot be applied. Instead, the motion equation system of the generators needs to be solved by numerical integration. The resulting time-series of the oscillations of the rotor angle show the transient behavior of the generator and are needed to obtain the time-series of all other electric and mechanical information. In contrast to the mechanical osciallations of the rotor, the electric transients in the grid are damped rapidly, such that the grid can be considered steady-state again. The necessity of steady-state grid analysis and dynamic rotor motion calculation results in an algebro-differential equation system which is typical for quasi steady-state analysis. The question of transient stability is answered within the first couple of

seconds after a disturbance. This fact can be used to simplify the analysis by making the following assumptions:

- The transient generated voltage is constant, due to the voltage controllers have not reacted in such a short period of time.
- The torque of the turbine is constant, due to the governor is slow.
- Loads are constant and can still be modeled as equivalent admittances.
- Frequency control has not reacted due to the rotor frequency is still within the tolerable bounds.

In combination with the three-phase short-circuit but with exception of the first assumption, this represents the worst-case. In a real system, the generator would be more stable than predicted by these assumptions.

7.6.1 Demonstration of transient stability using the single-machine problem

The principles of transient stability are visualized using again the single-machine problem given in Fig. 34. Therefore, a three-phase fault on one of the lines close to the bus bar is assumed. The fault is later on cleared by switching off the faulty line. This results in three different single line diagrams: prior to the fault, during the fault and after clearance of the fault.

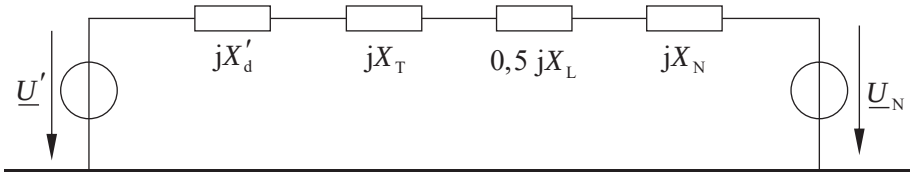

Fig. 38: single line diagram prior to the fault

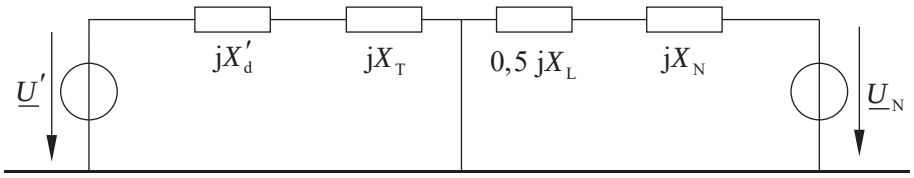

Fig. 39: single line diagram during the fault

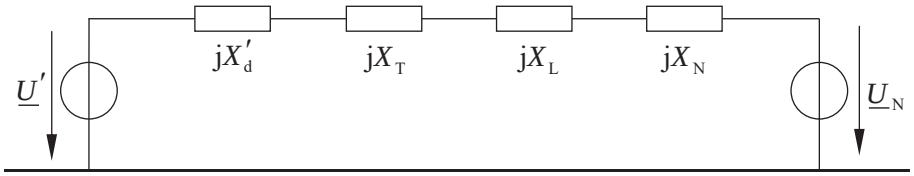

Fig. 40: single line diagram after the fault

First, the initial values of δ' and $\underline{U}'$ or $\underline{I}'_q$, respectively, are based on a load flow calculation of the system prior to the fault. The generator is operated at a stable operation point. Using the generator terminal voltage $\underline{U}_G$ the transient generated voltage is obtained

$$\underline{U}' = U' \, \mathrm{e}^{\mathrm{j}\vartheta'} = \underline{U}_\mathrm{G} - \mathrm{j}X_\mathrm{d} \, \underline{I}_\mathrm{G} \tag{7.30}$$

with

$$\vartheta' = \delta' + \vartheta_\mathrm{N} \tag{7.31}$$

Usually, the reference phase angle of the grid voltage is set to zero such that $\vartheta' = \delta'$. Similar to the synchronous generated voltage, the transient generated voltage is fixed to the rotor, too. This means that δ' can also be used to model the motion of the rotor. The system was in steady-state before the fault, so the initial values of the variables of the motion equation are all zero, if the motion equation is related to the synchronous speed.

Due to the three-phase fault, the generator cannot provide any power to the grid anymore. The generator current abruptly shifts to the transient short-circuit current

$$\underline{I}'_\mathrm{k} = \frac{\underline{U}'}{\mathrm{j}\left(X'_\mathrm{d} + X_\mathrm{T}\right)} \tag{7.32}$$

This is a pure reactive current. The power provided by the turbine is fully used to accelerate the generator, resulting in a change of the rotor speed.

$$\dot{\omega} = k_\mathrm{m} \, P_\mathrm{T} \tag{7.33}$$

So, the rotor angle increases quadratically over time for the duration of the fault.

$$\delta'(t) = \int \omega \, \mathrm{d}t = \iint \dot{\omega} \, \mathrm{d}t \, \mathrm{d}t = \frac{1}{2} k_\mathrm{m} \, P_\mathrm{T} \, t^2 + \delta'_0 \tag{7.34}$$

At the moment of clearance of the fault, the transient generated voltage phase angle is δ'_FC. From that moment on, the generator is able again to feed power to the grid according to its power curve. Clearance of the fault resulted in a topological change of the system, due to one of the lines has been switched off. That is why the power curve now is below the original one. According to the curve, the generator provides more power to the grid than it receives from the turbine. As already known from small-signal stability analysis, the generator starts to slow down. Due to the rotor is considerably faster than the grid, it takes some time to slow it down, until it is synchronous again. Up to then, the transient rotor angle is still increasing. Such a point of synchronism can only be found left from the instable, second operation point. Otherwise, the generator would already be accelerated again and starts to overrun. In this case the generator is transiently instable and needs to be switched off.

If there is a first point of synchronism, the provided electric power there is superior to the power of the turbine, which means the rotor starts to slow down and the rotor angle decreases. The rotor speed is now slower than the grid frequency, so the rotor overshoots the stable operation point and needs to be accelerated again. It becomes apparent, that the generator reaches its new stable operation point by a damped oscillation. The process is shown in Fig. 41.

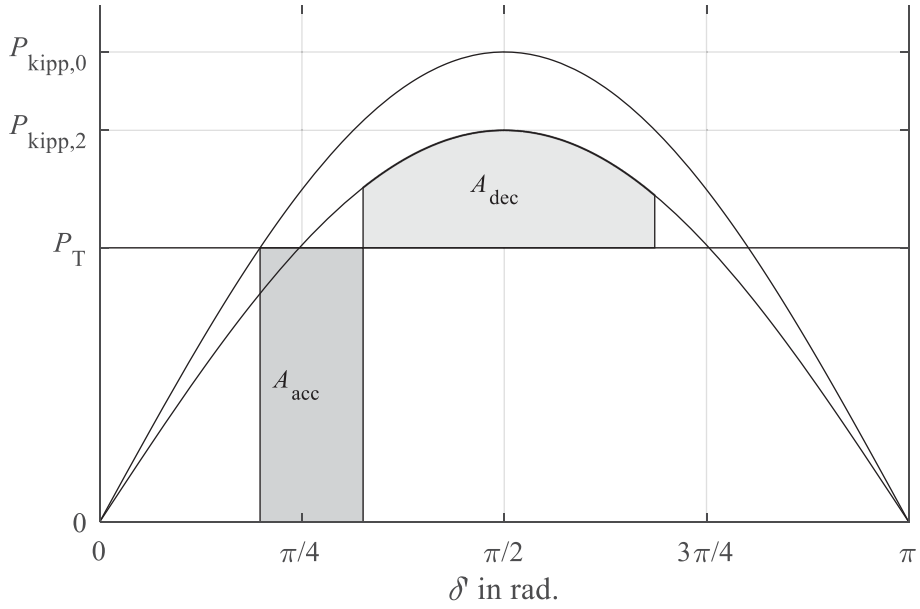

Fig. 41: acceleration and breaking areas of the single machine problem

The question of transient stability is therefore a question of the existence of the first point of synchronism. It can also be answered by having a look at the change of the kinetic energy of the generator. During the fault, the kinetic energy of the rotor increases.

$$\Delta E_{\mathrm{kin}} = \frac{1}{2}\frac{J}{p^2}\Delta\omega_{\mathrm{L}}^2 = \frac{1}{2}J\Delta\Omega_{\mathrm{L}}^2 = \frac{1}{\omega_0}P_{\mathrm{T}}\left(\delta'_{\mathrm{FC}} - \delta'_0\right) = \frac{1}{\omega_0}A_{\mathrm{acc}} \tag{7.35}$$

This increase is proportional the product of the turbine power and the rotor angle difference prior to and after the fault. This product corresponds to an area A_{acc} in Fig. 41, which is therefore called acceleration area.

The same considerations can be made for the time after the fault clearance and the first point of synchronism. During this time, the rotor is slowed down which is why the resulting area A_{dec} is called breaking area. The area is

$$A_{\mathrm{dec}} = \int_{\delta'_{\mathrm{FC}}}^{\delta'_{\mathrm{max}}} P_{\mathrm{T}} - P_{\mathrm{G}}\left(\delta'\right)\mathrm{d}\delta' \tag{7.36}$$

If there is a solution for eq. (7.36), which means there is a δ'_{max}, with

$$A_{\mathrm{dec}}\left(\delta'_{\mathrm{max}}\right) = A_{\mathrm{acc}} \tag{7.37}$$

in this case, the generator is transiently stable.

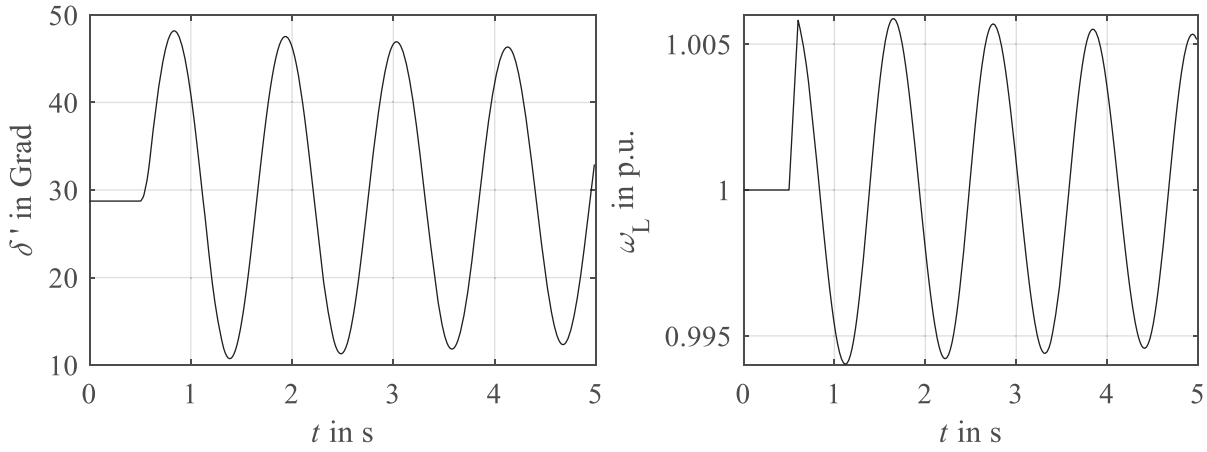

Fig. 42: time-series and roto speed for a transiently stable generator

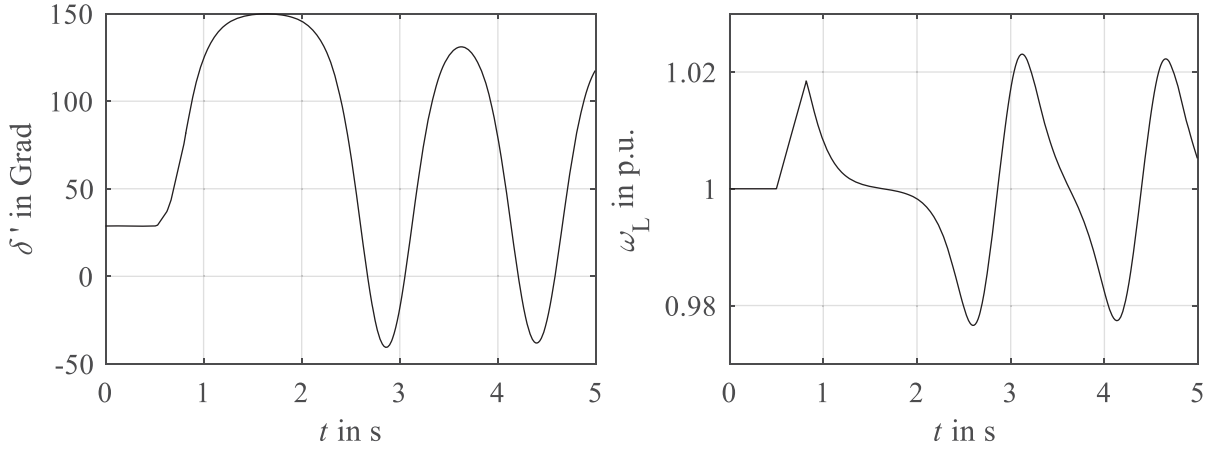

Fig. 43: critically stable time-series of roto angle and rotor speed

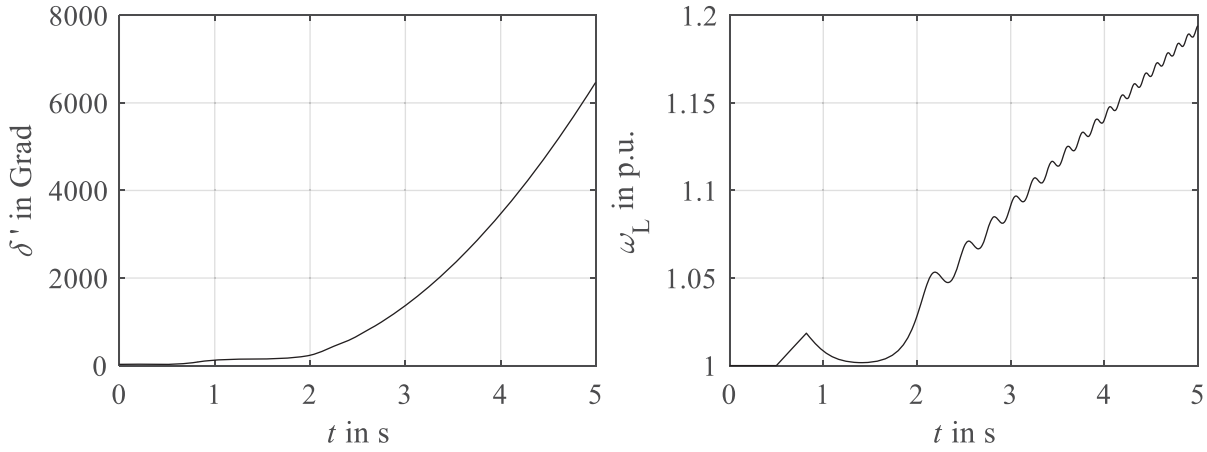

Fig. 44: instable stable time-series of roto angle and rotor speed

It is obvious, that transient stability does not only depend on the operation point of the generator but also on secondary factors like the fault location and the duration of the fault.

7.6.2 General determination of transient stability in grids with several generators

In real grids which are fed by a variety of different generators it is usually impossible to rely on a synchronous equivalent network. In fact, the oscillations of the generators among themselves are analyzed. A grid containing g generators results in a differential equation system with $2\,g$ variables according to eq. (7.22). The generator currents and transient generated voltages can be used to calculate the electric active powers $\boldsymbol{p}_\mathrm{e}$ which are needed to numerically solve the differential equation system. This results in a time-series of the rotor angle motions. Their behavior is used to decide, whether the system is transiently stable or not. If the rotor angles settle at a new steady-state value and stay close to each other, the system is transiently stable. If one of the angles diverges from the others, this generator is instable.

Instead of the reference angle of an equivalent network, the center of inertia of the generators can be used as reference value. It is obtained by the weighted average of the rotor angles.

$$\delta'_\mathrm{Z} = \frac{\sum_{i=1}^{g}\left(S_{\mathrm{rG},i}\; T_{\mathrm{m},i}\; \delta'_i\right)}{\sum_{i=1}^{g}\left(S_{\mathrm{rG},i}\; T_{\mathrm{m},i}\right)} \tag{7.38}$$

The generators oscillate around their common center of inertia. Topological properties of the grid may lead to distinct groups of generators that will form their respective centers of inertia. These groups can be used to aggregate generators and save computational time by simply analyzing the mutual motion of the aggregated groups.

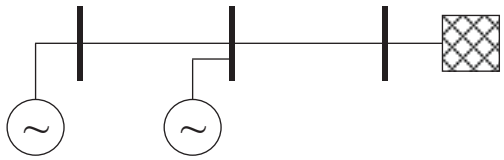

Fig. 45: multi-machine problem

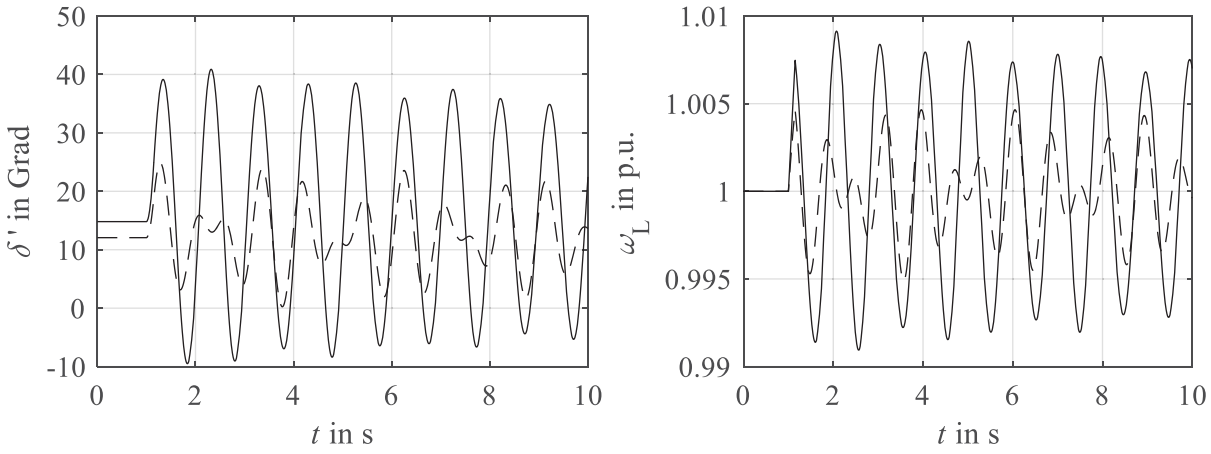

Fig. 46: stable time-series of rotor angle and speed (fault duration: 150 ms)

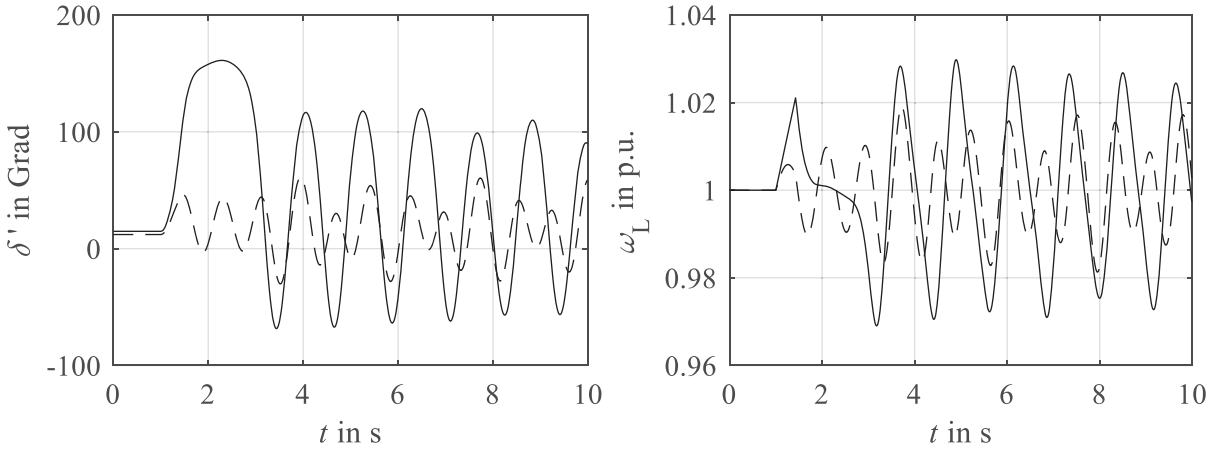

Fig. 47: critically stable time-series of rotor angle and speed (fault duration: 425 ms)

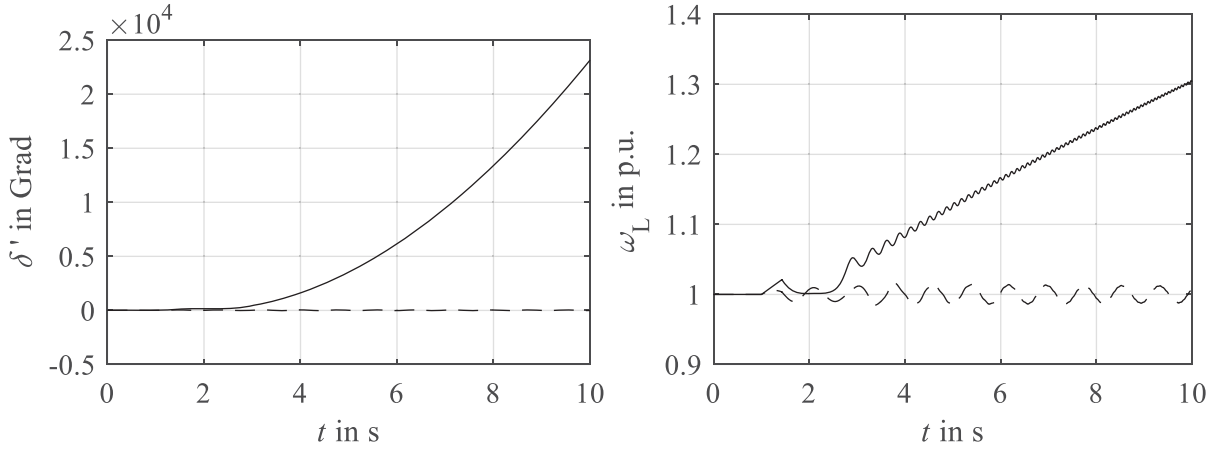

Fig. 48: instable time-series of rotor angle and speed (fault duration: 426 ms)

7.6.3 Measures to increase transient stability

To improve transient stability, it is necessary to provide sufficient reserves for slowing down or accelerating the rotor again after clearance of the fault. This can be achieved by maximizing the quotient of breakdown power and turbine power. Several options are available:

- High magnitude of U', that means high excitation, resulting in small transient rotor angles δ'
- Small grid impedance, which can be achieved with meshing or series compensation, similar to small-signal stability
- Selective and fast fault clearance
- Fast turbine governors
- Damping of rotor oscillations using additional controllers, so called Power System Stabilizers (PSS)

8 Modelling of shunt and series faults

In the electric power system, the occurrence of faults is inevitable. All possible sorts of faults must therefore be considered during grid planning and grid operation to not endanger assets, people and system security, if a fault occurs. In general, faults are divided into series and shunt faults:

- Shunt faults are faults that occur orthogonal to the power flow direction. They establish a conducting connection between phase and ground or between other phases (and potentially with ground). The perturbation and the intensity of the fault current depends on the constellation of the fault. If the fault current is high, it is called short-circuit current.
- Series faults are faults that occur in the direction of the power flow. They may be an increase of impedance up to a total interruption of the line. On the other hand, short-circuiting of an aspired interruption, e.g. a breaker that has not opened correctly, is seen as a series fault as well.

Shunt and series faults can occur balanced or unbalanced, as single or multiple parallel faults in any arbitrary constellation and combination and at different positions in the grid. This is typical for some sorts of faults. E.g. a single-line-to-ground fault causes the voltage to increase by the factor of $\sqrt{3}$ in the healthy lines of ungrounded grids which may lead to secondary short-circuits if the insulation cannot bear the voltage rise.

To calculate unbalanced faults, usually, the fault constellation, which is known in natural coordinates, needs to be transformed into symmetrical components. Therefore, the network descriptions of the positive, negative and zero sequence system need to be interconnected at the fault location depending on the fault. This gets very complicated in case of several parallel faults. Using the fault matrix method described here, the interconnection of these systems can be done in an easy and systematic way by integrating the fault conditions into the current equation of the grid. Thereby, the fault matrix method is independent from the actually used coordination systems and works with natural coordinates as well as every modal transformation. Besides, it offers some additional advantages:

- All matrices that need to be inverted are not singular.
- The number of nodes and terminals stays constant and is does not depend on the faults or the switching state.
- Shunt faults without an impedance ($\underline{Y} \to \infty$) and series faults without an admittance ($\underline{Z} \to \infty$) can be expressed and integrated without any numerical assumptions.

8.1 Fault conditions

The relations between voltages and currents at the fault location are called fault conditions. Independent from the used coordinate system, in a three-phase grid, there are always three dual voltage and current constraints which combine to the fault conditions. They can therefore be expressed using a characteristic 3×3 fault matrix $\boldsymbol{F}$.

8.1.1 Fault conditions in natural coordinates

To model shunt faults, at the respective location fault impedances $\underline{Z}_F$ are included into the line diagram. They carry the fault current $\underline{I}_F$

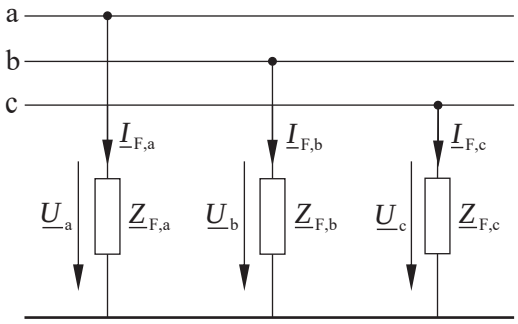

Fig. 49: modelling of shunt faults

In the healthy phases, the fault current is zero. In the faulty phases, the impedance creates a new mesh. The sum of voltages in this mesh must be zero. These two conditions can be expressed using the above-mentioned fault matrix.

$$\boldsymbol{F}\begin{bmatrix}\underline{I}_{F,a}\\ \underline{I}_{F,b}\\ \underline{I}_{F,c}\end{bmatrix}=\boldsymbol{0} \tag{8.1}$$

and

$$\left(\boldsymbol{E}-\boldsymbol{F}^{T}\right)\left(\begin{bmatrix}\underline{U}_a\\ \underline{U}_b\\ \underline{U}_c\end{bmatrix}-\begin{bmatrix}\underline{Z}_{F,a} & & \\ & \underline{Z}_{F,b} & \\ & & \underline{Z}_{F,c}\end{bmatrix}\begin{bmatrix}\underline{I}_{F,a}\\ \underline{I}_{F,b}\\ \underline{I}_{F,c}\end{bmatrix}\right)=\boldsymbol{0} \tag{8.2}$$

Series faults are modelled by including fault admittances $\underline{Y}_F$ into the line diagram at the respective location bearing a series fault voltage $\underline{U}_F$.

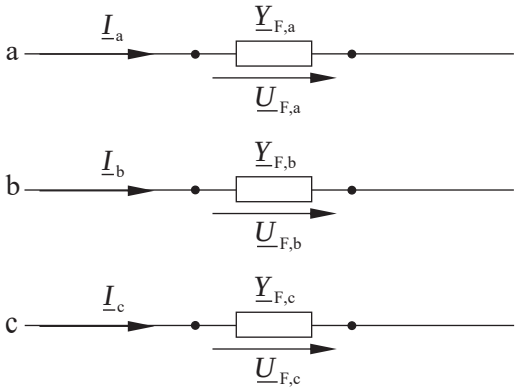

Fig. 50: modelling of series faults

In the healthy phases, the fault voltage is zero. On the other hand, in faulty lines, the fault admittance forms an additional fork, at which the sums of currents must be zero, according to Kirchhoff's first law. Both constraints can again be combined using the fault matrix.

$$\boldsymbol{F}\begin{bmatrix}\underline{U}_{\mathrm{F,a}}\\ \underline{U}_{\mathrm{F,b}}\\ \underline{U}_{\mathrm{F,c}}\end{bmatrix}=\boldsymbol{0} \tag{8.3}$$

and

$$\left(\boldsymbol{E}-\boldsymbol{F}^{\mathrm{T}}\right)\left(\begin{bmatrix}\underline{I}_{\mathrm{a}}\\ \underline{I}_{\mathrm{b}}\\ \underline{I}_{\mathrm{c}}\end{bmatrix}-\begin{bmatrix}\underline{Y}_{\mathrm{F,a}} & & \\ & \underline{Y}_{\mathrm{F,b}} & \\ & & \underline{Y}_{\mathrm{F,c}}\end{bmatrix}\begin{bmatrix}\underline{U}_{\mathrm{F,a}}\\ \underline{U}_{\mathrm{F,b}}\\ \underline{U}_{\mathrm{F,c}}\end{bmatrix}\right)=\boldsymbol{0} \tag{8.4}$$

Table 5: overview of fault matrices

shunt faults		series faults		fault matrix
no shunt fault	$\underline{I}_{\mathrm{F,a}}=0$ $\underline{I}_{\mathrm{F,b}}=0$ $\underline{I}_{\mathrm{F,c}}=0$	no series fault	$\underline{U}_{\mathrm{F,a}}=0$ $\underline{U}_{\mathrm{F,b}}=0$ $\underline{U}_{\mathrm{F,c}}=0$	$\begin{bmatrix}1&0&0\\0&1&0\\0&0&1\end{bmatrix}$
single phase to ground	$\underline{U}_{\mathrm{a}}-\underline{Z}_{\mathrm{F,a}}\,\underline{I}_{\mathrm{F,a}}=0$ $\underline{I}_{\mathrm{F,b}}=0$ $\underline{I}_{\mathrm{F,c}}=0$	single phase open	$\underline{I}_{\mathrm{a}}-\underline{Y}_{\mathrm{F,a}}\,\underline{U}_{\mathrm{F,a}}=0$ $\underline{U}_{\mathrm{F,b}}=0$ $\underline{U}_{\mathrm{F,c}}=0$	$\begin{bmatrix}0&0&0\\0&1&0\\0&0&1\end{bmatrix}$
two phases to ground	$\underline{I}_{\mathrm{F,a}}=0$ $\underline{U}_{\mathrm{b}}-\underline{Z}_{\mathrm{F,b}}\,\underline{I}_{\mathrm{F,b}}=0$ $\underline{U}_{\mathrm{c}}-\underline{Z}_{\mathrm{F,c}}\,\underline{I}_{\mathrm{F,c}}=0$	two phases open	$\underline{U}_{\mathrm{F,a}}=0$ $\underline{I}_{\mathrm{b}}-\underline{Y}_{\mathrm{F,b}}\,\underline{U}_{\mathrm{F,b}}=0$ $\underline{I}_{\mathrm{c}}-\underline{Y}_{\mathrm{F,c}}\,\underline{U}_{\mathrm{F,c}}=0$	$\begin{bmatrix}1&0&0\\0&0&0\\0&0&0\end{bmatrix}$
three phases to ground	$\underline{U}_{\mathrm{a}}-\underline{Z}_{\mathrm{F,a}}\,\underline{I}_{\mathrm{F,a}}=0$ $\underline{U}_{\mathrm{b}}-\underline{Z}_{\mathrm{F,b}}\,\underline{I}_{\mathrm{F,b}}=0$ $\underline{U}_{\mathrm{c}}-\underline{Z}_{\mathrm{F,c}}\,\underline{I}_{\mathrm{F,c}}=0$	three phases open	$\underline{I}_{\mathrm{a}}-\underline{Y}_{\mathrm{F,a}}\,\underline{U}_{\mathrm{F,a}}=0$ $\underline{I}_{\mathrm{b}}-\underline{Y}_{\mathrm{F,b}}\,\underline{U}_{\mathrm{F,b}}=0$ $\underline{I}_{\mathrm{c}}-\underline{Y}_{\mathrm{F,c}}\,\underline{U}_{\mathrm{F,c}}=0$	$\begin{bmatrix}0&0&0\\0&0&0\\0&0&0\end{bmatrix}$
two phase short-circuit without ground	$\underline{I}_{\mathrm{F,a}}=0$ $\underline{I}_{\mathrm{F,b}}+\underline{I}_{\mathrm{F,c}}=0$ $\left(\underline{U}_{\mathrm{c}}-\underline{Z}_{\mathrm{F,c}}\,\underline{I}_{\mathrm{F,c}}\right)$ $-\left(\underline{U}_{\mathrm{b}}-\underline{Z}_{\mathrm{F,b}}\,\underline{I}_{\mathrm{F,b}}\right)=0$			$\begin{bmatrix}1&0&0\\0&1&1\\0&0&0\end{bmatrix}$
three phase short-circuit without ground	$\underline{I}_{\mathrm{F,a}}+\underline{I}_{\mathrm{F,b}}+\underline{I}_{\mathrm{F,c}}=0$ $\left(\underline{U}_{\mathrm{b}}-\underline{Z}_{\mathrm{F,b}}\,\underline{I}_{\mathrm{F,b}}\right)$ $-\left(\underline{U}_{\mathrm{a}}-\underline{Z}_{\mathrm{F,a}}\,\underline{I}_{\mathrm{F,a}}\right)=0$ $\left(\underline{U}_{\mathrm{c}}-\underline{Z}_{\mathrm{F,c}}\,\underline{I}_{\mathrm{F,c}}\right)$ $-\left(\underline{U}_{\mathrm{a}}-\underline{Z}_{\mathrm{F,a}}\,\underline{I}_{\mathrm{F,a}}\right)=0$			$\begin{bmatrix}1&1&1\\0&0&0\\0&0&0\end{bmatrix}$

The fault matrices for the so-called main-faults are given in Table 5. Main fault means, that the fault is symmetric to the reference phase a. All other faults, e.g. a single line to ground fault in phase b, is modelled in the exact same way by setting the ones and zeros accordingly in the fault matrix.

Shunt and series faults are modelled using the same fault matrices. This fact is called duality. Only for the two-phase and three-phase short-circuit without ground contact there is no corresponding series fault.

If there is no fault, the fault matrix is the unity matrix. In this case in eq. (8.1) the fault currents are directly set to zero. In. eq. (8.2) the first term is zero. So, no artificial, numerically high impedances need to be assumed to approximate at faultless condition. The same is true for series faults. There is no need to include artificial admittances to approximate a connection with no impedance or an interruption with no admittance.

8.1.2 Fault conditions in symmetrical components

The description of faults in symmetrical components is done analogously to the natural coordinates. The system matrix $\underline{\boldsymbol{Z}}$, the fault matrix $\boldsymbol{F}$ and the fault impedances and admittances are transformed into the modal reference frame using the transformation matrix $\underline{\boldsymbol{T}}_{\mathrm{SK}}$. This results in the fault matrix

$$\underline{\boldsymbol{F}}_{\mathrm{SK}} = \underline{\boldsymbol{T}}_{\mathrm{SK}}^{-1}\, \boldsymbol{F}\, \underline{\boldsymbol{T}}_{\mathrm{SK}} \tag{8.5}$$

The fault matrix is now complex-valued. With

$$\underline{\boldsymbol{Z}}_{\mathrm{F,SK}} = \underline{\boldsymbol{T}}_{\mathrm{SK}}^{-1}\, \underline{\boldsymbol{Z}}_{\mathrm{F}}\, \underline{\boldsymbol{T}}_{\mathrm{SK}} \tag{8.6}$$

and

$$\underline{\boldsymbol{Y}}_{\mathrm{F,SK}} = \underline{\boldsymbol{T}}_{\mathrm{SK}}^{-1}\, \underline{\boldsymbol{Y}}_{\mathrm{F}}\, \underline{\boldsymbol{T}}_{\mathrm{SK}} \tag{8.7}$$

the shunt and series faults are calculated in the exact same way as in natural coordinates. Shunt faults are calculated according to

$$\begin{aligned} \underline{\boldsymbol{F}}_{\mathrm{SK}} \begin{bmatrix} \underline{I}_{\mathrm{F},1} \\ \underline{I}_{\mathrm{F},2} \\ \underline{I}_{\mathrm{F},0} \end{bmatrix} &= \boldsymbol{0} \\ \left(\boldsymbol{E} - \underline{\boldsymbol{F}}_{\mathrm{SK}}^{\mathrm{T}*}\right) \left(\begin{bmatrix} \underline{U}_1 \\ \underline{U}_2 \\ \underline{U}_0 \end{bmatrix} - \begin{bmatrix} \underline{Z}_{\mathrm{F},1} & & \\ & \underline{Z}_{\mathrm{F},1} & \\ & & \underline{Z}_{\mathrm{F},0} \end{bmatrix} \begin{bmatrix} \underline{I}_{\mathrm{F},1} \\ \underline{I}_{\mathrm{F},2} \\ \underline{I}_{\mathrm{F},0} \end{bmatrix} \right) &= \boldsymbol{0} \end{aligned} \tag{8.8}$$

and series faults respectively

$$\begin{gathered}\boldsymbol{\underline{F}}_{\mathrm{SK}}\begin{bmatrix}\underline{U}_{\mathrm{F},1}\\ \underline{U}_{\mathrm{F},2}\\ \underline{U}_{\mathrm{F},0}\end{bmatrix}=\boldsymbol{0}\\ \left(\boldsymbol{E}-\boldsymbol{\underline{F}}_{\mathrm{SK}}^{\mathrm{T}*}\right)\left(\begin{bmatrix}\underline{I}_1\\ \underline{I}_2\\ \underline{I}_0\end{bmatrix}-\begin{bmatrix}\underline{Y}_{\mathrm{F},1} & & \\ & \underline{Y}_{\mathrm{F},2} & \\ & & \underline{Y}_{\mathrm{F},0}\end{bmatrix}\begin{bmatrix}\underline{U}_{\mathrm{F},1}\\ \underline{U}_{\mathrm{F},2}\\ \underline{U}_{\mathrm{F},0}\end{bmatrix}\right)=\boldsymbol{0}\end{gathered} \tag{8.9}$$

where

$$\boldsymbol{\underline{F}}_{\mathrm{SK}}^{\mathrm{T}*}=\left(\boldsymbol{\underline{T}}_{\mathrm{SK}}^{-1}\,\boldsymbol{F}\,\boldsymbol{\underline{T}}_{\mathrm{SK}}\right)^{\mathrm{T}*}=\boldsymbol{\underline{T}}_{\mathrm{SK}}^{\mathrm{T}*}\,\boldsymbol{F}^{\mathrm{T}}\left(\boldsymbol{\underline{T}}_{\mathrm{SK}}^{-1}\right)^{\mathrm{T}*}=\boldsymbol{\underline{T}}_{\mathrm{SK}}^{-1}\,\boldsymbol{F}^{\mathrm{T}}\,\boldsymbol{\underline{T}}_{\mathrm{SK}} \tag{8.10}$$

Obviously, it is advantageous to model the fault in natural coordinates first and then transform it into symmetrical components for calculation. The resulting phase voltages and currents are obtained by retransformation afterwards.

The shown procedure can be used in the same way with any modal component system.

8.2 General description of shunt faults

All sequence systems need to be considered to calculate unbalanced faults. Therefore, the current equation system is extended to calculate the negative and zero sequence system as well resulting in 3×3 submatrices instead of the scalars known from the positive sequence system.

$$\begin{bmatrix}\boldsymbol{\underline{Y}}_{1,1} & \boldsymbol{\underline{Y}}_{1,2} & \cdots & \boldsymbol{\underline{Y}}_{1,n}\\ \boldsymbol{\underline{Y}}_{2,1} & \boldsymbol{\underline{Y}}_{2,2} & \cdots & \boldsymbol{\underline{Y}}_{2,n}\\ \vdots & \vdots & \ddots & \vdots\\ \boldsymbol{\underline{Y}}_{n,1} & \boldsymbol{\underline{Y}}_{n,2} & \cdots & \boldsymbol{\underline{Y}}_{n,n}\end{bmatrix}\begin{bmatrix}\boldsymbol{\underline{u}}_{\mathrm{K},1}\\ \boldsymbol{\underline{u}}_{\mathrm{K},2}\\ \vdots\\ \boldsymbol{\underline{u}}_{\mathrm{K},n}\end{bmatrix}=\begin{bmatrix}\boldsymbol{\underline{i}}_{\mathrm{K},1}\\ \boldsymbol{\underline{i}}_{\mathrm{K},2}\\ \vdots\\ \boldsymbol{\underline{i}}_{\mathrm{K},n}\end{bmatrix} \tag{8.11}$$

$$\boldsymbol{\underline{Y}}_{\mathrm{KK}}\qquad\qquad\boldsymbol{\underline{u}}_{\mathrm{K}}\;=\;\boldsymbol{\underline{i}}_{\mathrm{K}}$$

with

$$\boldsymbol{\underline{Y}}_{i,j}=\begin{bmatrix}\underline{Y}_{1,i,j} & & \\ & \underline{Y}_{2,i,j} & \\ & & \underline{Y}_{0,i,j}\end{bmatrix} \tag{8.12}$$

In case of a fault, the nodal currents are superposed by the fault currents.

$$\begin{bmatrix}\boldsymbol{\underline{Y}}_{1,1} & \boldsymbol{\underline{Y}}_{1,2} & \cdots & \boldsymbol{\underline{Y}}_{1,n}\\ \boldsymbol{\underline{Y}}_{2,1} & \boldsymbol{\underline{Y}}_{2,2} & \cdots & \boldsymbol{\underline{Y}}_{2,n}\\ \vdots & \vdots & \ddots & \vdots\\ \boldsymbol{\underline{Y}}_{n,1} & \boldsymbol{\underline{Y}}_{n,2} & \cdots & \boldsymbol{\underline{Y}}_{n,n}\end{bmatrix}\begin{bmatrix}\boldsymbol{\underline{u}}_{\mathrm{K},1}\\ \boldsymbol{\underline{u}}_{\mathrm{K},2}\\ \vdots\\ \boldsymbol{\underline{u}}_{\mathrm{K},n}\end{bmatrix}=\begin{bmatrix}\boldsymbol{\underline{i}}_{\mathrm{K},1}\\ \boldsymbol{\underline{i}}_{\mathrm{K},2}\\ \vdots\\ \boldsymbol{\underline{i}}_{\mathrm{K},n}\end{bmatrix}+\begin{bmatrix}\boldsymbol{\underline{i}}_{\mathrm{F},1}\\ \boldsymbol{\underline{i}}_{\mathrm{F},2}\\ \vdots\\ \boldsymbol{\underline{i}}_{\mathrm{F},n}\end{bmatrix} \tag{8.13}$$

$$\boldsymbol{\underline{Y}}_{\mathrm{KK}}\qquad\qquad\boldsymbol{\underline{u}}_{\mathrm{K}}\;=\;\boldsymbol{\underline{i}}_{\mathrm{K}}\;+\;\boldsymbol{\underline{i}}_{\mathrm{F}}$$

According to Table 5 for each node a fault matrix and a fault impedance matrix can be defined. All nodal fault matrices are combined to a single fault matrix $\boldsymbol{\underline{F}}_{\mathrm{K}}$ which has block-diagonal

form. Thus, it is possible to model as many parallel faults as wanted without additional effort. According to eq. (8.8), the fault currents

$$\begin{bmatrix} \underline{\boldsymbol{F}}_{\mathrm{K},1} & & \\ & \ddots & \\ & & \underline{\boldsymbol{F}}_{\mathrm{K},n} \end{bmatrix} \begin{bmatrix} \underline{\boldsymbol{i}}_{\mathrm{F},1} \\ \vdots \\ \underline{\boldsymbol{i}}_{\mathrm{F},n} \end{bmatrix} = \underline{\boldsymbol{F}}_{\mathrm{K}}\, \underline{\boldsymbol{i}}_{\mathrm{F}} = \boldsymbol{0} \tag{8.14}$$

and the voltages are calculated

$$\begin{bmatrix} \boldsymbol{E} - \underline{\boldsymbol{F}}_{\mathrm{K},1}^{\mathrm{T}*} & & \\ & \ddots & \\ & & \boldsymbol{E} - \underline{\boldsymbol{F}}_{\mathrm{K},n}^{\mathrm{T}*} \end{bmatrix} \begin{bmatrix} \underline{\boldsymbol{u}}_{\mathrm{K},1} - \underline{\boldsymbol{Z}}_{\mathrm{F},1}\, \underline{\boldsymbol{i}}_{\mathrm{F},1} \\ \vdots \\ \underline{\boldsymbol{u}}_{\mathrm{K},n} - \underline{\boldsymbol{Z}}_{\mathrm{F},n}\, \underline{\boldsymbol{i}}_{\mathrm{F},n} \end{bmatrix} = \left(\boldsymbol{E} - \underline{\boldsymbol{F}}_{\mathrm{K}}^{\mathrm{T}*}\right)\left(\underline{\boldsymbol{u}}_{\mathrm{K}} - \underline{\boldsymbol{Z}}_{\mathrm{F}}\, \underline{\boldsymbol{i}}_{\mathrm{F}}\right) = \boldsymbol{0} \tag{8.15}$$

Eq. (8.13) is solved for the fault current. The result is inserted into eq. (8.14) and eq. (8.15).

$$\underline{\boldsymbol{F}}_{\mathrm{K}} \left(\underline{\boldsymbol{Y}}_{\mathrm{KK}}\, \underline{\boldsymbol{u}}_{\mathrm{K}} - \underline{\boldsymbol{i}}_{\mathrm{K}}\right) = \boldsymbol{0} \tag{8.16}$$

and

$$\left(\boldsymbol{E} - \underline{\boldsymbol{F}}_{\mathrm{K}}^{\mathrm{T}*}\right)\left(\underline{\boldsymbol{u}}_{\mathrm{K}} - \underline{\boldsymbol{Z}}_{\mathrm{F}} \left(\underline{\boldsymbol{Y}}_{\mathrm{KK}}\, \underline{\boldsymbol{u}}_{\mathrm{K}} - \underline{\boldsymbol{i}}_{\mathrm{K}}\right)\right) = \boldsymbol{0} \tag{8.17}$$

Reformulation of eq. (8.17) results in

$$\left(\boldsymbol{E} - \underline{\boldsymbol{F}}_{\mathrm{K}}^{\mathrm{T}*}\right)\left(\boldsymbol{E} - \underline{\boldsymbol{Z}}_{\mathrm{F}}\, \underline{\boldsymbol{Y}}_{\mathrm{KK}}\right)\underline{\boldsymbol{u}}_{\mathrm{K}} + \left(\boldsymbol{E} - \underline{\boldsymbol{F}}_{\mathrm{K}}^{\mathrm{T}*}\right)\underline{\boldsymbol{Z}}_{\mathrm{F}}\, \underline{\boldsymbol{i}}_{\mathrm{K}} = \boldsymbol{0} \tag{8.18}$$

Eq. (8.18) is a voltage constraint. It can be multiplied with $\underline{\boldsymbol{Y}}_{\mathrm{KK}}$ to formally convert it into a current constraint. After that, it is set equal to the current constraint from eq. (8.16).

$$\underline{\boldsymbol{F}}_{\mathrm{K}} \left(\underline{\boldsymbol{Y}}_{\mathrm{KK}}\, \underline{\boldsymbol{u}}_{\mathrm{K}} - \underline{\boldsymbol{i}}_{\mathrm{K}}\right) = \underline{\boldsymbol{Y}}_{\mathrm{KK}} \left(\left(\boldsymbol{E} - \underline{\boldsymbol{F}}_{\mathrm{K}}^{\mathrm{T}*}\right)\left(\boldsymbol{E} - \underline{\boldsymbol{Z}}_{\mathrm{F}}\, \underline{\boldsymbol{Y}}_{\mathrm{KK}}\right)\underline{\boldsymbol{u}}_{\mathrm{K}} + \left(\boldsymbol{E} - \underline{\boldsymbol{F}}_{\mathrm{K}}^{\mathrm{T}*}\right)\underline{\boldsymbol{Z}}_{\mathrm{F}}\, \underline{\boldsymbol{i}}_{\mathrm{K}}\right) \tag{8.19}$$

Using the auxiliary matrix

$$\underline{\boldsymbol{F}}_{\mathrm{ZF}} = \underline{\boldsymbol{Y}}_{\mathrm{KK}} \left(\boldsymbol{E} - \underline{\boldsymbol{F}}_{\mathrm{K}}^{\mathrm{T}*}\right) \underline{\boldsymbol{Z}}_{\mathrm{F}} \tag{8.20}$$

eq. (8.19) can be solved and reformulated into the well-known current equation form

$$\begin{gathered} \left(\underline{\boldsymbol{F}}_{\mathrm{K}}\, \underline{\boldsymbol{Y}}_{\mathrm{KK}} - \underline{\boldsymbol{Y}}_{\mathrm{KK}} \left(\boldsymbol{E} - \underline{\boldsymbol{F}}_{\mathrm{FZ}}\right) + \underline{\boldsymbol{Y}}_{\mathrm{KK}}\, \underline{\boldsymbol{F}}_{\mathrm{K}}^{\mathrm{T}*}\right) \underline{\boldsymbol{u}}_{\mathrm{K}} = \left(\underline{\boldsymbol{F}}_{\mathrm{K}} + \underline{\boldsymbol{F}}_{\mathrm{FZ}}\right) \underline{\boldsymbol{i}}_{\mathrm{K}} \\ \underline{\boldsymbol{Y}}_{\mathrm{KK,F}} \qquad\qquad\qquad \underline{\boldsymbol{u}}_{\mathrm{K}} = \qquad \underline{\boldsymbol{i}}_{\mathrm{K,F}} \end{gathered} \tag{8.21}$$

The fault matrix method obviously modifies the nodal bus admittance matrix and the right-hand-side of the current equation. The voltages of the faulty system can now be calculated by solving eq. (8.21) for $\underline{\boldsymbol{u}}_{\mathrm{K}}$. Afterwards the fault currents can be obtained.

$$\underline{\boldsymbol{i}}_{\mathrm{F}} = \underline{\boldsymbol{Y}}_{\mathrm{KK}}\, \underline{\boldsymbol{u}}_{\mathrm{K}} - \underline{\boldsymbol{i}}_{\mathrm{K}} \tag{8.22}$$

During the entire process, the size of the equation has not changed.

If all faults do not have an impedance, $\underline{\boldsymbol{Z}}_{\mathrm{F}}$ and $\underline{\boldsymbol{F}}_{\mathrm{ZF}}$ are zero matrices. In this case, eq. (8.21) can be simplified to

$$\left(\underline{\boldsymbol{F}}_{\mathrm{K}}\, \underline{\boldsymbol{Y}}_{\mathrm{KK}} - \underline{\boldsymbol{Y}}_{\mathrm{KK}} + \underline{\boldsymbol{Y}}_{\mathrm{KK}}\, \underline{\boldsymbol{F}}_{\mathrm{K}}^{\mathrm{T}*}\right) \underline{\boldsymbol{u}}_{\mathrm{K}} = \underline{\boldsymbol{F}}_{\mathrm{K}}\, \underline{\boldsymbol{i}}_{\mathrm{K}} \tag{8.23}$$

If there is no fault, $\underline{\boldsymbol{F}}_{\mathrm{K}}$ will be the unity matrix and $\boldsymbol{E}-\underline{\boldsymbol{F}}_{\mathrm{K}}^{\mathrm{T}*}$ a zero matrix, respectively. Eq. (8.23) will be the original current equation again.

8.3 General description of series faults

Series faults are changes to the physical behavior of assets. Thus, they are not directly modelled using the nodal current equation system but the terminal current equation system instead. Again, the fault matrix method aims at calculating interruptions without artificial inner nodes or terminals which would change the size of the equation systems depending on the number and type of the fault. For the reason of highest relevance, modelling of series faults is demonstrated using quadrupoles here. It is nevertheless suitable for any type of equipment and applied in the exact same way.

Similar to the shunt faults, the terminal current equation system needs to be extended by the negative and zero sequence system resulting in 3×3 submatrices instead of scalars.

$$\begin{bmatrix}\underline{\boldsymbol{i}}_{\mathrm{A}}\\ \underline{\boldsymbol{i}}_{\mathrm{B}}\end{bmatrix}=\begin{bmatrix}\underline{\boldsymbol{Y}}_{\mathrm{AA}} & \underline{\boldsymbol{Y}}_{\mathrm{AB}}\\ \underline{\boldsymbol{Y}}_{\mathrm{BA}} & \underline{\boldsymbol{Y}}_{\mathrm{BB}}\end{bmatrix}\begin{bmatrix}\underline{\boldsymbol{u}}_{\mathrm{A}}\\ \underline{\boldsymbol{u}}_{\mathrm{B}}\end{bmatrix} \tag{8.24}$$

At each terminal, a series fault can be modelled as a series voltage which superposes to the terminal voltages

$$\begin{bmatrix}\underline{\boldsymbol{i}}_{\mathrm{A,F}}\\ \underline{\boldsymbol{i}}_{\mathrm{B,F}}\end{bmatrix}=\begin{bmatrix}\underline{\boldsymbol{Y}}_{\mathrm{AA}} & \underline{\boldsymbol{Y}}_{\mathrm{AB}}\\ \underline{\boldsymbol{Y}}_{\mathrm{BA}} & \underline{\boldsymbol{Y}}_{\mathrm{BB}}\end{bmatrix}\left(\begin{bmatrix}\underline{\boldsymbol{u}}_{\mathrm{A}}\\ \underline{\boldsymbol{u}}_{\mathrm{B}}\end{bmatrix}-\begin{bmatrix}\underline{\boldsymbol{u}}_{\mathrm{F,A}}\\ \underline{\boldsymbol{u}}_{\mathrm{F,B}}\end{bmatrix}\right) \tag{8.25}$$

For both terminals, the voltage constraints

$$\begin{bmatrix}\underline{\boldsymbol{F}}_{\mathrm{T,A}} & \\ & \underline{\boldsymbol{F}}_{\mathrm{T,B}}\end{bmatrix}\begin{bmatrix}\underline{\boldsymbol{u}}_{\mathrm{F,A}}\\ \underline{\boldsymbol{u}}_{\mathrm{F,B}}\end{bmatrix}=\boldsymbol{0} \tag{8.26}$$

and current constraints

$$\left(\boldsymbol{E}-\underline{\boldsymbol{F}}_{\mathrm{T}}^{\mathrm{T}*}\right)\left(\begin{bmatrix}\underline{\boldsymbol{i}}_{\mathrm{A}}\\ \underline{\boldsymbol{i}}_{\mathrm{B}}\end{bmatrix}-\begin{bmatrix}\underline{\boldsymbol{Y}}_{\mathrm{F,A}} & \\ & \underline{\boldsymbol{Y}}_{\mathrm{F,A}}\end{bmatrix}\begin{bmatrix}\underline{\boldsymbol{u}}_{\mathrm{F,A}}\\ \underline{\boldsymbol{u}}_{\mathrm{F,B}}\end{bmatrix}\right)=\boldsymbol{0} \tag{8.27}$$

are defined. For the entire grid this results in

$$\underline{\boldsymbol{i}}_{\mathrm{T,F}}=\underline{\boldsymbol{Y}}_{\mathrm{T}}\left(\underline{\boldsymbol{u}}_{\mathrm{T}}-\underline{\boldsymbol{u}}_{\mathrm{F}}\right) \tag{8.28}$$

with the fault constraints

$$\underline{\boldsymbol{F}}_{\mathrm{T}}\,\underline{\boldsymbol{u}}_{\mathrm{F}}=\boldsymbol{0} \tag{8.29}$$

and

$$\left(\boldsymbol{E}-\underline{\boldsymbol{F}}_{\mathrm{T}}^{\mathrm{T}*}\right)\left(\underline{\boldsymbol{i}}_{\mathrm{T}}-\underline{\boldsymbol{Y}}_{\mathrm{F}}\,\underline{\boldsymbol{u}}_{\mathrm{F}}\right)=\boldsymbol{0} \tag{8.30}$$

Similar to the shunt faults, as a first step, the faulty, dependent values – in the case the terminal currents – are eliminated by inserting eq. (8.28) into eq. (8.30).

$$\left(\boldsymbol{E}-\underline{\boldsymbol{F}}_{\mathrm{T}}^{\mathrm{T}*}\right)\left(\underline{\boldsymbol{Y}}_{\mathrm{T}}\,\underline{\boldsymbol{u}}_{\mathrm{T}}-\left(\underline{\boldsymbol{Y}}_{\mathrm{T}}+\underline{\boldsymbol{Y}}_{\mathrm{F}}\right)\underline{\boldsymbol{u}}_{\mathrm{F}}\right)=\boldsymbol{0} \tag{8.31}$$

Using the auxiliary matrix

$$\underline{\boldsymbol{Y}}_{\mathrm{H}} = \underline{\boldsymbol{Y}}_{\mathrm{T}} + \underline{\boldsymbol{Y}}_{\mathrm{F}} \tag{8.32}$$

the voltage constraints are again formally converted into current constraints which are set equal to the current constraints given in eq. (8.31).

$$\left(\boldsymbol{E} - \underline{\boldsymbol{F}}_{\mathrm{T}}^{\mathrm{T}*}\right)\left(\underline{\boldsymbol{Y}}_{\mathrm{T}}\,\underline{\boldsymbol{u}}_{\mathrm{T}} - \underline{\boldsymbol{Y}}_{\mathrm{H}}\,\underline{\boldsymbol{u}}_{\mathrm{F}}\right) = \underline{\boldsymbol{Y}}_{\mathrm{H}}\,\underline{\boldsymbol{F}}_{\mathrm{T}}\,\underline{\boldsymbol{u}}_{\mathrm{F}} \tag{8.33}$$

Eq. (8.33) is now brought into the well-known current equation form

$$\left(\underline{\boldsymbol{Y}}_{\mathrm{H}} - \underline{\boldsymbol{F}}_{\mathrm{T}}^{\mathrm{T}*}\,\underline{\boldsymbol{Y}}_{\mathrm{H}} + \underline{\boldsymbol{Y}}_{\mathrm{H}}\,\underline{\boldsymbol{F}}_{\mathrm{T}}\right)\underline{\boldsymbol{u}}_{\mathrm{F}} = \left(\boldsymbol{E} - \underline{\boldsymbol{F}}_{\mathrm{T}}^{\mathrm{T}*}\right)\underline{\boldsymbol{Y}}_{\mathrm{T}}\,\underline{\boldsymbol{u}}_{\mathrm{T}} \tag{8.34}$$

and can be solved for $\underline{\boldsymbol{u}}_{\mathrm{F}}$ if there is no shunt-free equipment being completely disconnected from the grid.

$$\underline{\boldsymbol{u}}_{\mathrm{F}} = \left(\underline{\boldsymbol{Y}}_{\mathrm{H}} - \underline{\boldsymbol{F}}_{\mathrm{T}}^{\mathrm{T}*}\,\underline{\boldsymbol{Y}}_{\mathrm{H}} + \underline{\boldsymbol{Y}}_{\mathrm{H}}\,\underline{\boldsymbol{F}}_{\mathrm{T}}\right)^{-1}\left(\boldsymbol{E} - \underline{\boldsymbol{F}}_{\mathrm{T}}^{\mathrm{T}*}\right)\underline{\boldsymbol{Y}}_{\mathrm{T}}\,\underline{\boldsymbol{u}}_{\mathrm{T}} = \underline{\boldsymbol{Z}}_{\mathrm{FF}}\,\underline{\boldsymbol{Y}}_{\mathrm{T}}\,\underline{\boldsymbol{u}}_{\mathrm{T}} \tag{8.35}$$

Eq. (8.35) is inserted into the terminal current equation system which results in

$$\underline{\boldsymbol{i}}_{\mathrm{T}} = \left(\underline{\boldsymbol{Y}}_{\mathrm{T}} - \underline{\boldsymbol{Y}}_{\mathrm{T}}\,\underline{\boldsymbol{Z}}_{\mathrm{FF}}\,\underline{\boldsymbol{Y}}_{\mathrm{T}}\right)\underline{\boldsymbol{u}}_{\mathrm{T}} = \underline{\boldsymbol{Y}}_{\mathrm{T,F}}\,\underline{\boldsymbol{u}}_{\mathrm{T}} \tag{8.36}$$

The fault matrix method only modifies the coefficients of $\underline{\boldsymbol{Y}}_{\mathrm{T}}$ and therefore the physical behavior of the assets according to the faults. Due to $\underline{\boldsymbol{Y}}_{\mathrm{T}}$ and $\underline{\boldsymbol{Y}}_{\mathrm{T,F}}$ have the same size and terminal enumeration, $\underline{\boldsymbol{Y}}_{\mathrm{T,F}}$ can be used to calculate a bus admittance matrix $\underline{\boldsymbol{Y}}_{\mathrm{KK,F}}$ which then can be used to model shunt faults. Thus, multiple parallel shunt and series faults can be calculated simultaneously.

As described, eq. (8.35) cannot be solved, if an asset with no shunt elements is completely disconnected from the grid i.e. switched off. This would result in a non-invertible, singular admittance matrix due to for the disconnected part of the grid, no reference voltage can be given. Due to in this case, independent from the terminal voltages, such an asset cannot transmit any currents via its terminals, it is not necessary to model such behavior using the fault matrix method. Instead, it is faster and more convenient to directly set the corresponding coefficients of $\underline{\boldsymbol{Y}}_{\mathrm{T,F}}$ to zero in eq. (8.36).

Dipoles are often equipped with an inner current source. The fault matrix method can also be applied to such active equipment in the described manner, if the source current is considered in the equations. Eq. (8.35) is extended to

$$\underline{\boldsymbol{u}}_{\mathrm{F}} = \underline{\boldsymbol{Z}}_{\mathrm{FF}}\left(\underline{\boldsymbol{Y}}_{\mathrm{T}}\,\underline{\boldsymbol{u}}_{\mathrm{T}} + \underline{\boldsymbol{i}}_{\mathrm{q}}\right) \tag{8.37}$$

which results in a modified eq. (8.36)

$$\underline{\boldsymbol{i}}_{\mathrm{T}} = \left(\boldsymbol{E} - \underline{\boldsymbol{Y}}_{\mathrm{T}}\,\underline{\boldsymbol{Z}}_{\mathrm{FF}}\right)\left(\underline{\boldsymbol{Y}}_{\mathrm{T}}\,\underline{\boldsymbol{u}}_{\mathrm{T}} + \underline{\boldsymbol{i}}_{\mathrm{q}}\right) = \underline{\boldsymbol{Y}}_{\mathrm{T,F}}\,\underline{\boldsymbol{u}}_{\mathrm{T}} + \underline{\boldsymbol{i}}_{\mathrm{q,F}} \tag{8.38}$$

8.4 Balanced faults

In a balanced system, the negative and zero sequence system are passive and can be neglected. It is sufficient to only calculate the positive sequence system. This can be applied to balanced faults as well, i.e. three phase short-circuits with or without ground contact and three-phase series faults. In these cases, the fault matrix is reduced to a scalar which only represents the positive sequence system. A healthy state is therefore represented by a “1” and the faulty state is indicted by a “0”. The rest of the method works as described. So, all balanced short-circuits and series faults can be easily modeled.

To model balanced admittance-free switching operations, the method can be even further simplified. It is not necessary to perform all of the above-mentioned steps. Instead, the resulting admittance matrices can be directly given, which increases calculation speed. The resulting coefficients of the terminal admittance matrix of quadrupoles is given in Table 6.

Table 6: admittance matrices for switching operations

A	B	fault matrix	lines	two-winding transformers
closed	closed	$\begin{bmatrix} 1 & 0 \\ 0 & 1 \end{bmatrix}$	$\begin{bmatrix} \underline{Y}_{\mathrm{A}} + \underline{Y}_{\mathrm{M}} & -\underline{Y}_{\mathrm{M}} \\ -\underline{Y}_{\mathrm{M}} & \underline{Y}_{\mathrm{B}} + \underline{Y}_{\mathrm{M}} \end{bmatrix}$	$\begin{bmatrix} \underline{Y}_{\mathrm{AA}} & -\underline{\tau}\,\underline{Y}_{\mathrm{AB}} \\ -\underline{\tau}^{*}\,\underline{Y}_{\mathrm{BA}} & \lvert\underline{\tau}\rvert^{2}\,\underline{Y}_{\mathrm{BB}} \end{bmatrix}$
closed	open	$\begin{bmatrix} 1 & 0 \\ 0 & 0 \end{bmatrix}$	$\begin{bmatrix} \underline{Y}_{\mathrm{A}} + \dfrac{\underline{Y}_{\mathrm{B}}\,\underline{Y}_{\mathrm{C}}}{\underline{Y}_{\mathrm{B}} + \underline{Y}_{\mathrm{C}}} & 0 \\ 0 & 0 \end{bmatrix}$	$\begin{bmatrix} \underline{Y}_{\mathrm{AA}} - \underline{Y}_{\mathrm{AB}} + \dfrac{\underline{Y}_{\mathrm{AB}}\underline{Y}_{\mathrm{BB}} - \underline{Y}_{\mathrm{AB}}^{2}}{\underline{Y}_{\mathrm{BB}}} & 0 \\ 0 & 0 \end{bmatrix}$
open	closed	$\begin{bmatrix} 0 & 0 \\ 0 & 1 \end{bmatrix}$	$\begin{bmatrix} 0 & 0 \\ 0 & \underline{Y}_{\mathrm{B}} + \dfrac{\underline{Y}_{\mathrm{A}}\,\underline{Y}_{\mathrm{C}}}{\underline{Y}_{\mathrm{A}} + \underline{Y}_{\mathrm{C}}} \end{bmatrix}$	$\begin{bmatrix} 0 & 0 \\ 0 & \lvert\underline{\tau}\rvert^{2}\left(\underline{Y}_{\mathrm{BB}} - \underline{Y}_{\mathrm{BA}} + \dfrac{\underline{Y}_{\mathrm{BA}}\underline{Y}_{\mathrm{AA}} - \underline{Y}_{\mathrm{BA}}^{2}}{\underline{Y}_{\mathrm{AA}}}\right) \end{bmatrix}$
open	open	$\begin{bmatrix} 0 & 0 \\ 0 & 0 \end{bmatrix}$	$\begin{bmatrix} 0 & 0 \\ 0 & 0 \end{bmatrix}$	$\begin{bmatrix} 0 & 0 \\ 0 & 0 \end{bmatrix}$